

Development of Systems for Expression, Purification, and CK2-Mediated Phosphorylation of the
Histone Oligomers

by

Md Touhidul Islam

A thesis submitted in partial fulfillment of the requirements for the degree of

Master of Science

Department of Biochemistry
University of Alberta

Abstract

It is of extreme importance to investigate the DNA repair pathways that will lead to a better understanding to develop cancer treatments since the primary cause of cancer is the inability of the cell to restore the damaged DNA. Upon DNA damage, the histone tails of the nucleosomes near the DNA lesions undergo a group of extensive post-translational modifications that remodels the chromatin structures in order to repair the damage. DNA double-strand break (DSB) induces the phosphorylation of histone variant H2A.X at Serine 139 residue, that is recognized by the mediator of DNA damage checkpoint, MDC1. This interaction is imperative for the recruitment of the other downstream DNA damage response (DDR) proteins that enact in selecting the repair pathways. Structural basis of interaction of the MDC1 BRCT domain with the phospho-peptide tail of H2A.X was previously revealed. However, the impacts of this interaction on the overall chromatin structure, and the successive nucleosome modifications are still elusive. We hypothesize that MDC1 BRCT domain not only binds to the phosphorylated H2A.X tail, but this interaction might position MDC1 in a way that its basic patch might interact with the nucleosomal DNA, or with the conserved acidic patch of H2A.X/H2B. To investigate these concepts *in vitro*, a successful purification of the nucleosome containing γ H2A.X is the prerequisite. For decades, histones have been extracted from the cell lysate using urea denaturant with subsequent extensive dialysis to refold the heteromeric histone complexes. This method is time and cost intensive. Here, we have developed two rapid purification protocols using the co-expression systems for the recombinant human histone oligomers. Furthermore, we have established a system for the *in vitro* phosphorylation of H2A.X that will facilitate the structural analysis of MDC1 BRCT bound γ H2A.X nucleosome complex in the future.

Preface

This thesis is a collaborative work by Md Touhidul Islam, and Dr. Rashmi Panigrahi, led by Professor Mark Glover at the University of Alberta. The modified refolding of the octamer, one-step purification of the dimer, and the *in vitro* phosphorylation of the dimer were developed by Md Touhidul Islam, while the one-step purification of the tetramer, and the octamer were developed by Dr. Rashmi Panigrahi. No part of this thesis has been previously published.

Acknowledgements

In the name of Allah, the most merciful and magnificent, I would like to thank countless people for helping me achieve my goal, however with space limitations, I will only name a few.

Firstly, thank you to my supervisor, Dr. Mark Glover, for guiding me throughout this journey and supporting me in every circumstance. You are the best supervisor one can ever have. Thank you to Dr. Rashmi Panigrahi, an incredible mentor, and co-worker, for all your contributions to help me reach this goal. Thank you to Dr. Luxin Sun for guiding me at the beginning of the project. Thank you to Dr. Curtis D Hodge for your assistance in the project. Thank you Morenike Ajidagba, Samuel Yang, Sherry Xu, and Mackenzie Credicott for your contributions. Thank you to my committee members Dr. Michael Hendzel and Dr. Ismail Hassan Ismail for your continual support and guidance. Thank you to Dr. Michael Ellison for agreeing to be an external evaluator for my defense. Thank you to Dr. David Stuart and Dr. Andrew MacMillan for evaluating my 670, 671, and 626 talks. Thank you to Dr. Jonathan Parrish, Dr. Deanna Davis, and Dr. Joanne Lemieux for helping me fulfill my professional requirements. Thank you to Kelsey Robertson for keeping me updated about the deadlines and for preparing the brochures for my seminar. Thank you to Dean Schieve for helping out with technical difficulties. Thanks to the wonderful graduate students and associates: Zabed Mahmud, Gaddafi Danmaliki, Catharine Trieber, Suad Rashid, Sayed Madi, Charanpal Grewal, Ayat Omer, Laine Lysyk, Emmanuella Takyi, Elena Arutyunova, Ayodeji Kulepa, Andrew Song, George Han, Brianna Greenwood, Anagha Krishnan, Jack Moore, Cameron Murray, Rabih Abou Farraj, Hyeong Jin Kim, Shiyun Peng, Jun Lu, Ross Edwards, Andrew Xiao, Zahra Havalishahriari, and Robyn A. Millott.

Thank you to Leslie Weigl, Afshin Arefi, Farah Masri, Anabelle C. Jones, Maja Matlinska, Ashley Davis, Dalal Awwad, Pedram Veisi and countless of others for being in my life and helping me grow. Thanks to my relatives and my parents for your perpetual blessings.

TABLE OF CONTENTS

CHAPTER ONE: INTRODUCTION	1
1.1 DNA DAMAGE TO TUMORIGENESIS	2
1.2 DIFFERENT TYPES OF DNA REPAIR MECHANISMS.....	3
1.3 GENOME ORGANIZATION: CHROMOSOME TO NUCLEOSOME	6
1.4 HISTONE FOLD, NUCLEOSOME STRUCTURE & HISTONE VARIANTS	8
1.5 H2A.X TO γ H2A.X	18
1.6 THE DEFENDER OF THE GENOME: FORMATION OF IRIF	21
1.7 TREATING OR TERMINATING: DI-PHOSPHORYLATION OF H2A.X	23
1.8 SUMMARY OF THE DSB REPAIR INITIATION.....	23
1.9 MDC1 INDEPENDENT UBIQUITINATION	24
1.10 STRUCTURE OF MDC1 BRCT BOUND γ H2A.X TAIL.....	26
1.11 AIM TO ATTAIN: RESEARCH QUESTIONS & HYPOTHESIS	27
CHAPTER TWO: MATERIALS AND METHODS	29
2.1 SITE-DIRECTED MUTAGENESIS OF H2A.X	30
2.2 CLONING OF HISTONES AND MDC1-BRCT	31
2.3 OVEREXPRESSION OF PROTEIN	33
2.4 PURIFICATION OF THE OCTAMER.....	34
2.4.1 MODIFIED REFOLDING OF THE OCTAMER	34
2.4.1.1 OVEREXPRESSION OF THE RECOMBINANT SINGLE HISTONES	34
2.4.1.2 PURIFICATION OF HISTONE	34
2.4.1.3 FORMATION OF THE H2A.X-H2B DIMER	35
2.4.1.4 FORMATION OF THE (H3.1-H4) ₂ TETRAMER	35
2.4.1.5 FORMATION OF THE (H2A.X-H2B-H3.1-H4) ₂ OCTAMER.....	36
2.4.2 ONE-STEP PURIFICATION OF THE DIMER AND THE TETRAMER	36
2.4.2.1 SEPARATE OVEREXPRESSION OF THE HISTONE PAIRS.....	36
2.4.2.2 PURIFICATION OF THE H2A.X-H2B DIMER	37
2.4.2.3 PURIFICATION OF THE (H3.1-H4) ₂ TETRAMER.....	38
2.4.2.4 FORMATION OF THE (H2A.X-H2B-H3.1-H4) ₂ OCTAMER.....	38
2.4.3 ONE-STEP PURIFICATION OF THE OCTAMER.....	39
2.4.3.1 COMBINED OVEREXPRESSION OF THE HISTONE PAIRS.....	39
2.4.3.2 PURIFICATION OF THE (H2A.X-H2B-H3.1-H4) ₂ OCTAMER.....	39
2.4 <i>IN VITRO</i> PHOSPHORYLATION OF THE H2A.X-H2B DIMER.....	40
CHAPTER THREE: RESULTS & DISCUSSIONS	41
3.0 PREAMBLE.....	42

3.1 RESULT: OVEREXPRESSION OF THE SINGLE HISTONES	44
3.2 DISCUSSION: OVEREXPRESSION OF THE SINGLE HISTONES	45
3.3 RESULT: SEPARATE OVEREXPRESSION OF THE HISTONES PAIRS	47
3.4 DISCUSSION: SEPARATE OVEREXPRESSION OF THE HISTONE PAIRS	50
3.5 RESULT: COMBINED OVEREXPRESSION OF THE HISTONES PAIRS	54
3.6 DISCUSSION: COMBINED OVEREXPRESSION OF THE HISTONE PAIRS	55
3.7 RESULT: MODIFIED REFOLDING OF THE OCTAMER	56
3.7.1 Ni ²⁺ AFFINITY PULL-DOWN PURIFICATION OF THE SINGLE HISTONES	56
3.7.2 SEC OF THE (His) ₆ -H2A.X-(His) ₆ -H2B DIMER	57
3.7.3 SEC OF THE [(His) ₆ -H3.1-(His) ₆ -H4] ₂ TETRAMER.....	58
3.7.4 SEC OF THE OCTAMER	59
3.7.5 YIELD OF THE HISTONE OLIGOMERS	60
3.8 DISCUSSION: MODIFIED REFOLDING OF THE OCTAMER.....	60
3.9 RESULT: ONE-STEP PURIFICATION OF THE DIMER AND THE TETRAMER.....	62
3.9.1 Ni ²⁺ AFFINITY PULL-DOWN PURIFICATION OF THE HISTONE PAIRS	62
3.9.2 SEC OF THE CO-EXPRESSED (His) ₆ -TEV-H2A.X-H2B DIMER.....	63
3.9.3 SEC OF THE CO-EXPRESSED [(His) ₆ -TEV-H4-H3.1] ₂ TETRAMER	64
3.9.4 SEC OF THE CO-EXPRESSED [(His) ₆ -TEV-H3.1-H4] ₂ TETRAMER	65
3.9.5 SEC OF THE OCTAMER	66
3.9.6 YIELD OF THE HISTONE OLIGOMERS	67
3.10 DISCUSSION: ONE-STEP PURIFICATION OF THE DIMER AND THE TETRAMER.....	67
3.11 RESULT: ONE-STEP PURIFICATION OF THE OCTAMER.....	69
3.11.1 Ni ²⁺ AFFINITY PULL-DOWN PURIFICATION OF THE OCTAMER.....	69
3.11.2 SEC OF THE OCTAMER.....	70
3.11.3 YIELD OF THE OCTAMER.....	72
3.12 DISCUSSION: ONE-STEP PURIFICATION OF THE OCTAMER	72
3.13 RESULT: MALDI-IMS CONFIRMATION OF THE DIMER	73
3.14 DISCUSSION: MALDI-IMS CONFIRMATION OF THE DIMER	73
3.15 RESULT: <i>IN VITRO</i> PHOSPHORYLATION OF THE H2A.X-H2B DIMER	74
3.16 DISCUSSION: <i>IN VITRO</i> PHOSPHORYLATION OF THE H2A.X-H2B DIMER.....	76
CHAPTER FOUR: CONCLUSION AND FUTURE DIRECTION	78
REFERENCES	84
APPENDICES	97
I- VECTORS, PRIMERS, RESTRICTION ENZYMES, AND ANTIBIOTICS	98
II- PROTOCOLS	100
PROTOCOL 1-TOUCH DOWN PCR.....	100
PROTOCOL 2-COLONY PCR	102

PROTOCOL 3-PCR CLEANUP	103
PROTOCOL 4-DOUBLE RESTRICTION DIGEST REACTION	103
PROTOCOL 5-LIGATION REACTION	104
PROTOCOL 6-RECOMBINANT DNA TRANSFORMATION.....	105
PROTOCOL 7-AGAROSE GEL CASTING & RUNNING	106
PROTOCOL 8-PLASMID MINIPREP PROTOCOL	107
PROTOCOL 9-SEQUENCING THE PLASMID TO CONFIRM THE INSERT	107
PROTOCOL 10-OVEREXPRESSION CHECKING	107
PROTOCOL 11-SDS PAGE	108
PROTOCOL 12-BRADFORD ASSAY	109
PROTOCOL 13-MODIFIED REFOLDING OF THE OCTAMER.....	110
PROTOCOL 14-ONE-STEP PURIFICATION OF THE DIMER & THE TETRAMER	115
PROTOCOL 15-ONE-STEP PURIFICATION OF THE OCTAMER	119
PROTOCOL 16- <i>IN VITRO</i> PHOSPHORYLATION OF THE H2A.X-H2B DIMER .	121
PROTOCOL 17- <i>SIZE EXCLUSION COLUMN (SEC)</i>	124
III-BUFFERS.....	126
IV-CLONING IMAGES	129
V-CELL LINES	134

LIST OF TABLES

TABLE 1.1 DIFFERENT HISTONE VARIANTS AND THEIR SPECIFICATIONS.	17
TABLE 2.1 THE LIMITATIONS WITH THE ATM KINASE & THE ADVANTAGES WITH THE CK2A.	31
TABLE 2.2 LIST OF THE RECOMBINANT CONSTRUCTS WITH THEIR RESPECTIVE OVEREXPRESSION CELL LINES.	33
TABLE 3.1 YIELD OF THE SINGLE HISTONES.	45
TABLE 3.2 YIELD OF THE REFOLDED HISTONE OLIGOMERS.	60
TABLE 3.3 YIELD OF THE CO-EXPRESSED HISTONE OLIGOMERS.	67
TABLE 3.4 YIELD OF THE ONE-STEP PURIFIED OCTAMER.	72
TABLE 4 A COMPARISON AMONG ALL THE PURIFICATION PROCESSES.	82
TABLE I-1 SPECIFICATIONS OF THE USED VECTORS AND THE DESIGNED PRIMERS.	98
TABLE I-2 LIST OF BACTERIAL EXPRESSION CELL LINES WITH THEIR INTRINSIC ANTIBIOTIC RESISTANCE	100
TABLE II-P1.1 TOUCH DOWN PCR REACTION TABLE	100
TABLE II-P1.2 PCR PRODUCT SIZES AND THE CALCULATED PCR EXTENSION TIME	100
TABLE II-P2.1 COLONY PCR REACTION TABLE	102
TABLE II-P4.1 DOUBLE DIGEST REACTION SETUP	103
TABLE II-P4.2 USED DOUBLE DIGEST PAIRS	104
TABLE II-P5.1 SIZE OF THE DIGESTED VECTORS FROM SERIAL CLONER 2.6	104
TABLE II-P5.2 LIGATION REACTION SETUP	105
TABLE II-P11 SDS POLYACRYLAMIDE GEL CASTING	108
TABLE II-P13.1 CONCENTRATION CALCULATION FOR THE HISTONES	111
TABLE II-P13.2 CONCENTRATION CALCULATION FOR THE HISTONE OLIGOMERS.	113
TABLE II-P14.1 CONCENTRATION CALCULATION FOR THE HISTONE OLIGOMERS.	117
TABLE II-P16.1 ATP MIX: 1MM ATP	121
TABLE II-P16.2 KINASE ASSAY REACTION SETUP	122
TABLE II-P16.3 QUENCHING OF KINASE REACTION	122
TABLE II-P17.1 SIZE EXCLUSION COLUMN INFORMATION	124
TABLE II-P17.2 SEC METHOD INFORMATION	125
TABLE III-1 ALL BUFFER COMPOSITIONS	126
TABLE V-1 DESCRIPTION OF THE CELL LINES USED IN THIS STUDY	134
TABLE V-2 DESCRIPTION OF THE TERMINOLOGIES USED IN THE CELL LINES SPECIFICATIONS	136

LIST OF FIGURES

FIGURE 1.1 DIFFERENT TYPES OF DNA DAMAGE.	5
FIGURE 1.2 DEPICTION OF GENOME ORGANIZATION IN EUKARYOTES WITH A SERIES OF SCHEMATIC DIAGRAMS AND TRANSMISSION ELECTRON MICROGRAPHS.	7
FIGURE 1.3 HISTONE FOLD AND HANDSHAKE MOTIF.	8
FIGURE 1.4 HISTONE FOLD HELPS IN FORMING HISTONE OLIGOMERS.	9
FIGURE 1.5 THE FOUR-HELIX BUNDLE FORMING THE OCTAMER.	10
FIGURE 1.6 PLACEMENT OF THE HISTONE TAILS IN THE NUCLEOSOME.	11
FIGURE 1.7 INTERACTION BETWEEN THE HISTONE FOLDS AND THE NUCLEOSOMAL DNA.	12
FIGURE 1.8 WIDOM 601 SEQUENCE AND SUPER HELICAL LOCATIONS.	13
FIGURE 1.9 SCHEMATIC DIAGRAM OF HISTONE SECONDARY STRUCTURE ARRANGEMENT.	14
FIGURE 1.10 DIFFERENT HISTONE SUBTYPE.	15
FIGURE 1.11 CURRENTLY IDENTIFIED POST TRANSLATIONAL MODIFICATION ON CANONICAL HISTONES.	16
FIGURE 1.12 SEQUENCE ALIGNMENT AND SECONDARY STRUCTURE PREDICTION BETWEEN CANONICAL H2A AND VARIANT H2A.X.	18
FIGURE 1.13 VARIOUS DSB SOURCES THAT LEADS TO γH2A.X FORMATION.	19
FIGURE 1.14 PTMS ON H2A/H2A.X.	20
FIGURE 1.15 A PREDICTED SCHEMATIC DIAGRAM OF INITIAL DSB RESPONSE. ...	24
FIGURE 1.16 SCHEMATIC DIAGRAM OF BMI1-RNF2 MEDIATED MONO-UBIQUITINATION.	25
FIGURE 1.17 STRUCTURAL BASIS OF THE INTERACTION BETWEEN THE MDC1 TANDEM BRCT DOMAIN AND γH2A.X PHOSPHOPEPTIDE TAIL.	26
FIGURE 1.18 BASIC REGION IN HUMAN MDC1 BRCT DOMAIN.	27
FIGURE 1.19 HYPOTHETICAL QUESTION OF HOW MDC1 BRCT IS INTERACTING WITH THE COMPLETE NUCLEOSOME.	28
FIGURE 2.1 MUTAGENESIS OF H2A.X.	31
FIGURE 3.0 SCHEMATIC DIAGRAM SHOWING THE DIFFERENCES AMONG THE THREE OLIGOMER PURIFICATION METHODS.	43
FIGURE 3.1 OVEREXPRESSION CHECK OF THE SINGLE HISTONES.	44
FIGURE 3.2 SCHEMATIC DIAGRAM OF THE PET47B(+)-HISTONE CONSTRUCT.	46
FIGURE 3.3 OVEREXPRESSION CHECK FOR THE H2A.X-H2B DIMER	48
FIGURE 3.4 OVEREXPRESSION CHECK FOR THE TEV-H4-H3.1 TETRAMER	49
FIGURE 3.5 OVEREXPRESSION CHECK FOR THE TEV-H3.1-H4 TETRAMER.	50
FIGURE 3.6 SCHEMATIC DIAGRAM OF THE PETDUET-1-H2A.X-H2B CONSTRUCT.	51

FIGURE 3.7 SCHEMATIC DIAGRAM OF THE PACYCDUET-1-TEV-H4-H3.1 AND THE PCDFDUET-1-TEV-H3.1-H4 CONSTRUCT.	52
FIGURE 3.8 OVEREXPRESSION CHECK FOR THE HISTONE OCTAMER.	54
FIGURE 3.9 Ni²⁺ AFFINITY PURIFICATION OF THE SINGLE HISTONES UNDER UREA DENATURING CONDITION.	56
FIGURE 3.10 SIZE EXCLUSION PROFILE OF THE RECONSTITUTED HISTONE DIMER.	57
FIGURE 3.11 SIZE EXCLUSION PROFILE OF THE RECONSTITUTED HISTONE TETRAMER.	58
FIGURE 3.12 SIZE EXCLUSION PROFILE OF THE RECONSTITUTED HISTONE OCTAMER.	59
FIGURE 3.13 Ni²⁺ AFFINITY PURIFICATION OF THE CO-EXPRESSED HISTONE OLIGOMERS, THE H2A.X-H2B DIMER, AND (H3.1-H4)₂ TETRAMER.	62
FIGURE 3.14 SIZE EXCLUSION PROFILE OF THE CO-EXPRESSED (HIS)₆-TEV-H2A.X-H2B DIMER.	63
FIGURE 3.15 SIZE EXCLUSION PROFILE OF THE CO-EXPRESSED [(HIS)₆-TEV-H4-H3.1]₂ TETRAMER.	64
FIGURE 3.16 SIZE EXCLUSION PROFILE OF THE CO-EXPRESSED [(HIS)₆-TEV-H3.1-H4]₂ TETRAMER.	65
FIGURE 3.17 SIZE EXCLUSION PROFILE OF THE CO-EXPRESSED HISTONE OLIGOMERS ASSOCIATED OCTAMER.	66
FIGURE 3.18 Ni²⁺ AFFINITY PURIFICATION OF THE OCTAMER.	69
FIGURE 3.19 SIZE EXCLUSION PROFILE OF THE OCTAMER PURIFIED FROM THE ONE-STEP PURIFICATION SYSTEM.	70
FIGURE 3.20 SIZE EXCLUSION PROFILE OF THE OCTAMER IN SUPERDEX 200 10 300 AFTER THE SUPERDEX 200 16 60 RUN.	71
FIGURE 3.21 MALDI-IMS CONFORMATION OF THE (HIS)₆-H2A.X-(HIS)₆-H2B DIMER PREPARED FROM THE MODIFIED REFOLDING SYSTEM.	73
FIGURE 3.22 PHOSPHORYLATION OF THE REFOLDED (HIS)₆-H2A.X-(HIS)₆-H2B DIMER BY THE CK2.	74
FIGURE 3.23 PHOSPHORYLATION OF THE CO-EXPRESSED (HIS)₆-H2A.X-H2B DIMER BY THE CK2.	75
FIGURE 3.24 PHOSPHORYLATION OF THE XRCC4 BY THE CK2.	75
FIGURE 3.24 Y57 OF H2A IS A POTENTIAL SUBSTRATE FOR THE CK2.	77
FIGURE 4.1 FLOWCHAT SHOWING THE CHOICE OF THE HISTONE OLIGOMER PURIFICATION PROCESS.	81
FIGURE IV-1 COLONY PCR CONFIRMATION FOR SUCCESSFUL CLONING.	129
FIGURE IV-2 COLONY PCR CONFIRMATION FOR SUCCESSFUL CLONING.	130
FIGURE IV-3 COLONY PCR CONFIRMATION FOR SUCCESSFUL CLONING.	131
FIGURE IV-4 COLONY PCR CONFIRMATION FOR SUCCESSFUL CLONING.	132
FIGURE IV-5 COLONY PCR CONFIRMATION FOR SUCCESSFUL CLONING.	133

Introduction

1.1 DNA Damage to Tumorigenesis

The stability and the successful transmission of DNA are vital for the survival of the living organisms since DNA is the storehouse of all the genetic information. According to the RNA world hypothesis ¹, DNA has evolved from its ancestor RNA in order to gain stability, and as a result, has become the unit of cellular inheritance. However, evolution has yet not provided DNA with inveterate stability. In fact, DNA is subjected to innumerable alterations that not only perform a pivotal role in the generation of genetic diversity but also give rise to numerous fatal diseases like cancer.

A single human cell undergoes 10^4 - 10^5 DNA damages per day ². To maintain the cell homeostasis, DNA must be restored with high efficacy by the cell. There is not a single form of DNA damage, but a variety of different unique types of DNA modifications resulting from either physiological processes or external environmental factors, such as UV lights or ionizing radiations ³. Therefore, the cells have evolved multifaceted cellular mechanisms to amend these diverse sets of DNA damages. The telltale sign of cancerous cells is the accumulation of DNA damages over time caused by the error-prone or dysfunctional DNA repair mechanisms ⁴.

Upon DNA damage, cells orchestrate a cascade of events, DNA Damage Response (DDR), in order to recognize and repair the injured DNA ⁵. DDR delays cell cycle progression through activating different checkpoints ⁶, however, DDR also triggers apoptosis if DNA damage is irreparable ⁷. DDR carries out the complete signal transduction pathway with the combination of three classes of proteins: DNA damage sensors that sense the damaged lesions, DNA damage transducers that amplify the damaged signal sensed by the sensors, and DNA damage effectors that eventually repair the lesions ⁸. The performance of all these proteins has to be coordinated in

a spatiotemporal manner to ensure the accuracy of the repair processes ⁹. Defects in maintaining cell homeostasis may appear if the coordination between the DDR proteins is disrupted.

1.2 Different Types of DNA Repair Mechanisms

Innumerable enzymes are involved in tackling various kinds of DNA injuries that are classified into different groups.

MMR

Mismatch Repair (MMR) is a high fidelity repair mechanism that corrects bases incorporated incorrectly during DNA replication ¹⁰ (Figure 1-a). Wrong bases can be incorporated either by random mutations or by insertion/deletion of bases ¹¹. MMR triggers post replicative machinery that removes the wrong bases and hence provides the DNA polymerases an opportunity to re-replicate without any error ¹².

BER/SSBR

Reactive oxygen species (ROS), alkylating or hydrolyzing agents can modify bases as well as can cause single-strand breaks in DNA ¹³. These anomalous lesions are then repaired by Base Excision Repair (BER) mechanism with high fidelity ¹⁴. DNA glycosylase enzymes recognize the lesion and create an abasic site that is repaired by a combined effort of DNA nucleases, polymerases and ligases ¹⁵ (Figure 1-b).

NER

Due to UV light and exogenous chemicals, significant distortion can happen to the DNA double helix, such as thymidine dimers. Distorted helices are repaired by Nucleotide Excision Repair (NER) mechanism ¹⁶. Specific endonucleases cleave off the oligonucleotides and create a single strand DNA that works as a template for DNA polymerase before ligation happens using DNA ligase ¹⁷ (Figure 1-c).

DSBR

The most perilous form of DNA damage is the DNA Double Strand Break (DSB) that can be resulting from ionizing radiation (IR) such as X-rays, or from anti-tumor drugs ¹⁸. DSB is the most lethal form of DNA damage since the repair mechanisms involved in this pathway are not highly fidelitous. DSBs are handled by the cell through two DDR pathways: Non-homologous end joining (NHEJ) and homologous recombination (HR) (Figure 1-d). NHEJ can operate throughout the cell cycle, but mostly post-mitotic cells since it does not require an intact template DNA, and therefore, NHEJ is a highly error-prone mechanism ¹⁹. On the other hand, HR can only operate when there is a sister template present in the cell; therefore, it can only function in S (DNA synthesis phase) and G2 (pre-mitotic gap 2 phase) phases of the cell cycle ²⁰.

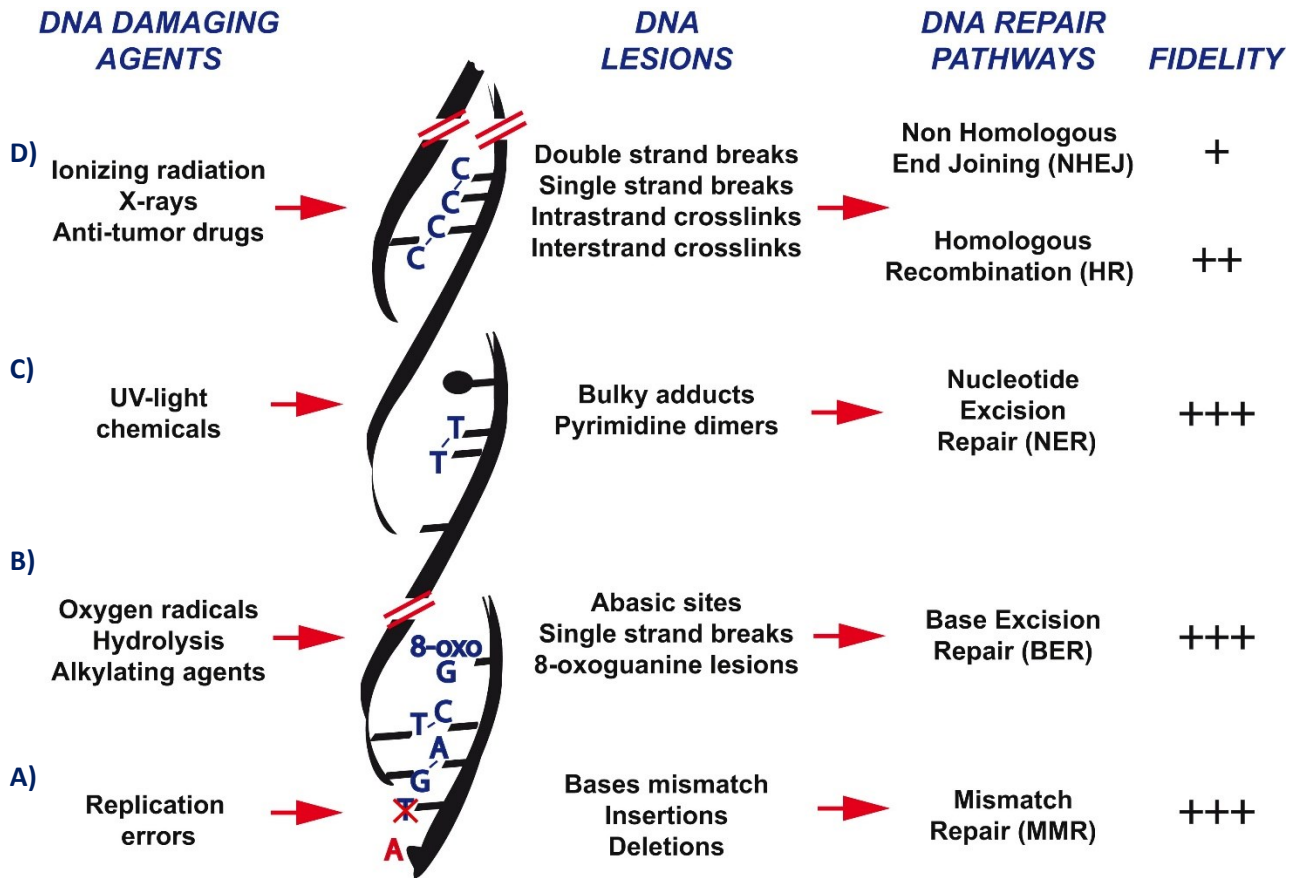


Figure 1.1 Different Types of DNA Damage. Adapted from “DNA-Damage Response in Tissue-Specific and Cancer Stem Cells,” by C. Blanpain, M. Mohrin, P. A. Sotiropoulou, and E. Passegué, 2011, *Cell Stem Cell*, 8(1), 16-29. Copyright 2018 by Elsevier Inc. Reprinted with permission.

The figure depicts different kinds of DNA injuries and their respective mechanisms. A) Replication-related mismatch errors are repaired by mismatch repair mechanism (MMR) with high fidelity. B) Base modification caused by oxygen radicals, alkylating and hydrolyzing agents is repaired by base excision repair (BER) with high fidelity. C) UV light can cause helix distortions. These distortions are repaired by nucleotide excision repair (NER) mechanisms. D) Ionizing radiation or anti-tumor drugs can induce DNA double-strand break (DSB), which is repaired by non-homologous end joining (NHEJ) or homologous recombination (HR) with relatively low fidelity compared to the other types of DNA damage repair processes ²¹.

1.3 Genome Organization: Chromosome to Nucleosome

The intricacy of DNA repair is augmented by the organizational style of the overall DNA in the cells. Eukaryotic DNA is ~2m long; this 2m long DNA thread is packaged into a condensed structure known as chromatin. The basic unit of chromatin is called the nucleosome, which is a nucleoprotein complex of 146bp DNA wrapped around four small highly basic proteins called histones. Albrecht Kossel first discovered histones in 1884^{22, 23}. Since then, how DNA forms the higher order structure, and how this arrangement regulates the overall cellular mechanisms have been the ever-evolving questions to be answered.

Two sets of four different types of histones, H2A, H2B, H3, and H4, form an octameric complex. At the very first stage of DNA packing, this octamer wraps itself with 146 bp of DNA double helix to form a single nucleosome (Figure 1.2). The arrangement of nucleosome on the DNA strand is analogous to a “beads on a string” formation that is visible at the interphase stage of the cell cycle. The DNA between the adjacent nucleosomes is called the linker DNA. Nucleosome with its histone tails and linker DNA interacts with the other nucleosomes in order to form a higher level of packaging. A fifth type of histone, H1 or linker histone, also facilitates this further compaction, and in turn, gives rise to 30 nm fiber. This 30 nm fiber then folds itself around a chromosomal scaffold complex to form 300 nm fiber. Further folding leads to 700 nm chromatid formation. Sister chromatid pair forms X shaped mitotic chromosome, which is visible at the metaphase stage under a light microscope (Figure 1.2)²⁴.

This complex structure of chromatin regulates transcription, replication, segregation, and repair of DNA. To carry out these functions chromatin remodeling is imperative.

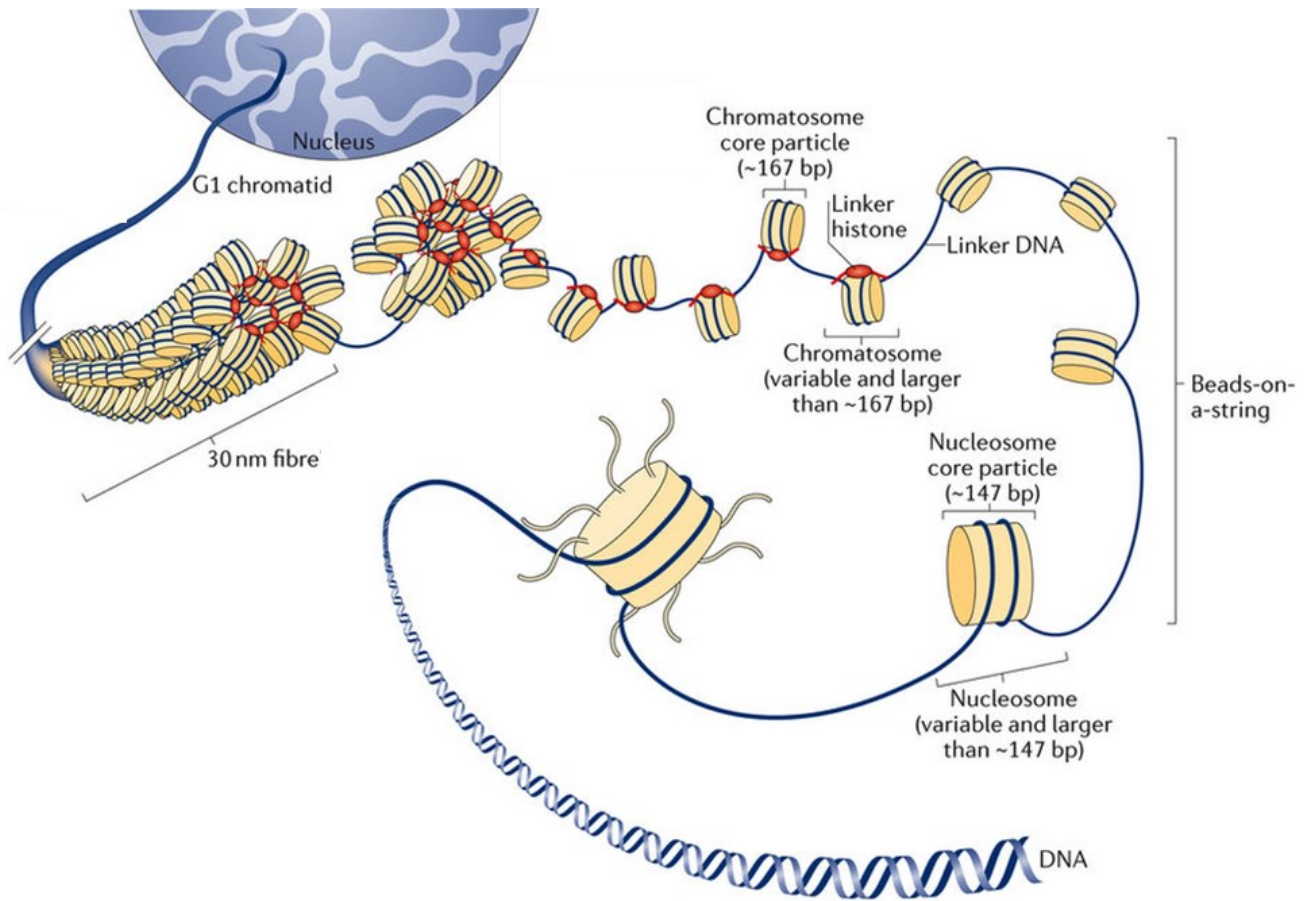


Figure 1.2 Depiction of Genome Organization in Eukaryotes. Adapted from “Emerging roles of linker histones in regulating chromatin structure and function”, by D. V. Fyodorov, B. Zhou, A. I. Skoultchi, and Y. Bai, 2018, *Nature Reviews Molecular Cell Biology*, 19(3), p. 192. Copyright 2018 Macmillan Publishers Limited, part of Springer Nature. Reprinted with permission.

The first level of DNA packing (10 nm) happens when double strand DNA helix (2 nm) wraps around four types of evolutionarily conserved histones, H2A, H2B, H3, and H4. The nucleoprotein complex is called nucleosome. The array of nucleosome on DNA strand resembles beads on a string conformation, where each bead is a nucleosome, and the string is called linker DNA. Next level of packaging (30 nm) occurs when one nucleosome with its histone tails and linker DNA comes into contact with other neighboring nucleosomes. A fifth type of histone called H1 or linker histone locks the overall nucleosomal complex and helps in forming this fiber like interphase chromatin organization^{24, 59}.

1.4 Histone Fold, Nucleosome Structure & Histone Variants

Concerning primary sequence, each type of histone is highly conserved, specially Histone H4 which has 95% conservation across species. Histone H1 or H5, which is known as linker histone and is responsible for higher-order chromatin packaging, is the least conserved histone; however, the core globular region is still conserved. This sequence conservation leads to the functional and structural conservation of each type of histone ²⁵.

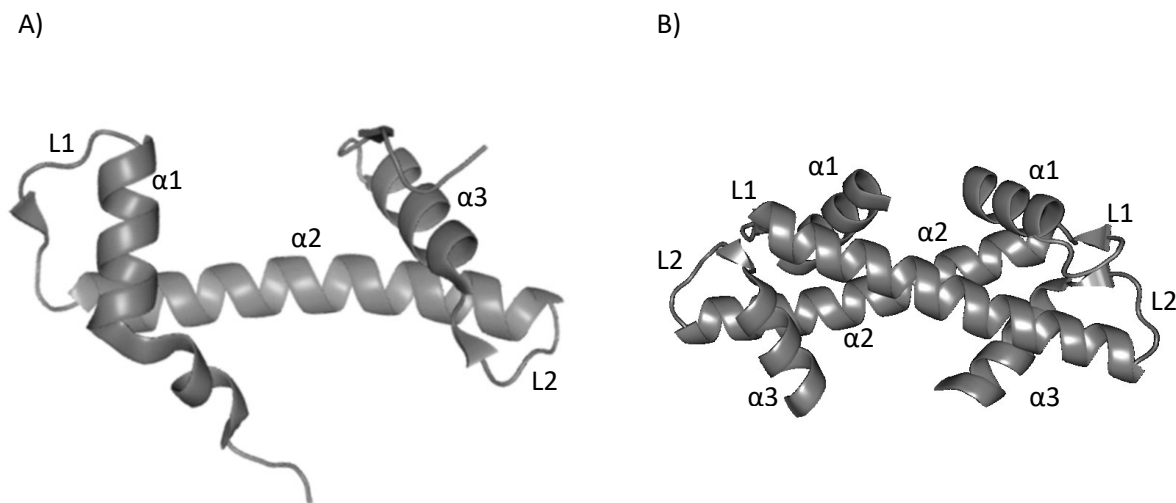


Figure 1.3 Histone Fold and Handshake Motif

A) All core histones have a distinctive structural similarity known as histone fold. Each histone fold consists of two helix strand helix (HSH) motifs. B) Histone fold helps in forming handshake motif between two histones in order to form a heteromeric oligomer.

All four core histones have low sequence conservation among themselves; in spite of this, all four core histones have a striking structural conservation. This structural motif is known as histone fold. Each histone fold has three alpha helices connected by two loops stated like $\alpha 1$ -L1- $\alpha 2$ -L2- $\alpha 3$. This particular arrangement of helix loop helix is also called helix strand helix (HSH) motif, and each histone fold has two HSH motifs that provide it with a 2-fold symmetry (Figure

1.3 A). This core histone motif mostly provides the histones with the ability to form a handshake motif with other respective histones in order to form the crescent-shaped hetero-oligomers, and hence leads to the creation of the overall nucleosome (Figure 1.3 B). This histone fold is the signature mark for all the core histones²⁶. H2A, H2B form a dimer, and H3 and H4 form a tetramer. Two dimers one tetramer interact in order to form an octamer (Figure 1.4).

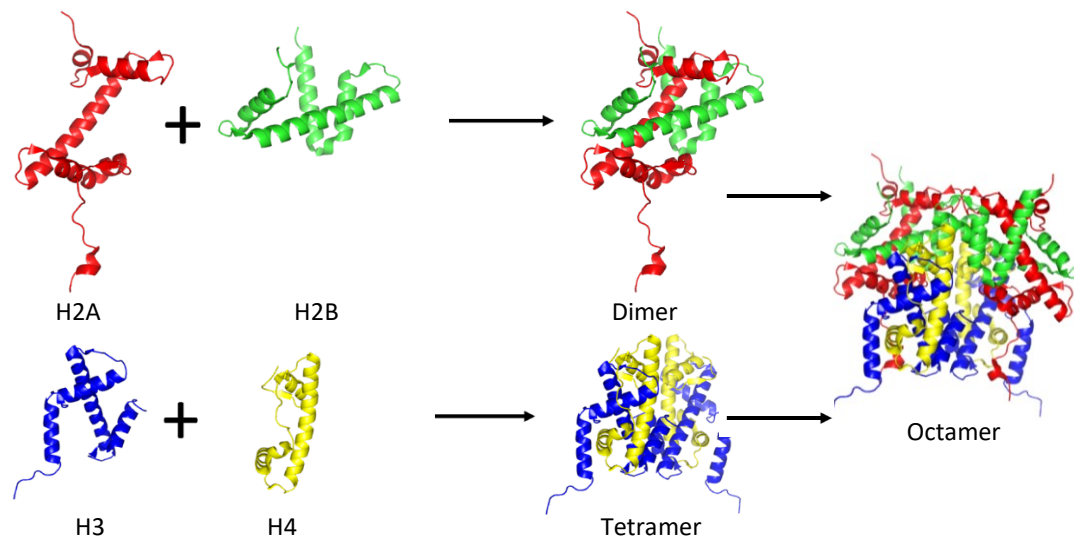


Figure 1.4 Histone Fold Helps in Forming Histone Oligomers.

Histone H2A and Histone H2B form a handshake motif together to form a heteromeric dimer, and H3 and H4 form a tetramer. Two dimers and one tetramer give rise to an octamer.

The legacy for deciphering nucleosome structure started back in 1980 when Klug et al. provided a 22Å resolution fiber structure showing that the histone octamer has a 2-fold axis of symmetry⁶⁸. Following this, in 1984 Richmond et al. submitted a 7Å resolution crystal structure of the nucleosome core particle that showed how the DNA bends and interacts with the histones⁶⁹. The breakthrough happened in 1991 when Arents et al. solved a 3.1Å resolution structure of the octamer which showed that the elongated histone chains are gathered in the octamer forming a distinctive handshake motif²⁶. The first high-resolution structure of the complete nucleosome at

2.8Å was solved by Luger et al. in 1997. In this structure, the finer details of protein-protein interactions and protein-DNA interactions were revealed ⁷⁰.

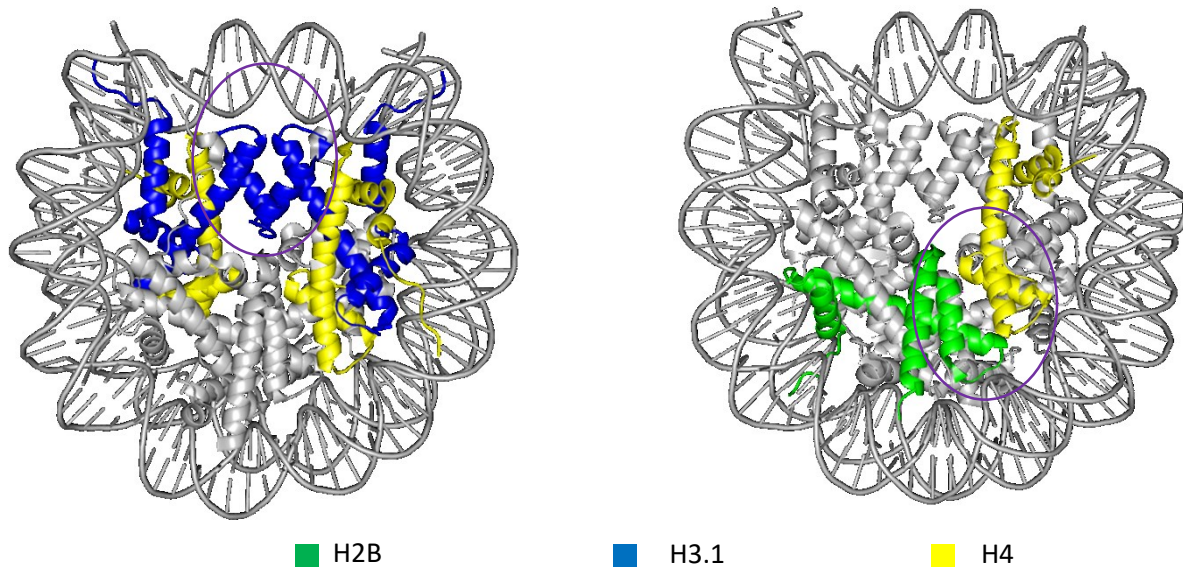


Figure 1.5 The Four-Helix Bundle Forming the Octamer (PDB: 5AVB).

A) The circled is the H3-H3 four-helix bundle. B) The circled is the H2B-H4 four-helix bundle.

According to the structure solved by Luger et al. 1997 ⁷⁰, the two H2A/H2B and the two H3/H4 form the overall octamer using a single structural motif known as the four-helix bundle, which is formed by the $\alpha 2$ and $\alpha 3$ helices from the adjacent histone-folds. The tetramer is formed when two H3/H4 pairs come into contact through a 4-helix bundle formed by H3/H3 histone folds (Figure 1.5 A). Each pair of H2A-H2B interacts with each half of the tetramer using another 4-helix bundle created by the histone folds of H2B and H4 (Figure 1.5 B). There are 10 histone tails that protrude outwards from the overall nucleosomal core particle, the eight N-terminal tail from all the histones and the two c-terminal tails from the H2A. H3 tail interacts with the nucleosomal DNA (~13 bp) at the entry-exit site, and H3 αN sits on top of the H4 (Figure 1.6 B). While the H2A αC terminal tail extends towards the dyad, H2B αC flips back from the center of the nucleosome opposite to the dyad (Figure 1.6 A). From the solved structure, it is evident that the

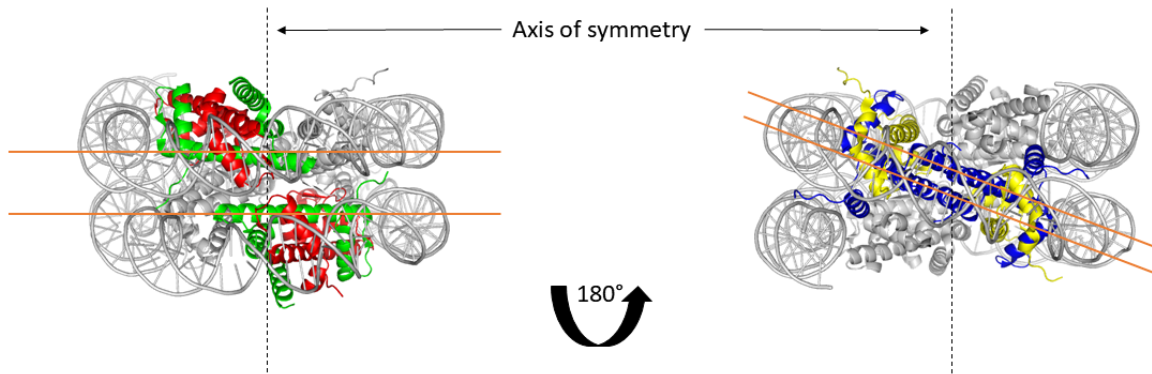


Figure 1.7 Interaction between the Histone Folds and the Nucleosomal DNA (PDB: 5AVB)

A) H2A-H2B interact with the nucleosomal DNA at two different parallel planes that are perpendicular to the axis of symmetry. B) H3-H4 interact with the nucleosomal DNA at two different parallel planes that are diagonally slanted with the axis of symmetry.

Three types of DNA sequences, the mixed genomic DNA, the 5S RNA coding sequence, and the human α -satellite repeat were mostly used in forming and solving the nucleosome structures before 1997. Widom 601 nucleosome positioning sequence has become more common recently. Through *in vitro studies*, Lowary and Widom found this synthetic DNA sequence that interacted tightly with the nucleosome⁷². The reason it binds tightly with the octameric core is that it has AT/TA/TT/AA base pairs at the minor groove of the DNA where it will interact with the octamer, while GG/GC/CG/CC base pairs will be found in the major groove does not come into contact with the octamer. These pyrimidine repeats after every 10bp provide the DNA with enough flexibility to gyre around the octamer without any steric hindrance. This 145bp palindromic Widom 601 sequence wraps around DNA at 1.67 left-handed super-helical turns. The dyad axis passes on a base pair rather than the middle of two bases. Therefore, both the nucleosomal half are wrapped around with 72bp DNA. Hence, Widom 609 sequence provides nucleosome with a perfect 2-fold symmetry, while the other sequences give rise to a pseudo 2-fold symmetry. The

base pair that has the dyad axis passing through is labeled as superhelical location 0 (SHL0). The next clockwise superhelical turns are called SHL+1, SHL+2, ..., SHL+7, while the next counterclockwise turn is labeled as SHL-1, SHL-2, ..., SHL-7. The dyad axis passes through the SHL0 and the SHL \pm 4^{70,72} (Figure 1.8).

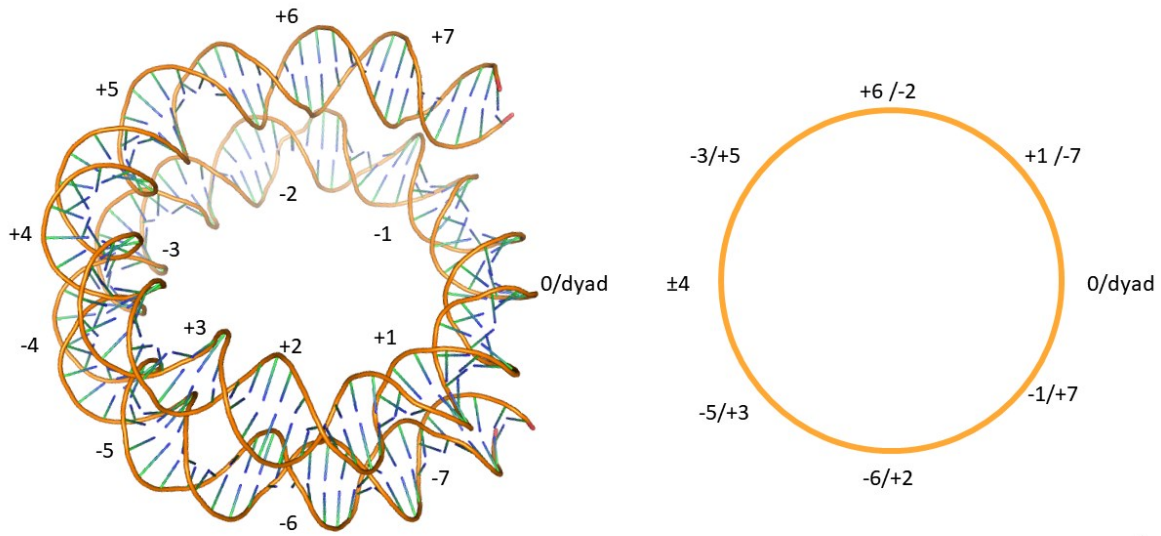


Figure 1.8 Widom 601 Sequence and Super Helical Locations.

The spiral turns are numbered with a positive integer (clockwise) or a negative integer (counterclockwise). From the top certain superhelical location overlaps on each other.

The coiled shape nucleosome has a diameter of $\sim 100\text{\AA}$ and a width of $\sim 60\text{\AA}$ ⁷⁰. The circumference of the nucleosome is a high negatively charged surface because of the phosphodiester backbone of the wrapped DNA. There is one more negatively charged surface at the groove of H2A/H2B dimer known as the nucleosome acidic patch. This acidic patch is comprised of eight acidic residues, two from H2B (E102 and E110) and six from H2A (E56, E61, E64, D90, E91, and E92)⁷⁰. This acidic patch is considered to be the docking site for extrinsic non-nucleosomal protein factors.

The functional differences of each histone are governed by their differences in both the terminal tail regions (Figure 1.9). These tails are enriched with highly polar amino acids, and therefore, they flank the nucleosomal core. These tail regions are important for the regulation of chromosomal packaging and remodeling. Hence, they play a crucial role in the DNA transcription, replication, and repair processes ²⁷.

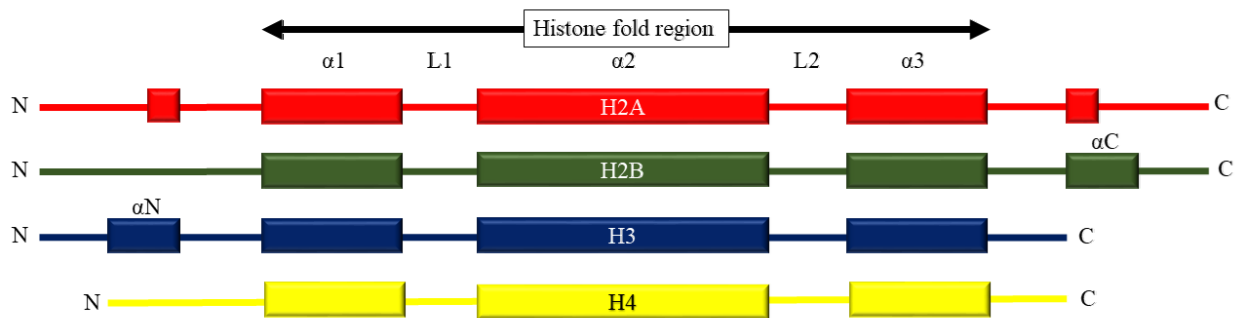


Figure 1.9 Schematic Diagram of Histone Secondary Structure Arrangement

All four core histones have the structurally similar histone fold. The difference among them results from the length and the compositions of the amino acids at the N-terminal and the C-terminal tail regions.

Histone H2A, H2B, H3, and H4 are the canonical histones. Except for H4, all the other histones have different variants known as histone subtypes (Figure 1.10). Again, the difference between each subtype rises in the terminal tail regions. Different subtypes carry out different functions through various type of post-translational modifications (PTMs) at different amino acids in the tail regions. These variants of histones are crucial for the regulation of various cellular functions such as DNA damage repair (Table 1.1) ²⁸.

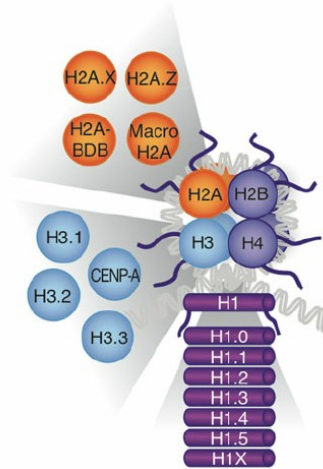


Figure 1.10 Different Histone Subtypes. Adapted from “Epigenetics Components of Aging in the Central Nervous System,” by Y. Q. Zhao, K. Jordan, V. V. Lunyak, 2013, *Neurotherapeutics*, 10(4), 647-663. Copyright 2013 by The American Society for Experimental NeuroTherapeutics, Inc. Reprinted with permission.

Except for H4, each canonical histone has different variants. Histone H1, which is the least conserved among all the histones, has the highest number of variants. Histone H2A has four major subtypes: H2A.X, H2A.Z, H2A-BDB, and MacroH2A. Histone H2B, which is second highly conserved after H4, has only one known variant, TSH2B. Histone H3 has eight known variants H3.1, H3.2, H3.3, H3.4, H3.5, H3.X, H3.Y, and CENP-A⁷³.

A large number of histone PTMs has been reported. Figure 1.11 shows PTMs that occur in canonical histones²⁹. Aside from these PTMs, there are PTMs that also happen in different subtypes. Therefore, the number of PTMs and their functional configurations are still a mystery. Each of these modifications has distinct purposes and is responsible for the different chromatin configurations which characterize the different stages in DDR.

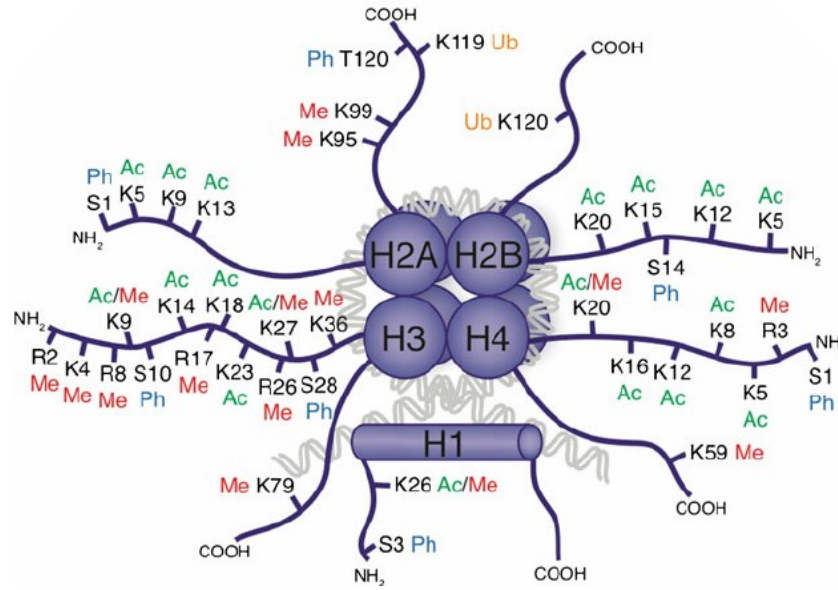


Figure 1.11 Currently Identified Post Translational Modifications on Canonical Histones. Adapted from “Epigenetics Components of Aging in the Central Nervous System,” by Y. Q. Zhao, K. Jordan, V. V. Lunyak, 2013, *Neurotherapeutics*, 10(4), 647-663. Copyright 2013 by The American Society for Experimental NeuroTherapeutics, Inc. Reprinted with permission.

Post-translational modifications found on canonical histones are responsible for chromatin remodeling. Each of these modifications serves different purposes either solo or in combination with other modifications (Ac = Acetylation, Ph = Phosphorylation, Me = Methylation, Ub =Ubiquitination) ⁷³.

Table 1.1: Different histone variants and their specifications. Adapted from “Every amino acid matters: essential contributions of histone variants to mammalian development and disease,” by I. Maze, K. Noh, A. A. Soshnev, C.D. Allis, 2014). *Nature Reviews Genetics* 15, 259–271. Copyright 2018 by Macmillan Publishers limited, part of Springer Nature. Reprinted with permission.

This table outlines the histone variants, their redundancies, expression dependencies, localizations, functions, and knockout phenotypes.

Histone	Number of gene copies	Cell-cycle expression	Location	Function	Knockout phenotype
H2A	15	RD	Throughout the genome	Core histone	ND
H2A.X	1	RI	Throughout the genome	DNA repair (mediated by the phosphorylated form γ H2A.X) and genome integrity	Male infertility (that is, defects in sperm meiosis) in mice
H2A.Z	2	RI	Throughout the genome	Gene activation, gene silencing and chromosome segregation	Embryonic lethality in H2A.Z.1-knockout mice at E4.5–E7.5
MacroH2A	2	Possibly RI	Inactive X chromosome	Gene silencing	Brain malformation in zebrafish
H2A.Bbd	3	RI	Active X chromosome and euchromatin	Active transcription	ND
H2B	17	RD	Throughout the genome	Core histone	ND
TSH2B	1	Possibly RI	Throughout the sperm genome and in telomeres of somatic cells	Chromatin-to-nucleoprotamine transition	ND
H2BFWT	1	Possibly RI	Primate telomeres in sperm	ND	ND, as there is no gene product in mice
H2BE	1	RI	Throughout the genome of olfactory neurons	ND	Overexpression of olfactory receptor in mice
H3.1	10	RD	Throughout the genome	Core histone	ND
H3.2	3	RD	Throughout the genome	Core histone	ND
H3.3	2	RD and RI	Throughout the genome	Gene activation, silencing and chromosome segregation	ND; adult infertility in H3.3A-gene-trap and H3.3B-knockout mice
H3.4	1	RI	Sperm genome and nucleolus of somatic cells	ND	ND
H3.5	1	Possibly RI	Euchromatin in hominid testis	ND	ND, as there is no gene product in mice
H3.X and H3.Y	1 of each	Possibly RI	Euchromatin in primates	ND	ND, as there is no gene product in mice
CENP-A	1	RI	Centromeres	Chromosome segregation	Embryonic lethality at E3.5–E8.5 in mice
H4	14	RD	Throughout the genome	Core histone	ND

CENP-A, histone H3-like centromeric protein A; E, embryonic day; H2BFWT, histone H2B type W-T; ND, not determined; RD, replication dependent; RI, replication independent.

1.5 H2A.X to γ H2A.X

H2A.X is a variant of H2A family. It is highly similar to canonical H2A in terms of sequence except for the C-terminal region (Figure 1.12). H2A.X has some more amino acids at the carboxyl-terminal that can be post-translationally modified to provide diverse cellular signals specific to DSB repair. The content of H2A.X is cell and tissue-specific, ranging from 2 to 25% of total H2A³⁰.

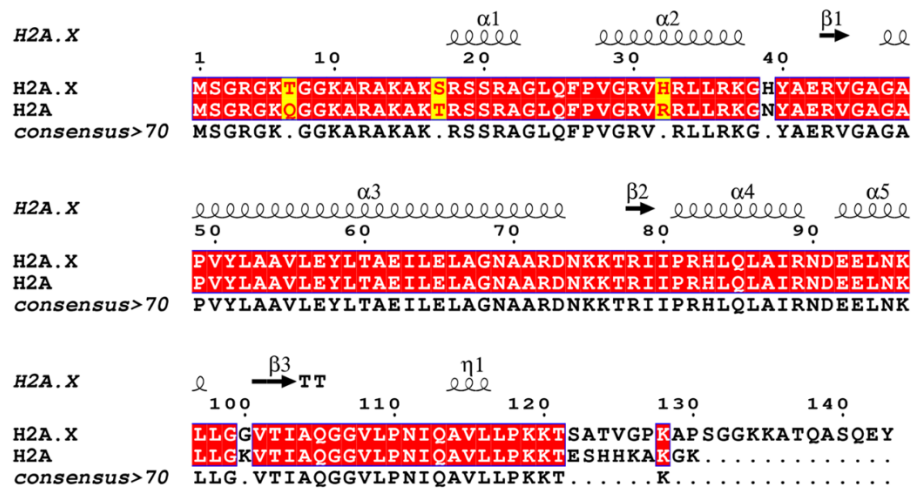


Figure 1.12 Sequence Alignment and Secondary Structure Prediction between Canonical H2A and Variant H2A.X

The core sequences are highly similar between H2A and H2A.X. The sequences differ at C-terminal region after residue 120, and this is the basis of functional differences between H2A and H2A.X³¹.

Upon DSB, H2A.X is phosphorylated at serine 139 residue. This phosphorylated H2A.X is called gamma-H2A.X (γ H2A.X). γ H2A.X is a well-established hallmark for DSBs as the other types of DNA injuries do not produce γ H2A.X^{32, 33, 34}. On the other hand, cellular or extracellular incidents that lead to DSB formation lead to the γ H2A.X formation (Figure 1.13)³⁵.

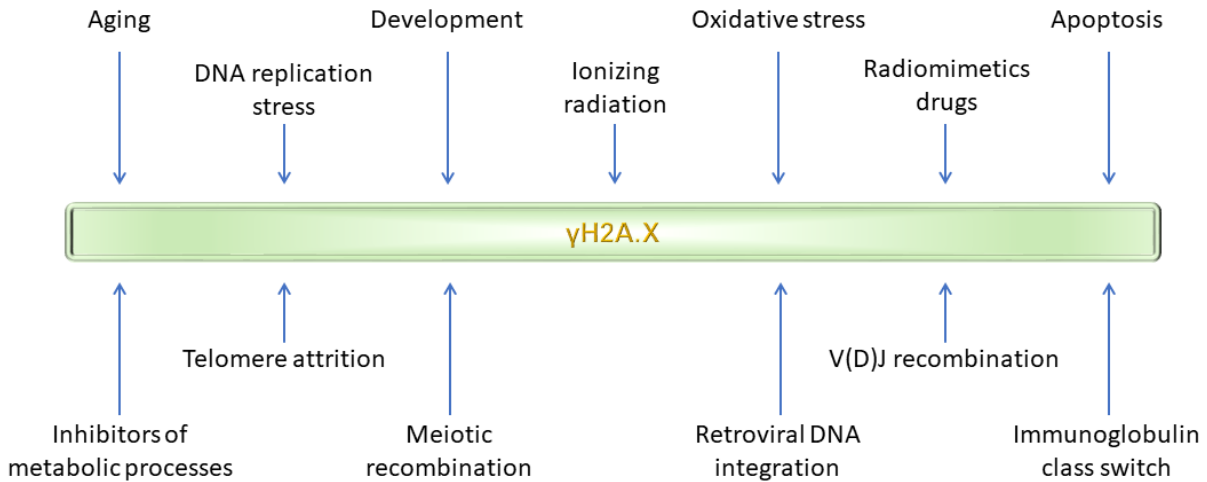


Figure 1.13 Various DSB Sources that Lead to γ H2A.X Formation. Adapted from “Genome Instability and γ H2AX”, by A. Georgoulis, C. E. Vorgias, G. P. Chrousos, and E. P. Rogakou, 2017, *International Journal of Molecular Science*, 18(9), p. 1979. Licensed under CC BY 4.0.

This figure shows multiple sources of DNA double-strand break (DSB) damage. All these incidents can lead to the formation of γ H2A.X

In order to carry out successful repair of DSB lesions, either H2A or H2A.X or both undergo extensive PTMs. Phosphorylation at tyrosine 142 residue of H2A.X determines whether cell proceeds towards apoptosis pathway, while phosphorylation at serine 139 residue and ubiquitination of various lysine residues (13, 15 or 119) determines whether a cell would try to repair the DNA (Figure 1.14) ⁵⁸.

γ H2A.X is a hallmark for DSB. Formation of it is imperative for the cell to execute other downstream activity involved in DSB repair pathways. γ H2A.X^{-/-} mice show pleiotropic phenotypes related to genomic instability, defects in repair processes, and compromised recruitment of other downstream DDR proteins to the site of DNA damage ³⁶.

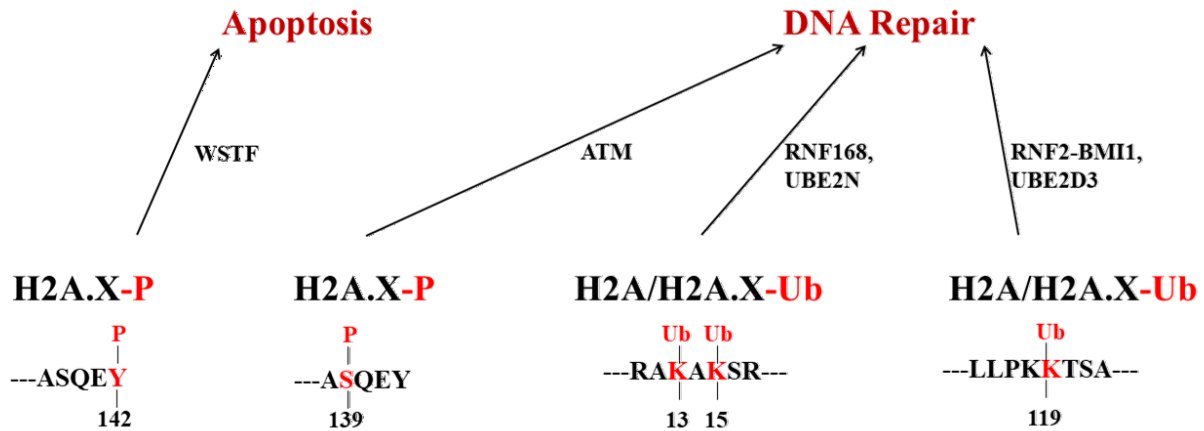


Figure 1.14 PTMs on H2A/H2A.X

Different PTMs or combination of PTMs on H2A/H2A.X determine different fate upon DSB. WSTF (William syndrome transcription factor) constitutively phosphorylates Y142 of H2A.X, while ATM (ataxia-telangiectasia mutated) phosphorylates S139 of H2A.X upon DSB, and decides if the cell should move on to the DNA repair pathway or the apoptotic pathway depending on the presence of pY142. Additionally, ubiquitination of K13/K15 by RNF168-UBE2N and K119 by RNF2-BMI1-UBE2D3 determine whether the repair would carry out through HR or NHEJ pathway.

Upon DSB, the S139 at SQ motif of H2A.X is phosphorylated by phosphatidylinositol 3 family kinases, namely ATM (Ataxia-telangiectasia mutated), ATR (ATM-Rad3 related) or DNA-PK (DNA dependent protein kinase)^{37,38}. ATM is the main kinase that reacts promptly with DSB. However, other kinases would also phosphorylate H2A.X if ATM activity is compromised or reduced³⁹. In fact, ATR is the major kinase for γ H2A.X creation at replication arrest^{40,41}. Aside from these kinases, γ H2A.X is created by other kinases in various other cellular events, for example, Apoptosis⁴².

1.6 The Defenders of the Genome: Formation of IRIF

DSB induced by IR causes the formation of γ H2A.X spanning megabases of chromatin. γ H2A.X acts as a signal amplifier and helps hundreds of DDR proteins to accumulate near the site of DNA lesion forming nuclear foci called ionizing radiation-induced foci (IRIF)⁴³. γ H2A.X is pervasive at all the stages of the cell cycle after DSB and recruits other downstream DDR mediator and effector proteins at the site of DSB at different cell cycles. The role of accumulated DDR proteins and their overall organization in IRIF are still not understood⁴⁴. However, studies have shown that all these proteins have crucial significance in conducting successful repair mechanisms.

Upon DSB, a number of proteins co-localizes with γ H2A.X, therefore, contributes to the formation of IRIF⁴⁵. P-ATM, which is the activated ATM, co-localizes with γ H2A.X, and takes part in phosphorylating other DDR proteins. Mre11 (meiotic recombination 11 homolog), Rad50 (radiation sensitive 50), are proteins that maintain telomere integrity and meiosis, are also found in the IRIF region⁴⁶. Nbs1 (Nijmegen breakage syndrome protein 1) is a major cell cycle checkpoint protein that as well is found in the same site as IRIF⁴⁷. Mre11, Rad 50, Nbs1 form a complex called MRN complex that tethers broken DNA ends, and is also required for direct activation of ATM^{48,49}.

E3 ubiquitin ligases, RNF8 (Ring finger like 8) and RNF168 (Ring finger like 168) also co-localize with γ H2A.X induced foci^{50,51}, respectively. RNF8 ubiquitinates linker histone, H1 through lysine 63 (K63) linked poly-ubiquitination that acts as a substrate for RNF168⁵². Docked RNF168 on poly-ubiquitinated H1 (poly-ub-K63-H1) mono-ubiquitinates H2A and H2A.X through K63 linked poly-ubiquitination via E2 ubiquitin ligase UBE2N, which provides subsequent docking sites for more RNF168 to amplify the ubiquitination signal in the DDR pathway⁵³. RNF168 also poly-ubiquitinates H2A and H2A.X through lysine 27 (K27) linked

ubiquitination, which is a result of auto-ubiquitination and auto-selectivity nature of RNF168. This ubiquitination phenomenon has been proven crucial for the subsequent recruitment of the downstream effector proteins like BRCA1 (Breast Cancer Associated 1) for HR, or TP53BP1 (Tumor suppressor P53 binding protein 1) for NHEJ repair pathway ⁵⁴.

Not only these proteins but lots of other proteins involved in DSB repair pathway show co-localization with γ H2A.X. However, after pATM phosphorylates the S139 residue at H2A.X, the very first mediator protein that interacts with pS139 via a tandem BRCT domain is MDC1 (Mediator of DNA Damage Check Point 1) in order to provide a docking site for other downstream proteins. MDC1 is the first in sequence to create the supramolecular complex that spans through megabases of DNA. Therefore, MDC1 also co-localizes with γ H2A.X upon DSB ⁵⁵, and the absence of MDC1 hinders the downstream ubiquitination activity as RNF8 needs to interact with MDC1 to locate itself at the foci ⁵⁰.

1.7 Treating or Terminating: Di-phosphorylation of H2A.X

Aside from S139 phosphorylation that happens as a response to DSB, H2A.X has a tyrosine 142 residue, that is constitutively phosphorylated by an unusual tyrosine kinase namely WSTF (William Syndrome Transcription Factor) ⁵⁶. Upon DSB, when ATM phosphorylates S139, both pS139 and pY142 are recognized by a pair of tandem BRCT domain of MCPH1 (Microcephalin 1) ⁵⁷. MCPH1 mediates the recruitment of pro-apoptotic kinase, JNK1 (JUN amino-terminal kinase 1), and directs cell towards apoptotic pathway ⁵⁸.

pY142 prevents MDC1 from binding the epitope pS139 of γ H2A.X ⁵⁶, but as DSB happens, Y142 gradually gets dephosphorylated by Eya1 (Eye absent 1) and Eya3 (Eye absent 3) ⁶⁰. As a result, MDC1 can bind to pS139, and carry out the repair pathway.

1.8 Summary of the DSB Repair Initiation

Upon DSB, MRN complex binds the lesions, and activates ATM kinase. ATM kinase then phosphorylates S139 and creates γ H2A.X. pS139 and Constitutively phosphorylated pY142 are recognized by MCPH1 with its two tandem BRCT domains. MCPH1 falls off as Eya1 or Eya3 dephosphorylates the Y142 residue, and helps the cell to proceed forward with the repair process rather than the self-termination process. MDC1 with its tandem BRCT domain then interacts with the γ H2A.X. ATM also phosphorylates FHA domain of MDC1, which is recognized by E3 ubiquitin ligase RNF8. RNF8 in conjunction with Ubc13/UBE2N poly-ubiquitinates linker histone, H1 through K63 linked ubiquitination. This poly-ubiquitinated chain is recognized by RNF168. RNF168 in conjunction with Ubc13/UBE2N monoubiquitinates K13 or K15 of H2A.X. This ubiquitination cascade eventually leads to the recruitment of other effector proteins to repair the injured DNA ^{63, 74}.

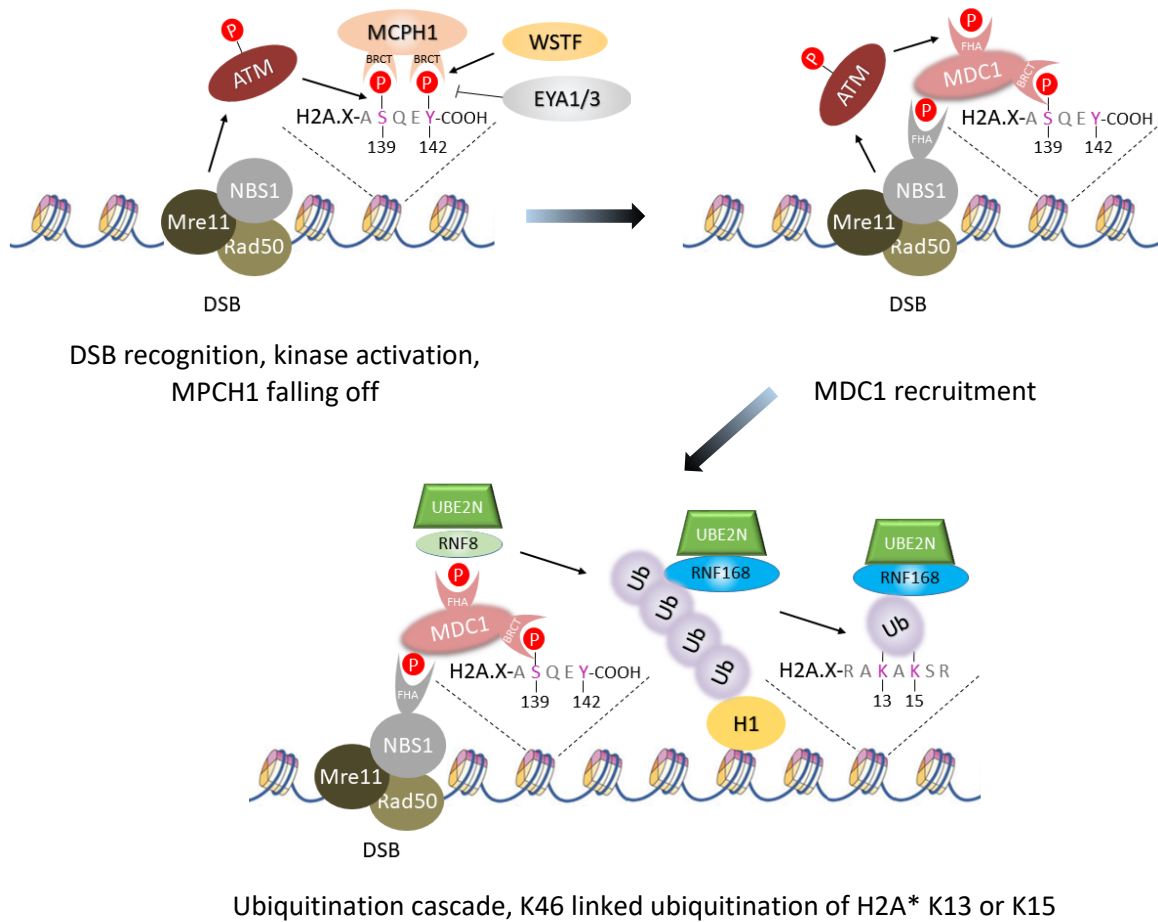


Figure 1.15 A Predicted Schematic Diagram of Initial DSB Response.

Upon creation of γ H2A.X, MDC1 binds the pS139 and mediates the downstream ubiquitination events through providing a docking site for UBE2N-RNF8 complex⁶³. (* can either be H2A or H2A.X)

1.9 MDC1 Independent Ubiquitination

MDC1 recruitment is crucial for RNF8 mediated ubiquitination. However, another different E3 ubiquitin ligase, Polycomb complex protein BMI1 (B cell-specific Moloney murine leukemia virus integration site 1) in complex with RNF2 (Ring finger like 2) mono-ubiquitinates lysine 119 (K119) of H2A or H2A.X (Figure 1.16); this mono-ubiquitination is imperative for successful repair of DSB ⁶⁴. BMI1 is found in IRIF, and the recruitment of BMI1 is independent of MDC1- γ H2A.X interaction ⁶⁵.

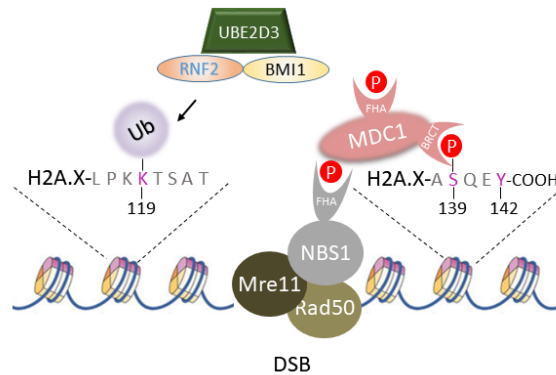


Figure 1.16 Schematic diagram of BMI1-RNF2 mediated mono-ubiquitination

BMI1-RNF2 mono-ubiquitinates K119 of H2A.X upon DSB. This ubiquitination is independent of MDC1- γ H2A.X interaction.

Now we know that there are two different nucleosome ubiquitination pathways that are involved in the DSB repair mechanism. What we do not know is whether these ubiquitinations happen on the same nucleosome docking MDC1 or different nucleosomes juxtaposing the MDC1 interacting nucleosomes.

1.10 Structure of MDC1 BRCT Bound γ H2A.X Tail

Since MDC1 is one of the major players in the DSB repair pathway, understanding how MDC1 interacts with the phosphopeptide tail would reveal some mystery associated with the downstream applications. Therefore, researchers crystallized MDC1 BRCT bound γ H2A.X phosphopeptide tail to elucidate the organizational behavior of this interaction (Figure 1.17 A) ⁵⁵.

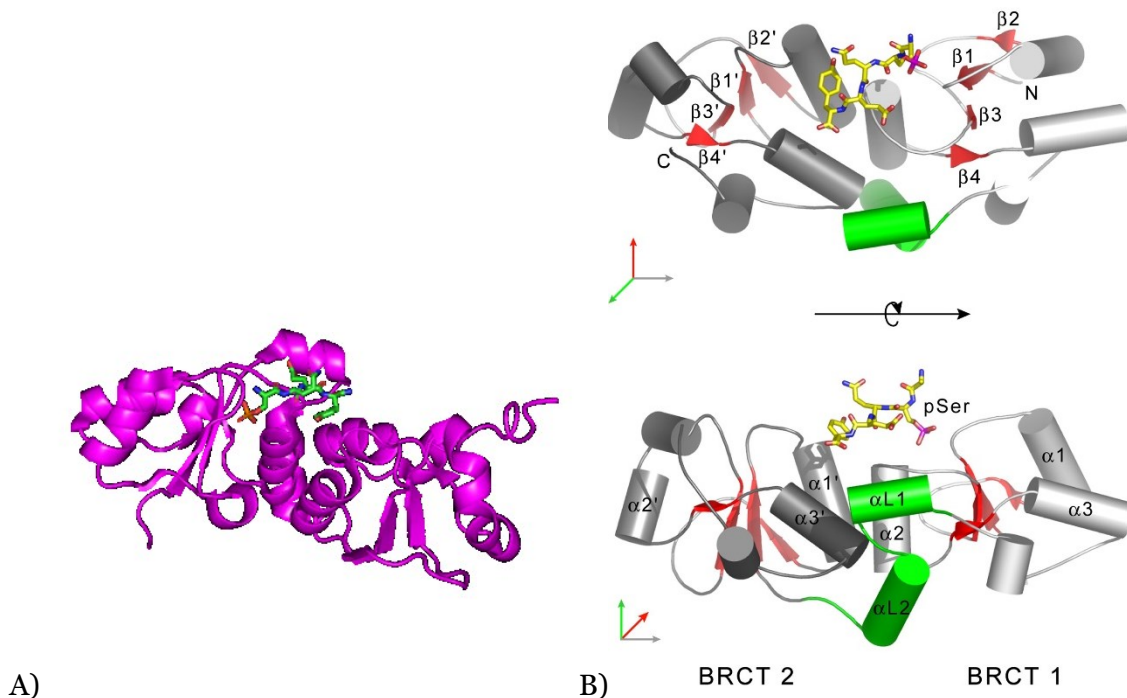


Figure 1.17 Structural basis of the interaction between the MDC1 tandem BRCT domain and γ H2A.X phosphopeptide tail. Adapted from “MDC1 Directly Binds Phosphorylated Histone H2AX to Regulate Cellular Responses to DNA Double-Strand Breaks” by M. Stucki, J. A. Clapperton, D. Mohammed, M. B. Yaffe, S. J. Smerdon, S. P. Jackson, 2005, *Cell*, 123(7), Copyright 2018 by Elsevier Inc. Reprinted with permission.

A) Crystal structure of MDC1 tandem BRCT bound γ H2A.X phosphopeptide tail (PDB-2AZM).
B) Schematic interaction diagram. Each BRCT repeat has three helices, and four beta strand connected by loops, as well as one helix strand helix motif at the C-terminal. γ H2A.X peptide tail sits between the furrow of the two BRCT repeat contact point ⁵⁵.

A typical tandem BRCT fold has two BRCT repeats. Each repeat has a compact α/β connected with a linker region. $\alpha 2$ of BRCT1 interacts with an $\alpha 1'/\alpha 3'$ loop of BRCT2. The helix-

loop-helix folds (α L1 and α L2) both interact at the BRCT interface. γ H2A.X binds between the groove at the contact point between the two BRCT repeats. It interacts with β 1/ α 1 loop and the N-terminal ends of α 2 and α 1' (Figure 1.17 B) ⁵⁵. There is a not highly basic region observed in human MDC1 BRCT (Figure 1.18).

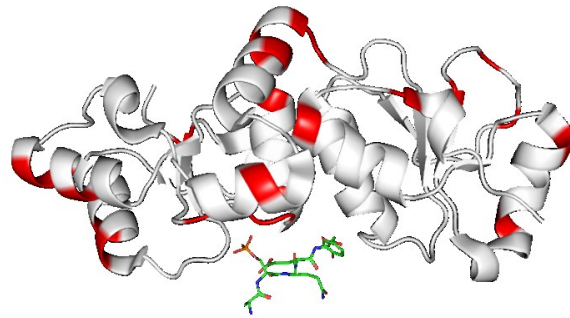


Figure 1.18 Basic region in human MDC1 BRCT domain.

The basic region in human BRCT domain is marked in red.

1.11 Aim to Attain: Research Questions & Hypothesis

The crystal structure of MDC1 tandem BRCT domain bound γ H2A.X tail tells us the tale of how the BRCT domain interacts with a small peptide and folds accordingly. However, in the cell, it is not a single γ H2A.X peptide tail that interacts with the MDC1 BRCT domain. In fact, MDC1 interacts with the overall nucleosome at the damage lesion and helps in forming the nuclear foci. Therefore, the interaction of MDC1 with this small peptide does not tell us how MDC1 positions itself in terms of the overall nucleosome, how the nucleosome remodels itself upon binding with MDC1, how MDC1 positioning affects the formation of IRIF, and the downstream applications like ubiquitination.

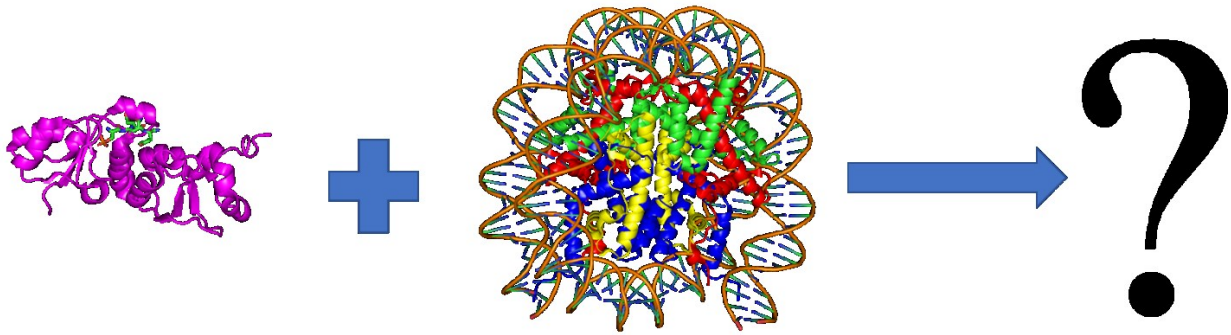


Figure 1.18 Hypothetical question of how MDC1 BRCT is interacting with the complete nucleosome.

Here we hypothesize that MDC1 BRCT domain not only binds to the phosphorylated γ H2A.X tail, but this interaction might position MDC1 in a way that its basic patch might interact with the nucleosomal DNA or with the conserved acidic patch of H2A.X/H2B.

To test this hypothesis *in vitro*, a successful purification and assembly of γ H2A.X containing nucleosome is the prerequisite. Previously, histones were extracted from the cell lysate using urea denaturant followed by extensive dialysis to refold the heteromeric histone complexes. This method is cost, and time intensive. Here we have established and contrasted two rapid purification protocols using the co-expression systems for the recombinant human histone oligomers. Moreover, we have also developed a system for the *in vitro* phosphorylation of H2A.X that will facilitate the structural analysis of MDC1 BRCT bound γ H2A.X nucleosome complex.

Materials & Methods

2.1 Site-Directed Mutagenesis of H2A.X

For our studies, *in vitro* enzymatic phosphorylation of S139 is necessary to produce sufficient amount of γ H2A.X. Inside the cell, ATM kinase phosphorylates S139 of H2A.X upon DSB. However, large-scale purification of ATM kinase is problematic because it is a large protein of 350.7 kDa. Moreover, the activity of ATM kinase is not well defined.

We have decided to use GST tagged casein kinase II alpha subunit (GST-CK2 α) to phosphorylate S139 of H2A.X. Therefore, we mutagenized the C-terminal tail of H2A.X with a CK2 recognition motif in order to produce modified γ H2A.X (Figure 2.1). To have a control for our kinase assay, we introduced an alanine mutation at S139 residue of CK2 α recognition site mutagenized H2A.X. From now on, we will refer S139 and A139 containing CK2 recognition site modified H2A.X as H2A.X(CK2-S) and H2A.X (CK2-A).

CK2 requires some acidic patches flanking the S/T residue in order to bind and phosphorylate the S/T successfully, and studies showed that it requires a negatively charged residue at +3 position (Figure 2.1) ⁶⁷. Due to that, we decided to change A138 (-1) and Q140 (+1) residues into D, and E respectively; however, if we introduce A138D (-1), T136 (-3) becomes a potential unwanted substrate for CK2. Therefore, we introduced T136E (-3) in order to prevent the unwanted phosphorylation and to provide a more negative patch for CK2 to bind the H2A.X tail (Figure 2.1). These changes were incorporated in-frame to the open reading frame (ORF) of H2A.X through designing a reverse primer that contains all the appropriate mutations (Appendix i-Table i-1).

Due to expression inconsistencies, each histone was re-cloned into the pET47b(+) (Novagen-Cat. # 71461-3) vector with an N-terminal Human Rhinovirus (HRV) 3C Protease cleavable hexahistidine tag. These pET47b(+)-Histone constructs were used for traditional refolding purification of histones.

To co-express histone pairs, we have used different duet vectors, namely, pETDuet-1 (Novagen-Cat. # 71146-3), pACYCDuet-1 (Novagen-Cat. # 71147-3), and pCDFDuet-1 (Novagen-Cat # 71340-3). These vectors have two multiple cloning sites (MCSs). Each MCS has its own inducible T7 promoter. One of the MCSs has an N-terminal hexahistidine tag, while the other one does not. We introduced a Tobacco Etch Virus (TEV) Protease cleavage site with the histone that was cloned into the tagged MCS (Appendix i Table i-1).

In order to clone, we needed to introduce two different restriction sites at the ends of the histone fragments, so that particular restriction enzymes (REs) (Appendix i Table i-1) could generate two asymmetric sticky ends flanking the fragment. These asymmetric sticky ends would allow the fragment to be ligated in the vector with the right direction. These restriction sites were incorporated through PCR reaction using appropriate primers. We designed multiple sets of primers using Serial Cloner 2.6 software to confirm the presence of ORF without any frameshift mutation. The primers were further checked and ordered using OligoAnalyzer Tool from Integrated DNA Technologies (IDT) (Appendix i Table i-1). The ordered primer was processed upon arrival following the instructions on the specification paper provided by IDT with the primer package.

In order to incorporate the restriction endonuclease sites at both the ends of histone DNA sequence, PCR reaction was performed using the appropriate set of primers (Appendix ii protocol 1). After PCR Clean up (Appendix ii Protocol 3), double restriction digest reaction was performed

on both the vector and the insert (Appendix ii Protocol 4). The digested insert was ligated with the digested vector. The directionality of the ligated insert was ensured by the asymmetric sticky ends that were present at both the ends of the insert (Appendix ii Protocol 5). After transforming the recombinant construct into the DH5 α cell, the positive colonies were checked using colony PCR method (Appendix ii Protocol 6).

During the time of PCR reaction, spontaneous mutation can happen in the desired insert fragment. So, the recombinant vectors were sent for sequencing (Appendix ii Protocol 9).

2.3 Overexpression of protein

In order to figure out which bacterial cell line expresses our protein of interest at the optimal temperature and within the optimal time, we transformed different bacterial cells with the different recombinant constructs (Table 2.2) and performed small-scale overexpression check (Appendix ii Protocol 10).

Table 2.2 List of the Recombinant Constructs with Their Respective Overexpression Cell lines. (green – confirmed for larger scale production)

Recombinant Construct	Cell lines used	Temperature tested
pET47b(+)-H2A.X	BL21(DE3)	37°C
pET47b(+)-H2B	BL21(DE3)	37°C
pET47b(+)-H3.1	BL21(DE3)	37°C
pET47b(+)-H4	BL21(DE3)	37°C
pETDuet-TEV-H2B-H2A	C41(DE3), Rosetta 2, Rosetta 2(DE3)	18°C, 30°C, 37°C
pETDuet-1-TEV-H2A.X-H2B	Rosetta 2(DE3)	18°C, 30°C, 37°C
pCDFDuet-1-TEV-H3.1-H4	BL21(DE3), BL21(DE3) pLysS, Rosetta 2, Rosetta 2(DE3)	18°C, 30°C
pACYCDuet-1-TEV-H4-H3.1	C41(DE3), C43(DE3), BL21(DE3)	18°C, 30°C, 37°C
pETDuet -1-TEV-H2A.X-H2B + pCDFDuet-1-His-H3.1-H4	Rosetta 2(DE3)	24°C, 30°C
pETDuet-1-TEV-H2A.X-H2B pACYCDuet-1-TEV-H4-H3.1	BL21(DE3)	30°C

2.4 Purification of the Octamer

We have developed three methods for the extraction of the human histone oligomer complexes using bacterial expression system. The first one is the modified version of the traditional refolding method for the oligomer purification which is based on the *in vitro* folding of the four histones to reconstitute the heteromeric oligomers. The second and the third methods involve co-purification of different histone oligomers where histone pairs are folded *in vivo* to give rise to soluble complexes.

2.4.1 Modified Refolding of the Octamer

Here we combined and modified the nucleosome purification methods from Lugar et al. 1999⁷⁷ and Tanaka et al. 2004⁷⁸. (Detailed protocol is written in Appendix II-Protocol 13)

Overexpression of the recombinant single histones

pET47b(+)-Histone plasmids transformed BL21(DE3) were grown in 500ml Kanamycin containing LB medium at 37°C for 16 hours. 50ml of pre-inoculum was transferred into 1L Kanamycin containing LB medium and was grown at 37°C. At OD₆₀₀ = 0.6, the culture was induced with 1mM IPTG to overexpress the histone proteins for 5 hours. Cells were harvested and stored at -80°C for future use.

Purification of histone

4L cells were resuspended in 40ml buffer A containing 100µl protease inhibitor cocktail (Cat #. P8849), 1mM PMSF, 0.1g lysozyme. Cells were lysed using sonicator or emulsiflex cell disruptor. The lysate was spun down at 17,000 RPM for 20 minutes at 4°C. Discard the supernatant containing all the soluble protein fractions. The inclusion body containing histone was resuspended

in 40ml buffer B containing 6M urea. The resuspended suspension was spun down at 17,000 RPM for 45 minutes at 4°C. The supernatant was collected and incubated with 5ml Ni²⁺ resins for 2 hours. After 2 hours, the beads were loaded on a column and flow through was collected. The beads were washed with 250ml buffer C containing 10mM imidazole. Followed by this, the Ni²⁺ bound histone was eluted out using 5ml of buffer D containing 300mM imidazole until the Bradford assay gave a negative result. The fractions were run on a 16% SDS PAGE.

Formation of the H2A.X-H2B dimer

Purified H2A.X and H2B were mixed in the equimolar ratio at a concentration of 5mg/ml in a dialysis bag of 8,000 kDa cutoff, and an appropriate amount of protease inhibitor cocktail was added (100µl/50ml), and the mixture was dialyzed in 1L buffer E for 12 hours at 4°C. After 12 hours, the mixture was dialyzed in buffer F at 4°C for another 12 hours with two rounds of buffer exchange. If no precipitation was observed, then the mixture was dialyzed further with buffer G for 2 hours, and with buffer H for another 2 hours at 4°C. Following this, the mixture was dialyzed for either 2 hours or 16 hours in buffer I. The solution was concentrated using Amicon Ultra-15 Centrifugal Filter Unit NMWL 10 with mixing for every 15 minutes. The concentrated solution was loaded on the Superdex 200 16 60 size exclusion column equilibrated in buffer I. The dimer peak fractions around the 82ml region were collected and stored at -80°C after concentrating for future use.

Formation of the (H3.1-H4)₂ tetramer

Purified H3.1 and H4 were mixed in the equimolar ratio at a concentration of 5mg/ml in a dialysis bag of 8,000 kDa cutoff, and an appropriate amount of protease inhibitor cocktail was added (100µl/50ml). The mixture was dialyzed in 1L buffer E for 12 hours at 4°C. After 12 hours,

the mixture was dialyzed in buffer F at 4°C for another 12 hours with two rounds of buffer exchange. (The lower salt dialysis for tetramer is tricky and should only be performed if H3.1 and H4 were purified using ion exchange column after the Ni²⁺ column purification.) The solution was concentrated using Amicon Ultra-15 Centrifugal Filter Unit NMWL 30 with mixing for every 15 minutes. The concentrated solution was loaded on the Superdex 200 16 60 size exclusion column equilibrated in buffer F. The tetramer peak fractions around the 72ml region were collected and stored at -80°C after concentrating for future use.

Formation of the (H2A.X-H2B-H3.1-H4)₂ octamer

The dimer and the tetramer were mixed in 2.5:1 molar ratio at a concentration of 5mg/ml. The mixture was dialyzed for 24 hours in buffer F at 4°C with at least 2 rounds of buffer exchange. (At this point, the salt concentration can be gradually brought down to 250mM). The octamer was concentrated using Amicon Ultra-15 Centrifugal Filter Unit NMWL 10 with mixing after every 10 minutes. The concentrated octamer was loaded on a Superdex 300 16 60 analytical size exclusion column equilibrated with the buffer used in the very last dialysis step. The octamer peak fractions around the 12ml region were collected and stored at -80°C after concentrating for future use.

2.4.2 One-step Purification of the Dimer and the Tetramer

Here we have developed a quick purification protocol for each histone oligomers (Detailed protocol is written in Appendix ii-Protocol 14).

Separate Overexpression of the Histone Pairs

pETDuet-1-(His)₆-TEV-H2A.X-H2B plasmid transformed Rosetta 2(DE3) was grown in 500ml Ampicillin and Chloramphenicol containing TB medium at 37°C for 16 hours. 50ml of pre-

inoculum was transferred into 1L Ampicillin, and Chloramphenicol added TB medium and was grown at 37°C. At OD₆₀₀ = 0.8-1, the culture was induced with 1mM IPTG to overexpress the histone dimer for 7 hours at 30°C. Cells were harvested and stored at -80°C for future use.

pACYCDuet-1-(His)₆-TEV-H4-H3.1 plasmid transformed BL21(DE3) was grown in 500ml chloramphenicol containing TB medium at 37°C for 16 hours. 50ml of pre-inoculum was transferred into 1L chloramphenicol containing TB medium and was grown at 37°C. At OD₆₀₀ = 0.8-1, the culture was induced with 1mM IPTG to overexpress the histone tetramer for 7 hours at 30°C. Cells were harvested and stored at -80°C for future use.

Purification of the H2A.X-H2B dimer

4L cells were resuspended in 120ml buffer L containing protease inhibitor cocktail (100µl/50ml), 1mM PMSF, 0.1g lysozyme. Cells were lysed using the emulsiflex cell disruptor. The lysate was spun down at 17,000 RPM for 45 minutes at 4°C. The supernatant was collected and incubated with 15ml Ni²⁺ resins for 2 hours. After 2 hours, the beads were loaded on a column, and the flow-through was collected. The beads were washed with 250ml buffer W containing 30mM imidazole. Followed by this, the Ni²⁺ bound dimer was eluted out in a successive 5ml fractions using buffer E1 containing 100mM imidazole, E2 containing 250mM imidazole, buffer E3 containing 500mM imidazole, buffer E4 containing 1M imidazole, and buffer E5 containing 2M imidazole. The fractions were run on a 16% SDS PAGE.

The purest fractions were combined and concentrated using Amicon Ultra-15 Centrifugal Filter Unit NMWL 10 with mixing after every 10 minutes. The concentrated dimer was loaded on Superdex 200 16 60 size exclusion column pre-equilibrated with buffer S. The dimer fractions around 82ml peak were collected and stored at -80°C after concentrating for further use.

Purification of the (H3.1-H4)₂ tetramer

4L cells were resuspended in 120ml buffer L containing protease inhibitor cocktail (100µl/50ml), 1mM PMSF, 0.1g lysozyme. Cells were lysed using the emulsiflex cell disruptor. The lysate was spun down at 17,000 RPM for 45 minutes at 4°C. The supernatant was collected and incubated with 15ml Ni²⁺ resins for 2 hours. After 2 hours, the beads were loaded on a column and flow-through was collected. The beads were washed two times with 250ml buffer W containing 30mM imidazole. Followed by this, the Ni²⁺ bound tetramer was eluted out in a successive 5ml fractions using buffer E1 containing 100mM imidazole, buffer E2 containing 250mM imidazole, buffer E3 containing 500mM imidazole, buffer E4 containing 1M imidazole, and buffer E5 containing 2M imidazole. The fractions were run on a 16% SDS PAGE.

The purest fractions were combined and concentrated using Amicon Ultra-15 Centrifugal Filter Unit NMWL 50 with mixing after every 10 minutes. The concentrated tetramer was loaded on Superdex 200 16 60 size exclusion column pre-equilibrated with buffer S. The tetramer fractions around 76ml peak were collected and stored at -80°C after concentrating for further use.

Formation of the (H2A.X-H2B-H3.1-H4)₂ octamer

The dimer and the tetramer were mixed in 2.5:1 molar ratio at a concentration of 5mg/ml. The mixture was dialyzed for 24 hours in buffer S at 4°C with at least two rounds of buffer exchange. (At this point, the salt concentration can be gradually brought down to 250mM). The octamer was concentrated using Amicon Ultra-15 Centrifugal Filter Unit NMWL 10 with mixing after every 10 minutes. The concentrated octamer was loaded on a Superdex 200 10 300 analytical size exclusion column pre-equilibrated with the buffer used in the very last dialysis step. The

octamer peak fractions around the 12ml region were collected and stored at -80°C after concentrating for future use.

2.4.3 One-step Purification of the Octamer

Here we have developed a quick purification protocol for the complete octamer (Detailed protocol is written in Appendix ii-Protocol 15).

Combined Overexpression of the Histone Pairs

[pETDuet-1-(His)₆-TEV-H2A.X-H2B+pCDFDuet-1-(His)₆-TEV-H3.1-H4] transformed Rosetta 2(DE3) was grown in 500ml Ampicillin, streptomycin, and chloramphenicol containing TB medium at 37°C for 16 hours. 50ml of pre-inoculum was transferred into 1L Ampicillin, streptomycin, and chloramphenicol containing TB medium and was grown at 37°C . At $\text{OD}_{600} = 0.8-1$, the culture was induced with 1mM IPTG to overexpress the all four histones for 7 hours at 30°C . Cells were harvested and stored at -80°C for future use.

Purification of the (H2A.X-H2B-H3.1-H4)₂ octamer

4L cells were resuspended in 120ml buffer L containing protease inhibitor (100 μl /50ml), 1mM PMSF, 0.1g lysozyme. Cells were lysed using emulsiflex cell disruptor. The lysate was spun down at 17,000 RPM for 45 minutes at 4°C . The supernatant was collected and incubated with 15ml Ni^{2+} resins for 2 hours. After 2 hours, the beads were loaded on a column and flow through was collected. The beads were washed two times with 250ml buffer W containing 30mM imidazole. Followed by this, the Ni^{2+} bound octamer, tetramer and dimer were eluted out in a successive 5ml fractions using buffer E1 containing 100mM imidazole, buffer E2 containing 250mM imidazole, buffer E3 containing 500mM imidazole, buffer E4 containing 1M imidazole, and buffer E5 containing 2M imidazole. The fractions were run on a 16% SDS PAGE.

The purest fractions were combined and concentrated using Amicon Ultra-15 Centrifugal Filter Unit NMWL 10 with mixing after every 10 minutes. The concentrated tetramer was loaded on Superdex 200 16 60 size exclusion column pre-equilibrated with buffer S. The octamer fractions around 44ml peak were collected and concentrated to reload on a Superdex 200 10 300 column pre-equilibrated in buffer S. The octamer fractions around 12ml peak was collected and stored at -80°C after concentrating for future use.

2.5 *In Vitro* Phosphorylation of the H2A.X-H2B Dimer

We set up a system in order to produce γ H2A.X through *in vitro* kinase assay (Detailed protocol is written in Appendix ii- protocol 16). 20 molar of the dimer was mixed with 1 molar of the CK2 in a total reaction volume of 50 μ l containing 1x kinase buffer and 1mM ATP (γ ATP is 1/300 times diluted). The reaction mix was incubated at 30°C for 30 minutes. The sample was collected after every 10 minutes, and the reaction was quenched using 4x SDS buffer. After 30 minutes, the samples were run on a 16% SDS PAGE gel. The gel was wrapped with Saran wrap and placed on a phosphorscreen cassette. The pre-equilibrated phosphorscreen film was placed on top of the gel. The cassette was closed and incubated for 24 hours at room temperature. After that, the phosphorscreen was developed using typhoon scanner from Dr. Fhalmen's lab. X-ray film can also be used to develop the 32 P radioactive signal.

Results & Discussions

3.0 Preamble

The purpose of our study was to test the different approaches for the formation of the overall nucleosomes. We compared the amount of the nucleosomal complex produced by the modified traditional refolding method, and by the two co-expression methods developed by us. We also evaluated how much time and resources are required for each method to work successfully. In the modified traditional refolding method of the octamer preparation, our aim was to produce each histone separately from the inclusion bodies and then forming the different oligomeric states through performing dialysis. In the separate co-expression method, we wanted to produce the different oligomeric states separately in direct soluble form by allowing bacterial cell to fold the expressed histones. We further wanted to express all four histones together in the bacterial cell to produce a complete soluble octamer in one step without having any dialysis. The reason for extracting soluble protein complex is that it would allow us to produce faster with less manipulation and better yield.

In order to check these three methods, we had to extensively venture different cell lines to see which cell lines express the histones, both in singles and in different pairs. We exploited the different duet expression system vectors to co-express the compatible histone pairs. In turns, we ended up having eight different constructs, four for the single histone expression and four for the duet expression, that needed to be checked for the best overexpression cell lines. Figure 3.0 shows a schematic diagram of three different ways of histone oligomer preparation.

Lastly, we have also developed an *in vitro* rapid CK2 mediated phosphorylation of the modified H2A.X C-terminal tail in terms of the H2A.X-H2B dimer in order to form the γ H2A.X-H2B dimer. This γ H2A.X will be used to create the overall γ H2A.X containing nucleosome, which will further be used to structurally analyze the binding interaction between the MDC1 BRCT and the γ H2A.X containing nucleosome.

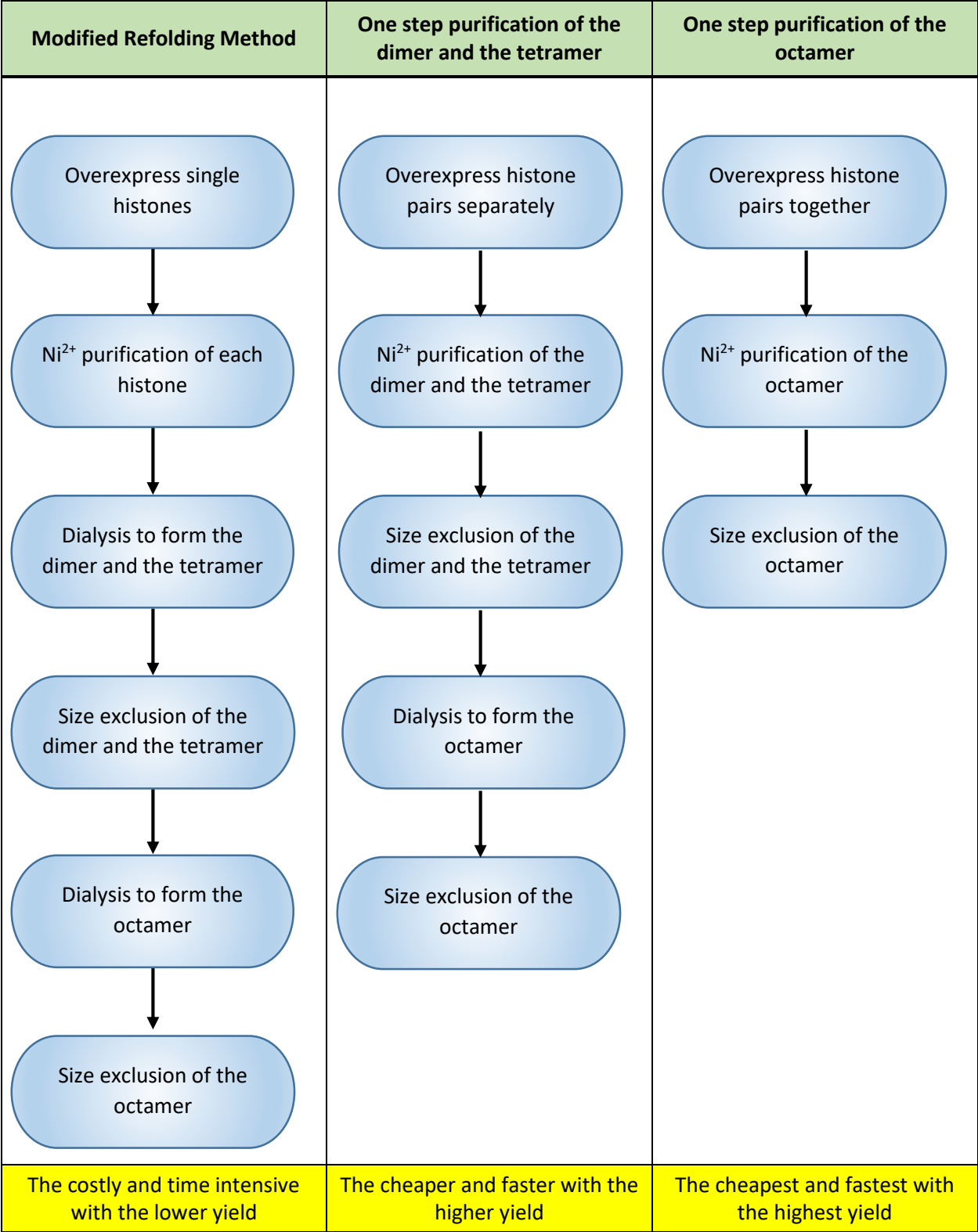


Figure 3.0 Schematic Diagram Showing the Difference between the Three Octamer Purification Methods

3.1 Result: Overexpression of the Single Histones

pET47b(+)-H2A.X*, pET47b(+)-H2B, pET47b(+)-H3.1, and pET47b(+)-H4 constructs were overexpressed in BL21(DE3) cell line under 1mM IPTG induction for 5 hours. Histone H2A.X*, H2B, and H3.1 were highly expressed, however, the expression of H4 was not as high compared to the other three histones (Figure 3.1).

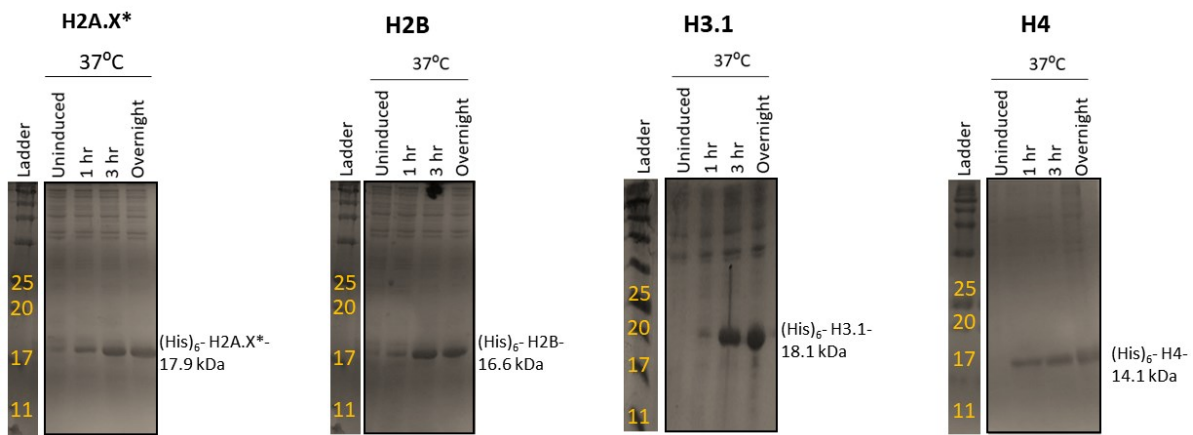


Figure 3.1 Overexpression Check of the Single Histones

pET47b(+)-H2A.X*, pET47b(+)-H2B, pET47b(+)-H3.1, and pET47b(+)-H4 constructs were overexpressed in BL21(DE3) under 1mM IPTG induction at 37°C for 5 hours. The expression level of H2A.X*, H2B, and H3.1 was higher than the expression level of H4. (H2A*→ Both wild type and mutant variants)

For large scale protein purification, 4L LB culture of each histone was grown. The yield is listed in table 3.1. The expression of H3.1 was the highest while the expression of H4 was the lowest. H2A.X* and H2B expressions were equal.

Table 3.1 Yield of the Single Histones. (Yield was calculated by measuring the absorbance at A280.)

Histones	Amount of Protein (mg/1 liter)
H2A.X*	~38
H2B	~40
H3.1	~42
H4	~22

3.2 Discussion: Overexpression of the Single Histone

Since the single histones would be purified from the inclusion bodies, not too much optimization was required for the expression of these histone constructs. Inclusion body formation due to overexpression was desired in this context. Therefore, the cells were allowed to grow at 37°C even after the 1mM IPTG induction at OD600 = 0.6. Enough protein got expressed in 5 hours after the induction.

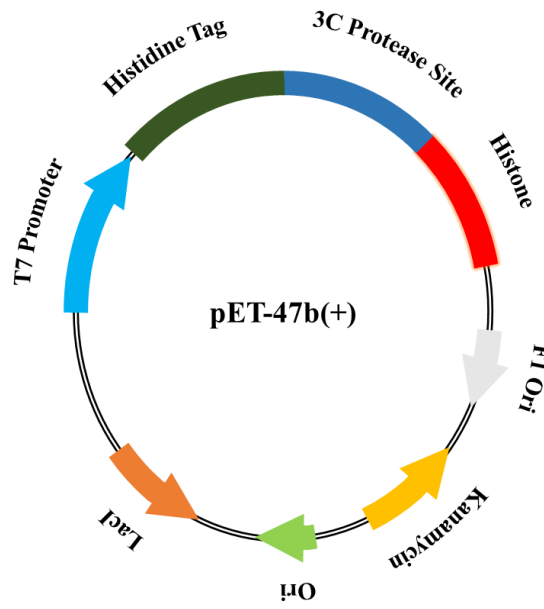


Figure 3.2: Schematic diagram of the pET47b(+)—Histone construct.

Each histone was cloned into pET47b(+) vector downstream to the T7 promoter site with a 3C cleavable hexahistidine tag. pET47b(+) carries kanamycin resistance and lac operon repressor gene LacI, which prevents non-induced expression by blocking the expression of T7 RNA polymerase.

The inducible pET47b(+)-T7 promoter allowed the optimal production of the histone using BL21(DE3) (Figure 3.2). After adding IPTG, IPTG blocked the lacI repressor protein and led to the production of T7 RNA polymerase from the chromosomal λ (DE3) to express the protein of interest.

Histones are not native bacterial proteins, and that might explain the low level of expression of H4. The amount of cell pellet observed after H4 induction was really less than the other three histones. This provided us with the idea that H4 might be toxic to the bacterial cells.

Since the level of expression for H4 was almost half of the level of expression for H3.1, therefore, growing double amount of H4 bacterial culture was sufficient to bypass the H4 expression issue.

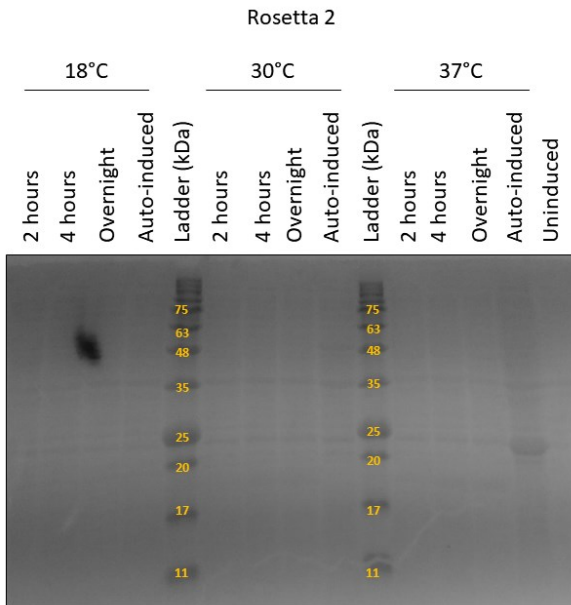
3.3 Result: Separate Overexpression of the Histone Pairs

The pETDuet-1-TEV-H2A.X*-H2B and pETDuet-1-TEV-H2B-H2A.X* expressions were checked in the different cell lines. Among all the cell lines Rosetta 2(DE3) showed the best expression level for both the constructs at 30°C and 37°C under 1mM IPTG induction, while the other cell lines had no detectable expression (Figure 3.3).

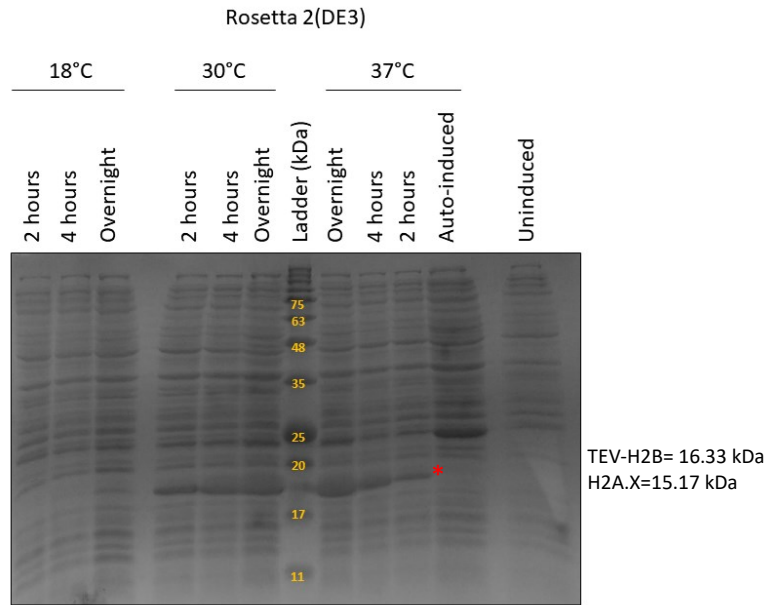
The pACYCDuet-1-TEV-H4-H3.1 was expressed in C41, C43, and BL21(DE3) cells under 1mM IPTG induction at 18°C, 30°C, and 37°C. Among all the cells BL21(DE3) gave the optimal expression both at 18°C and 30°C for 4 hours of incubation. Other cell lines did not show a detectable level of expression (Figure 3.4).

The pCDFDuet-1-TEV-H3.1-H4 was expressed in BL21(DE3), BL21(DE3) pLysS, Rosetta 2, and Rosetta 2(DE3). Among all the cell lines Rosetta 2(DE3) provided the optimal level of expression of both TEV-H3.1 and H4 at 18°C for overnight incubation (Figure 3.5).

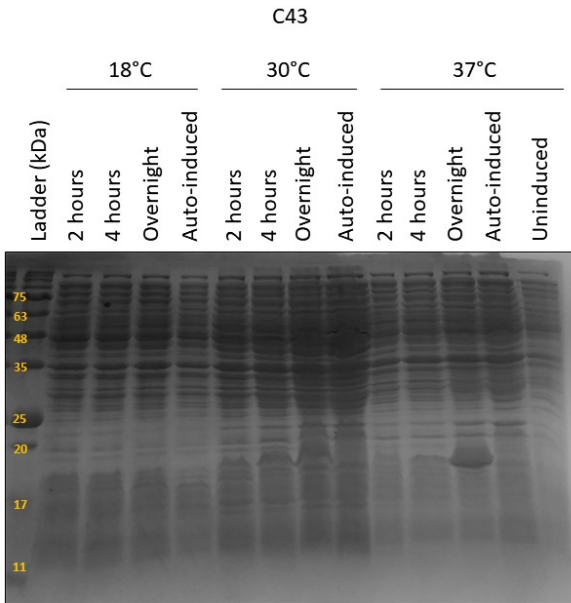
a) pETDuet-1-TEV-H2B-H2A.X(CK2-A) Overexpression



b) pETDuet-1-TEV-H2B-H2A.X(CK2-A) Overexpression



c) pETDuet-1-TEV-H2B-H2A.X(CK2-A) Overexpression



d) pETDuet-1-TEV-H2A.X(CK2-S)-H2B Overexpression

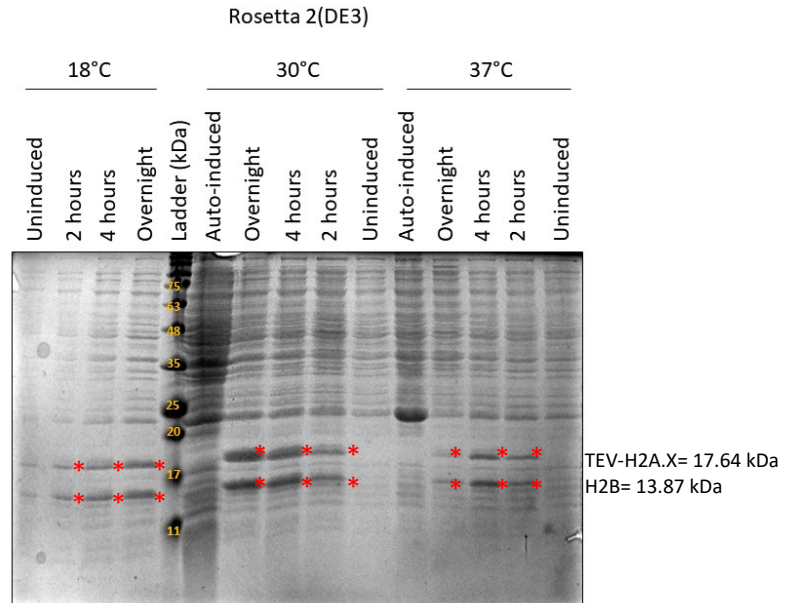


Figure 3.3 Overexpression Check for the H2A.X-H2B Dimer

pETDuet-1-TEV-H2B-H2A.X* was overexpressed in Rosetta 2, Rosetta 2(DE3), and C43. pETDuet-1-TEV-H2A.X*-H2B was overexpressed in Rosetta 2(DE3) under 1mM IPTG induction at 18°C, 30°C, and 37°C. (a), (c) show no detectable expression in Rosetta 2 and C43 respectively. (b), (d) However, both the constructs show detectable expression in Rosetta 2(DE3). In (b) TEV-

H2B (16.33 kDa) and H2A.X* (15.17 kDa) bands were unresolvable, while in (d) TEV-H2A.X*(17.64 kDa) and H2B (13.87 kDa) bands were resolvable.

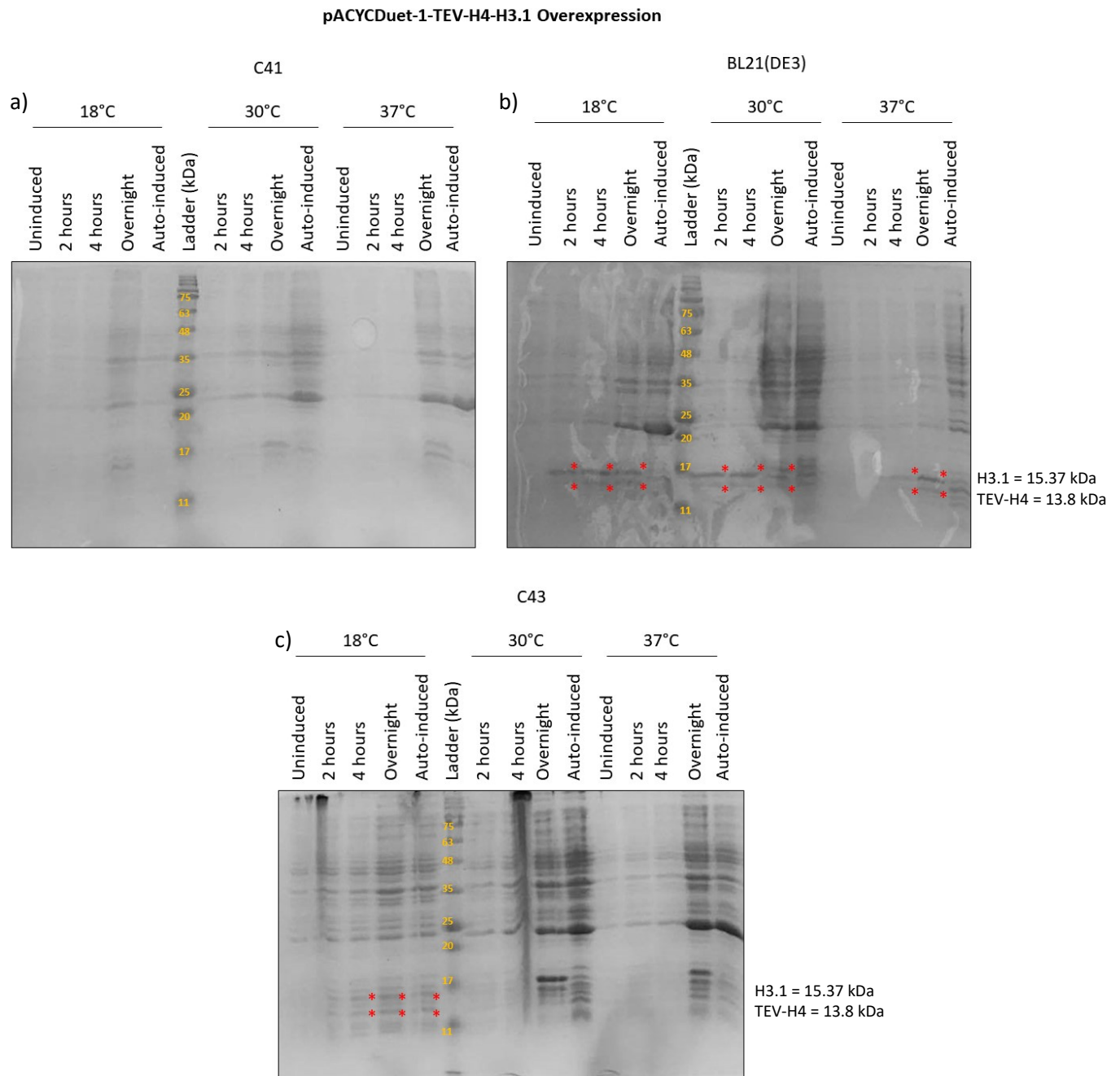


Figure 3.4 Overexpression check for TEV-H4-H3.1 tetramer

pACYCDuet-1-TEV-H4-H3.1 was overexpressed in C41, BL21(DE3), and C43 under 1mM IPTG induction at 18°C, 30°C, and 37°C. (a) showed no detectable expression in C41. (b), (c) However, showed detectable expression in BL21(DE3), and C43 respectively.

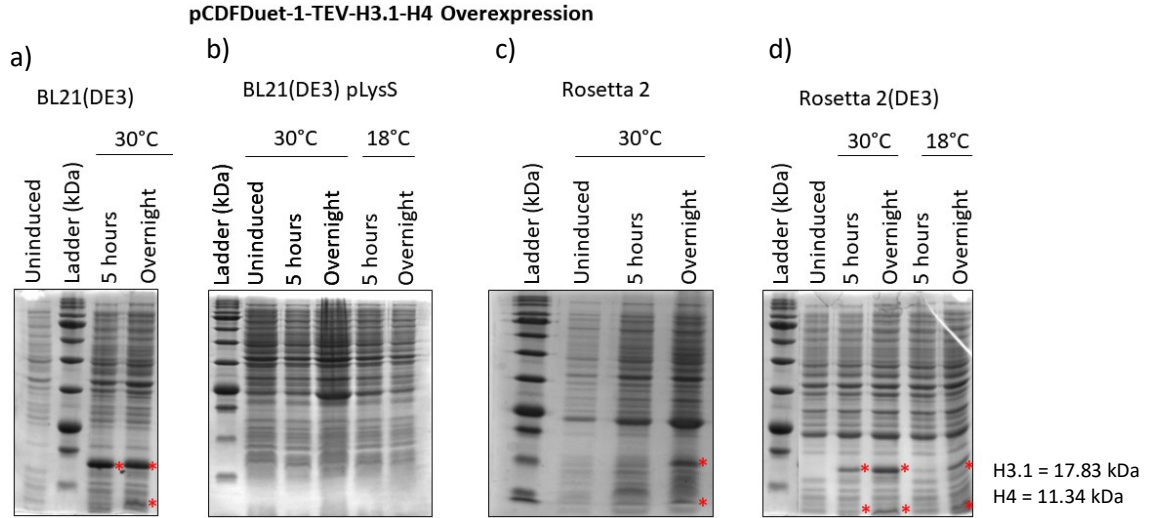


Figure 3.5 Overexpression check for TEV-H3.1-H4 tetramer (Image courtesy, Dr. Rashmi Panigrahi).

pCDFDuet-1-TEV-H3.1-H4 was overexpressed in BL21(DE3), BL21(DE3) pLysS, Rosetta 2 and Rosetta 2(DE3) under 1mM IPTG. (a) BL21(DE3) provided a good detectable expression of both TEV-H3.1 and H4 at 30°C for overnight, and only TEV-H3.1 at 30°C for 5 hours. (b) BL21(DE3) pLysS showed no detectable expression and (d) Rosetta 2 showed the presence of both TEV-H3.1 and H4 at 30°C overnight. (e) Rosetta 2(DE3) showed an optimal expression of both TEV-H3.1 and H4 at 18°C, and 30°C overnight as well as 30°C 5 hours.

For large scale protein purification, 4L TB culture of H2A.X-H2B dimer and 4L TB culture of (H3.1-H4)₂ were grown. The yield is listed in table 3.3.

3.4 Discussion: Separate Overexpression of the Histone Pairs

Histones are only soluble when they form a hetero-oligomeric complex with their other histone counterparts. H2A-H2B forms a soluble dimer, and H3.1-H4 forms a soluble tetramer. Therefore, we decided to express them together in order to perform soluble extraction of histone complexes.

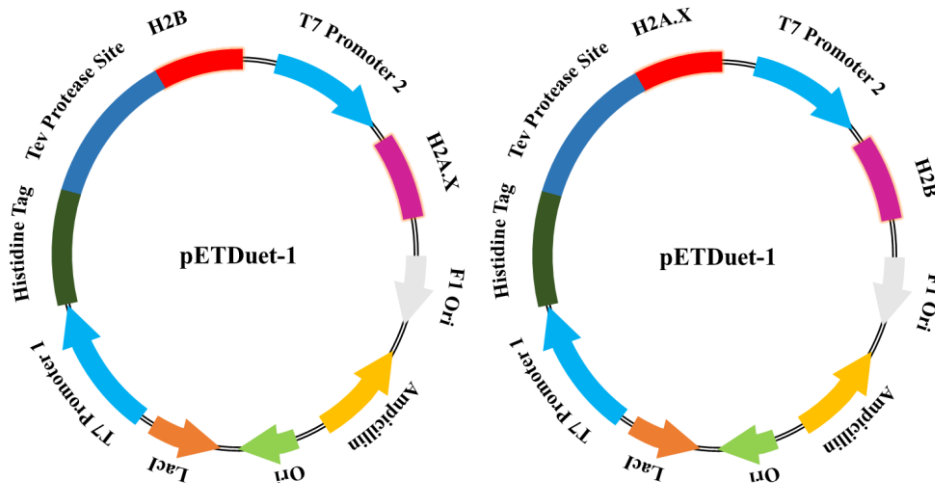


Figure 3.6 Schematic diagram of the pETDuet-1-H2A.X-H2B construct.

Ampicillin resistant pETDuet-1 vector has two inducible T7 promoters that allow simultaneous expression of both the downstream regions. A) H2B was cloned in the T7 promoter 1 region with a TEV protease cleavable hexahistidine tag, and H2A.X was cloned in the T7 promoter 2 region without any tag. B) H2A.X was cloned in the T7 promoter 1 region with a TEV protease cleavable hexahistidine tag, and H2B was cloned in the T7 promoter 2 region without any tag. This construct facilitated the simultaneous production of both the histones to produce the soluble dimer.

The H2A.X-H2B dimer had two cloned construct in the pETDuet-1 vector. In one construct, the TEV cleavable hexahistidine tag was on H2A.X, and in the other one, it was on H2B. The size of TEV-H2B is 16.33 kDa, which was almost the same size of untagged H2A.X (15.17 kDa). Therefore, they were not resolvable on the 16% SDS PAGE (Figure 3.3 a, b, c). Upon putting the tag on H2A.X, the size of TEV-H2A.X becomes 17.64 kDa, and the size of untagged H2B is 13.87 kDa. Therefore, TEV-H2A.X and H2B bands were nicely visible (Figure 3.3 d). Rosetta 2(DE3) cell line was chosen for large-scale purification for the dimer because it showed the best expression compared to the other cell line. Although C43 is suitable for producing toxic bacterial proteins, it lacks rare codon translating tRNAs. And, this might be the reason why C43 was not able to produce the proteins. On the other hand, both Rosetta 2 and Rosetta 2(DE3) cell lines have 7 rare codon producing tRNAs that allow the bacterial cells to translate the rare codon containing

eukaryotic genes. However, Rosetta 2 did not give good expression probably because unlike Rosetta 2(DE3), it lacks λ (DE3) lysogen containing T7 RNA polymerase gene in the chromosome. Therefore, expression in Rosetta 2 completely depends on the bacterial native RNA polymerases which are not as efficient as T7 RNA polymerase in recognizing the T7 promoter.

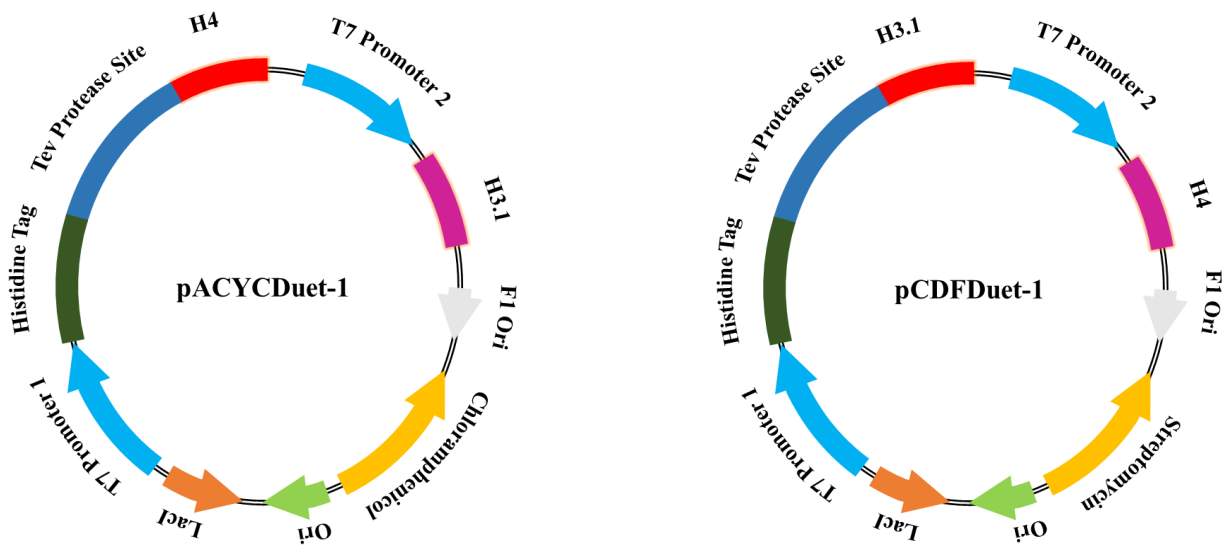


Figure 3.7 Schematic diagram of the pACYCDuet-1-TEV-H4-H3.1 and the pCDFDuet-1-TEV-H3.1-H4 constructs.

Chloramphenicol resistant pACYCDuet-1 vector, and so as Streptomycin resistant pCDFDuet-1 vector, has two inducible T7 promoters that allow simultaneous expression of both the downstream regions. A) In pACYCDuet-1, H4 was cloned in the T7 promoter 1 region with a TEV protease cleavable hexahistidine tag, and H3.1 was cloned in the T7 promoter 2 region without any tag. B) In pCDFDuet-1, H3.1 was cloned in the T7 promoter 1 region with a TEV protease cleavable hexahistidine tag, and H4 was cloned in the T7 promoter 2 region without any tag. These constructs facilitated the simultaneous production of both the histones to produce the soluble tetramer.

The H3.1 and H4 were also cloned in two recombinant vectors, the pACYCDuet-1 where the tag is on H4, and the pCDFDuet-1 where the tag is on H3.1. H3.1 and H4 did not have the resolution dilemma like H2A.X and H2B. In both the construct, they were visible. However, H3.1 was highly expressed than H4 in both the construct (Figure 3.4 and Figure 3.5).

For pACYCDuet-1 construct, Rosetta 2 and Rosetta 2(DE3) cell lines were not used because of the antibiotic selection incompatibility. Both Rosetta 2 and Rosetta 2(DE3) cell lines have intrinsic chloramphenicol resistance because of having the seven tRNA gene containing plasmid, and the selection antibiotic for pACYCDuet-1 vector is also chloramphenicol. Therefore, despite Rosetta 2(DE3) providing a good expression profile for pETDuet-1 constructs and pCDFDuet-1 constructs, the pACYCDuet-1 construct was not expressed in this cell line.

pACYCDuet-1 construct showed nice expression in both BL21(DE3) and C43, but not in C41. Although both C41 and C43 cells are suitable for toxic protein expression, C43 has few more modifications selected for different sets of toxic protein expression than C41. As H4 seemed to be toxic to the bacterial cells, C43 seemed to express better than C41. And, BL21(DE3) showed a good level of expression as well. We decided to use BL21(DE3) cells for larger scale protein purification.

pCDFDuet-1 construct showed a nice expression in BL21(DE3), Rosetta 2, and Rosetta 2(DE3). However, no expression was detected for BL21(DE3) pLysS. The pLysS produces T7 lysozyme to attenuate the basally expressed T7 RNA polymerase to provide stringent protein expression. This T7 lysozyme is also harmful to the bacteria itself because it degrades the bacterial cell wall. On top of that, both H3.1 and H4 were not native bacterial proteins, and H4 seemed toxic to the bacteria. Therefore, this strain died before producing a good amount of protein. We choose Rosetta 2(DE3) for large-scale tetramer production.

3.5 Result: Combined Overexpression of the Histone Pairs

[pETDuet-1-TEV-H2A.X-H2B - pACYCDuet-1-TEV-H4-H3.1] transformed BL21(DE3) and [pETDuet-1-TEV-H2A.X-H2B - pCDFDuet-1-TEV-H3.1-H4] transformed Rosetta 2(DE3) cells were induced with 1mM IPTG at different temperatures. Both the cell line showed the minor level of expression of all four histones.

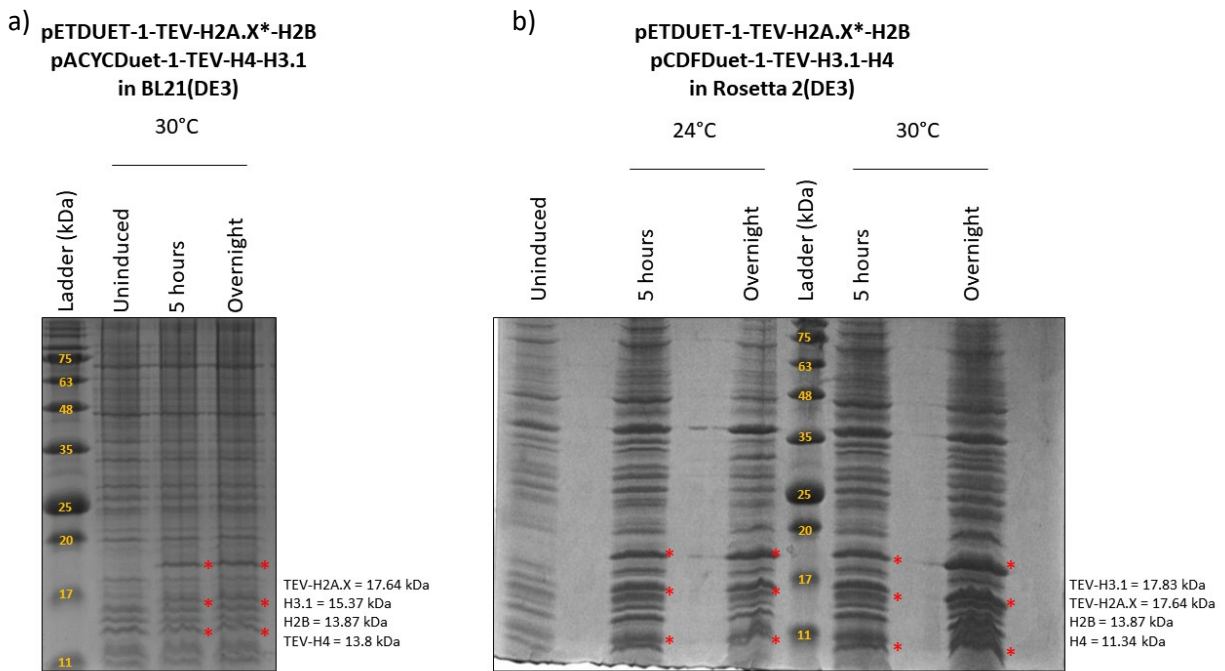


Figure 3.8 Overexpression Check of the Histone Octamer

a) pETDuet-1-TEV-H2A.X-H2B and pACYCDuet-1-TEV-H4-H3.1 both were expressed together in BL21(DE3). b) pETDuet-1-TEV-H2A.X-H2B and pACYCDuet-1-TEV-H4-H3.1 both were expressed together in Rosetta 2(DE3) under 1mM IPTG induction. In both the cases, some level of protein expression was observed (Image courtesy- Dr. Rashmi Panigrahi).

For large scale protein purification, 8L TB culture of each octamer producing strain was grown. The yield is listed in table 3.4.

3.6 Discussion: Combined Overexpression of the Histone Pairs

The expression check profile for the octamer from the 16% SDS PAGE was very confusing. Since the sizes of H2B (13.87 kDa) and TEV-H4 (13.8 kDa) were the same, we only see three bands on the gel in Figure 3.7 a. Same with Figure 3.7 b, the sizes of TEV-H2A.X (17.64 kDa) and TEV-H3.1 (17.83 kDa) were close enough for those two bands to merge together. However, Rosetta 2(DE3) expressed better than the BL21(DE3); the reason probably be again Rosetta 2(DE3) having the capability to encode for rare codons.

Aside from band dilemma, the expression levels of the four histones were not very high in the pETDuet-1 and the pACYCDuet-1 construct, however, the expression level of the four histones were good on the pETDuet-1 and the pCDFDuet-1 construct.

In order to rule out the confusions, large-scale protein purification was performed on both the constructs.

3.7 Result: Modified Refolding of the Octamer

3.7.1 Ni²⁺ affinity pull-down purification of the single histones

Single histone constructs were expressed separately in BL21(DE3) and were purified under urea denaturing condition using Ni²⁺ affinity pull-down purification. The eluents from the Ni²⁺ resins contained mostly the protein of interest, and also some impurities (Figure 3.9).

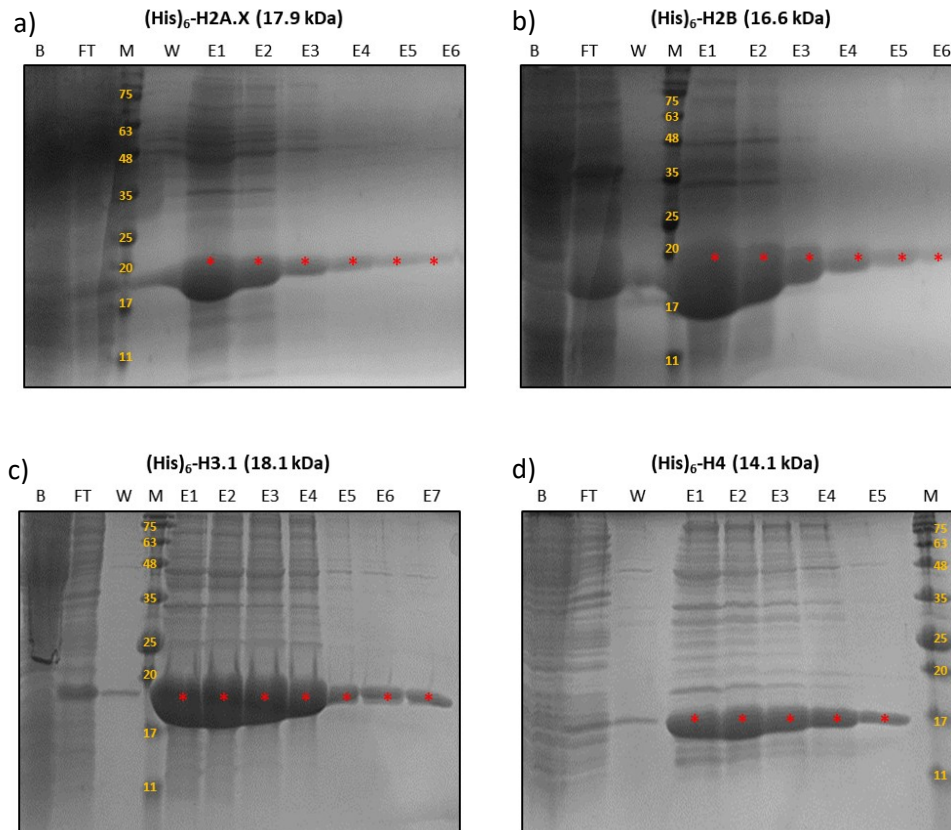


Figure 3.9 Ni²⁺ Affinity Purification of the Single Histones under Urea Denaturing Condition.

On a 16% SDS PAGE gel, B → background supernatant, which contains the soluble proteins, FT → Flow through after 2 hours of incubation with the Ni²⁺ resins, W → wash of the Ni²⁺ resins with 30mM imidazole, E* → elution fractions of 300mM imidazole elution, M → Protein marker (kDa). a) Ni²⁺ affinity purification of (His)₆-H2A.X. b) Ni²⁺ affinity purification of (His)₆-H2B. c) Ni²⁺ affinity purification of (His)₆-H3.1. d) Ni²⁺ affinity purification of (His)₆-H4.

3.7.2 Size Exclusion Chromatography of the (His)₆-H2A.X-(His)₆-H2B Dimer

Dialyzed 1:1 molar (His)₆-H2A.X and (His)₆-H2B were loaded on the Superdex 200 16/60 size exclusion column. In a 120 ml of elution volume column, the dimer (34.5 kDa) peak eluted out around 82 ml. Fractions from the peak region were loaded on a 16% SDS gel to confirm the presence of the dimer (Figure 3.10).

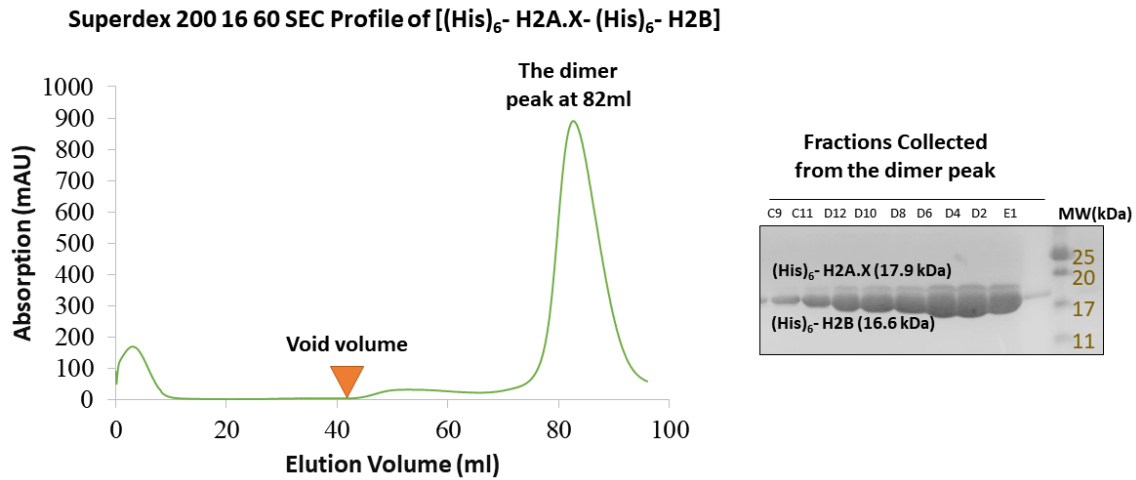


Figure 3.10 Size Exclusion Profile of the Reconstituted Histone Dimer (250mM NaCl).

The concentrated dimer was loaded on a Superdex 200 16 60 size exclusion column. The higher molecular weight contaminant and aggregates eluted out before the void volume (~40ml). The dimer peak eluted out around 82ml elution volume. Fractions from the peak region loaded on a 16% SDS PAGE gel showed the presence of the dimer.

3.7.3 Size Exclusion Chromatography of the [(His)₆-H3.1-(His)₆-H4]₂ Tetramer

Dialyzed 1.3:1 of (His)₆-H3.1 and (His)₆-H4 were loaded on the Superdex 200 16/60 size exclusion column. In a 120 ml of elution volume column, the tetramer (64.4 kDa) peak eluted out around 82 ml. Fractions from the peak region were loaded on a 16% SDS gel to confirm the presence of the dimer (Figure 3.11).

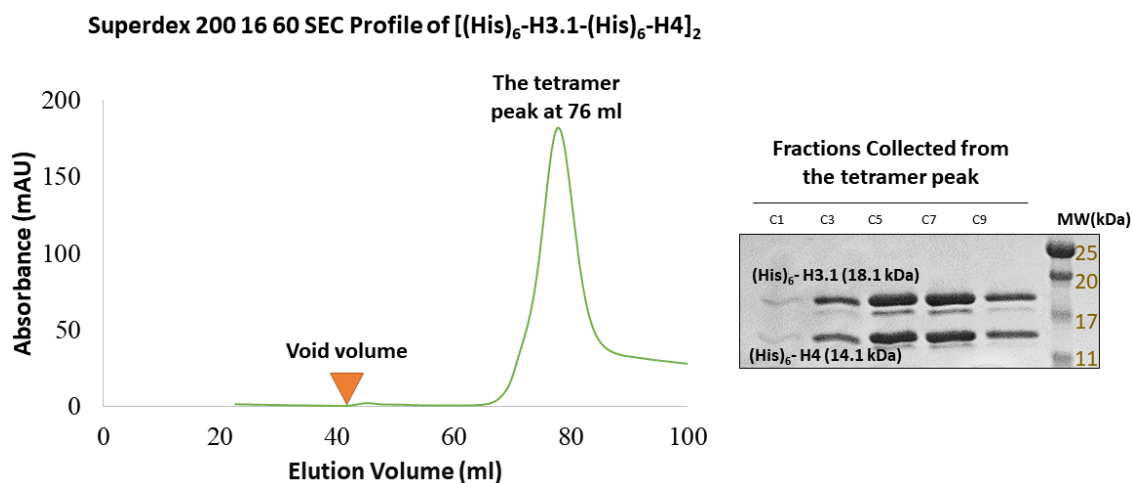


Figure 3.11 Size Exclusion profile of the Reconstituted Histone Tetramer (250mM NaCl).

The concentrated tetramer was loaded on a Superdex 200 16 60 size exclusion column. The higher molecular weight contaminant and aggregates eluted out before the void volume (~40ml). The tetramer peak eluted out around 76ml elution volume. Fractions from the peak region loaded on a 16% SDS PAGE gel showed the presence of the tetramer.

3.7.4 Size Exclusion Chromatography of the Octamer

Dialyzed 2.1:1 molar ratio of dimer and tetramer were loaded on the Superdex 200 10 300 size exclusion column. In a 25 ml of elution volume column, the octamer (133.4 kDa) peak eluted out around 12 ml. Fractions from the peak region were concentrated and digested with the 3C protease to remove hexahistidine tag. Both digested and undigested octamer were loaded on a 16% SDS gel to confirm the presence of the octamer (Figure 3.12).

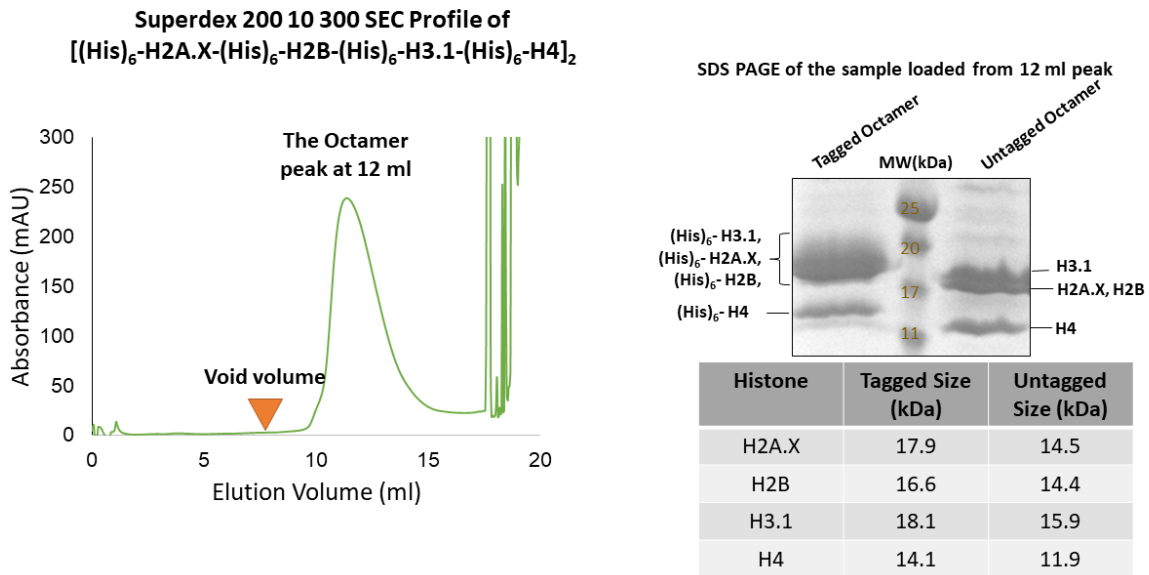


Figure 3.12 Size Exclusion profile of the reconstituted histone octamer (250mM NaCl).

Concentrated octamer was loaded on a Superdex 200 10 300 size exclusion column. The higher molecular weight contaminant and aggregates eluted out before the void volume (~8 ml). The octamer peak eluted out around 12 ml elution volume. Fractions from the peak region were concentrated and digested with the 3C protease. Both digested and undigested octamer were loaded on a 16% SDS PAGE gel to show the presence of the octamer.

3.7.5 Yield of the Histone Oligomers

The yield of the histone oligomers from modified refolding method was calculated, and table 3.2 listed the approximate amount.

Table 3.2 Yield of the Refolded Histone Oligomer. (Yield was calculated by measuring the concentration at A280).

Oligomers	Amount
Dimer	~ 30 mg / 8 liters
Tetramer	~ 10 mg / 8 liters
Octamer	~5 mg / 16 liters

3.8 Discussion: Modified Refolding of the Octamer

Eukaryotic histones were expressed separately in BL21(DE3) cells. Due to the amino acid compositions in the distinctive histone fold, each histone is not soluble as a singlet. Therefore, each histone was extracted from inclusion bodies using urea denaturant with a subsequent Ni^{2+} affinity column purification.

The Ni^{2+} affinity purification step for the single histones did not result in a completely pure histone. Due to the non-specific binding affinity of the Ni^{2+} resins, lots of other proteins bound on the beads that were not removed even after 250 ml of 30mM imidazole wash. However, the 16% SDS PAGE gel shows that the amount of histone bound onto the beads was significantly more than the amount of impurities.

(His)₆-H2A.X and (His)₆-H2B were mixed into equimolar ratio to form the dimers, and (His)₆-H3.1 and (His)₆-H4 were mixed into equimolar ratio to form the tetramers. Due to the presence of other impurities, this mixing was not perfect, and lots of precipitants were observed as the urea was being dialyzed out. While the mixing concentration of the (His)₆-H2A.X-(His)₆-H2B did not matter, (His)₆-H3.1-(His)₆-H4 precipitated out if the concentration in the dialysis bag was more than 0.2 mg/ml. Therefore, not a lot of dialysis bags were set up for (His)₆-H3.1-(His)₆-H4 tetramer formation. Another reason for (His)₆-H3.1-(His)₆-H4 tetramer to precipitate out frequently might be its high intrinsic affinity for the genomic DNA. One way to prevent the genomic DNA contamination is to use a higher concentration of salt while eluting the protein out from the Ni²⁺ beads or using a cation exchange column to purify the histones. As most of the precipitants during dialysis were mostly the insoluble bacterial proteins, the size exclusion column eluted out highly purified histone oligomers.

The dimer component was not resolvable on a 16% SDS gel due to the fact that (His)₆-H2A.X (17.9 kDa) and (His)₆-H2B (16.6 kDa) had almost the same sizes. Mass spectrometry was performed to figure out the presence of the two proteins in the dimer. The tetramer, on the other hand, was nicely confirmed on a 16% SDS gel. The dilemma persisted in the octamer as well. Only two bands were visible on a 16% SDS gel because (His)₆-H2A.X (17.9 kDa), (His)₆-H2B (16.6 kDa), and (His)₆-H3.1 (18.1 kDa) were clumped together and gave a broad smear. However, upon cleaving off the histidine tag, H2A.X (14.5 kDa), H2B (14.4 kDa), H3.1 (15.9 kDa) and H4 (11.9 kDa) gave rise to three bands as untagged H2A.X, and untagged H2B still remained merged together.

From 16 liters of initial culture, we were able to reconstitute ~20 mg of the dimer, and ~10 mg of the tetramer. And, overall ~5 mg of the octamer.

3.9 Result: One-step Purification of the Dimer and the Tetramer

3.9.1 Ni²⁺ Affinity Pull-down Purification of the Histone Pairs

Rosetta 2(DE3) cell line was used to express the pETDuet-1-TEV-H2A.X-H2B or the pETDuet-1-TEV-H2B-H2A.X and the pCDFDuet-1-TEV-H3.1-H4 constructs separately. The pACYCDuet-1-TEV-H4-H3.1 construct was expressed in BL21. The heteromeric oligomers were purified using Ni²⁺ affinity pull-down purification. The eluants from the Ni²⁺ resins contained mostly the protein of interest, and also some impurities (Figure 3.13). Each elution volume is 5ml. The purest fraction was loaded on the size exclusion column for further purification.

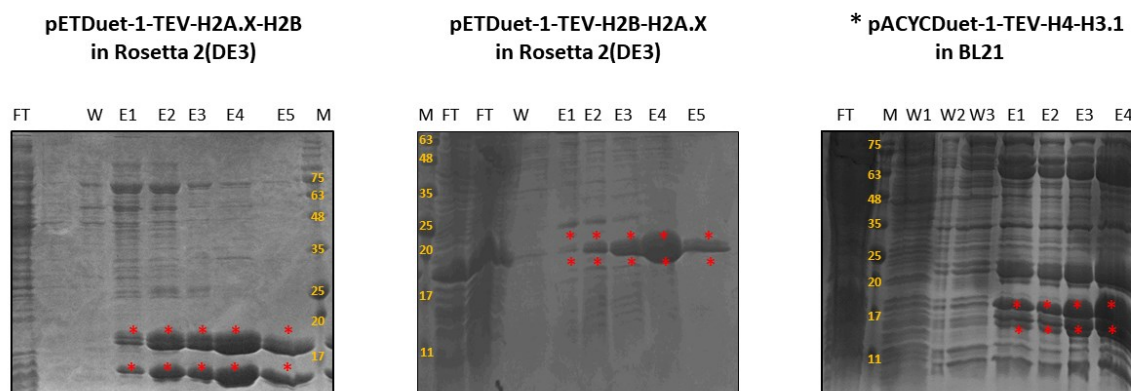


Figure 3.13 Ni²⁺ Affinity Purification of the Co-expressed Histone Oligomers, H2A.X-H2B dimer, and (H3.1-H4)₂ tetramer.

On a 16% SDS PAGE gel, FT → Flow through after 2 hours of incubation with the Ni²⁺ resins, W → wash of the Ni²⁺ resins with 30mM imidazole, E1 → 100mM imidazole elution fraction, E2 → 250mM imidazole elution fraction, E3 → 500mM imidazole elution fraction, E4 → 1mM imidazole elution fraction, E5 → 2mM imidazole elution fraction, M → Protein marker (kDa). a) Ni²⁺ affinity purification of (His)₆-TEV-H2A.X-H2B. b) Ni²⁺ affinity purification of (His)₆-TEV-H2B-H2A. c) Ni²⁺ affinity purification of (His)₆-TEV-H4-H3.1 (* → image courtesy, Dr. Rashmi Panigrahi).

3.9.2 Size Exclusion Chromatography of the Co-expressed (His)₆-TEV-H2A.X-H2B Dimer

The purest elution fraction for (His)₆-TEV-H2A.X-H2B was loaded on a Superdex 200 16 60 size exclusion column. In a 120 ml of elution volume column, the dimer (31.51 kDa) peak eluted out around 82 ml. Fractions from the peak region were loaded on 16% SDS gel to confirm the presence of the dimer (Figure 3.14).

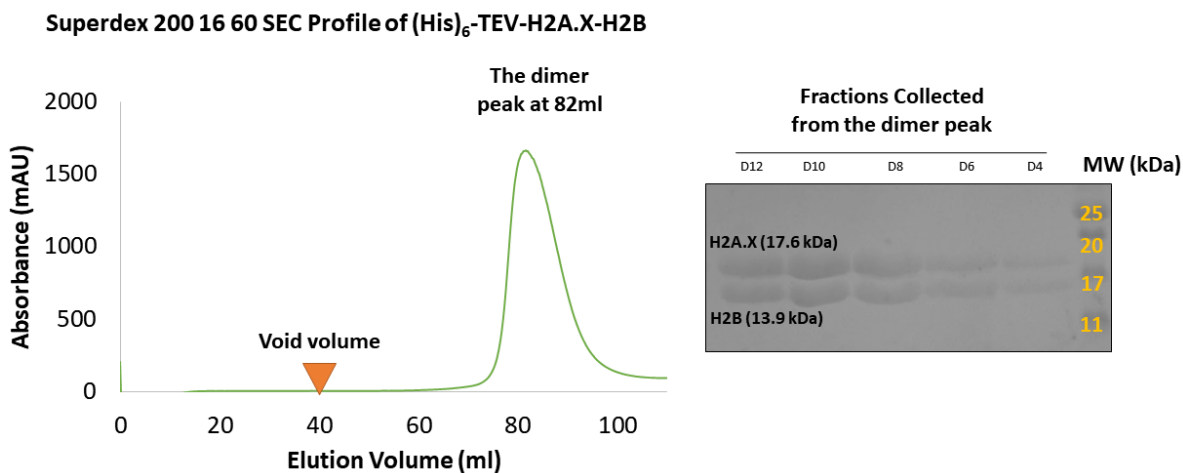


Figure 3.14 Size Exclusion Profile of the Co-expressed (His)₆-TEV-H2A.X-H2B Dimer (2M NaCl).

The Ni²⁺ purified dimer was loaded on a Superdex 200 16 60 size exclusion column. The higher molecular weight contaminant and aggregates eluted out before the void volume (~40 ml). The dimer peak eluted out around 82 ml elution volume. Fractions from the peak region were loaded on a 16% SDS PAGE gel to show the presence of the dimer.

3.9.3 Size Exclusion Chromatography of the Co-expressed [(His)₆-TEV-H4-H3.1]₂ Tetramer

The purest elution fraction for (His)₆-TEV-H4-H3.1 was loaded on a Superdex 200 16 60 size exclusion column. In a 120 ml of elution volume column, the tetramer (29.2 kDa) peak eluted out around 76 ml. Fractions from the peak region were loaded on 16% SDS gel to confirm the presence of the tetramer (Figure 3.15). The tetramer contained a few contaminants that needed to be purified further.

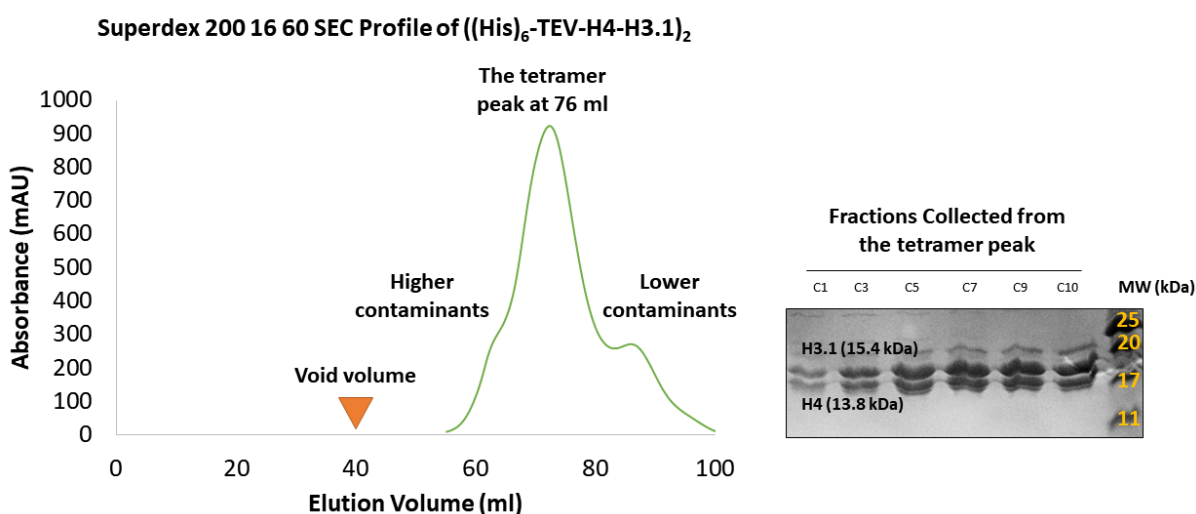


Figure 3.15 Size Exclusion Profile of the Co-expressed [(His)₆-TEV-H4-H3.1]₂ Tetramer (2M NaCl). (Image courtesy, Dr. Rashmi Panigrahi).

The Ni²⁺ purified tetramer was loaded on a Superdex 200 16 60 size exclusion column. The higher molecular weight contaminant and aggregates eluted out before the void volume (~40 ml). The tetramer peak eluted out around 76 ml elution volume. Fractions from the peak region were loaded on a 16% SDS PAGE gel to show the presence of the tetramer.

3.9.4 Size exclusion chromatography of the co-expressed [(His)₆-TEV-H3.1-H4]₂ tetramer

The purest elution fraction for (His)₆-TEV-H3.1-H4 was loaded on a Superdex 200 16 60 size exclusion column. In a 120 ml of elution volume column, the tetramer (58.34 kDa) peak eluted out around 76 ml. Fractions from the peak region were loaded on 16% SDS gel to confirm the presence of the tetramer (Figure 3.16). The yield for the tetramer from this pCDFDuet-1 construct was extremely low. The reason for this inconsistency probably because H3.1 got highly expressed than H4. There were two H3.1 bands near each other, and this was probably due to the contamination between both (His)₆-TEV-H3.1-H4 and H3.1-H4 constructs. Upon TEV digestion, all the H3.1 bands fell under one band.

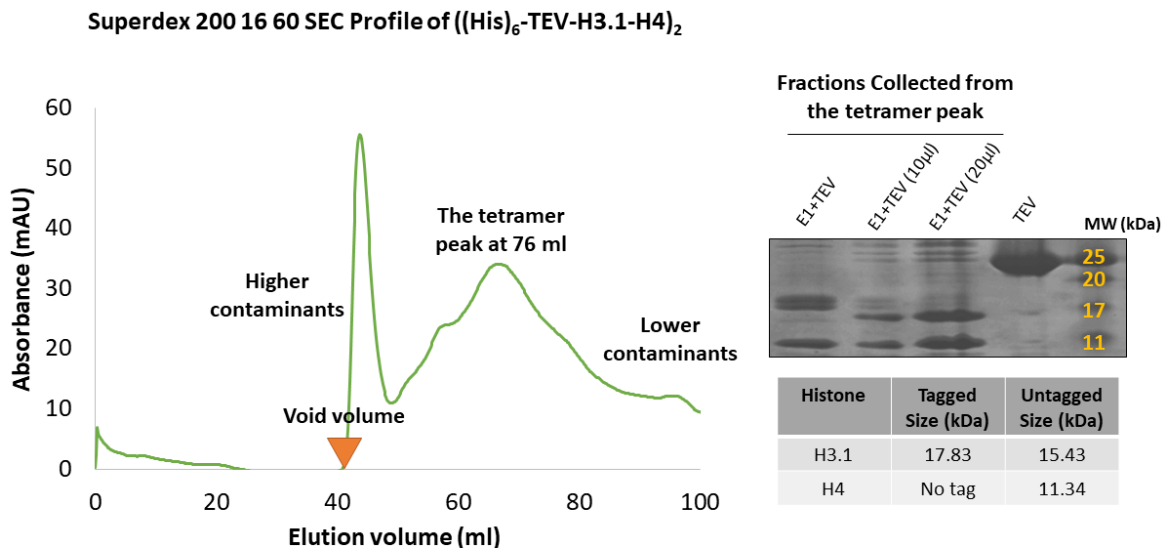


Figure 3.16 Size Exclusion Profile of the Co-expressed [(His)₆-TEV-H3.1-H4]₂ Tetramer (2M NaCl). (Image courtesy, Dr. Rashmi Panigrahi).

The Ni²⁺ purified tetramer was loaded on a Superdex 200 16 60 size exclusion column. The higher molecular weight contaminant and aggregates eluted out before the void volume (~40 ml). The tetramer peak eluted out around 76 ml elution volume. Fractions from the peak region were concentrated and loaded on a 16% SDS PAGE gel to show the presence of the tetramer. Upon TEV protease digestion, the H3.1 bands fell under one band.

3.9.5 Size Exclusion Chromatography of the Octamer

The two oligomers from pETDuet-1 construct and pACYCDuet-1 construct were then assembled together to form the octamer. Due to the short incubation period, the octamer did not form properly. Therefore, a longer incubation period is necessary in order for the dimer and the tetramer to form the octamer.

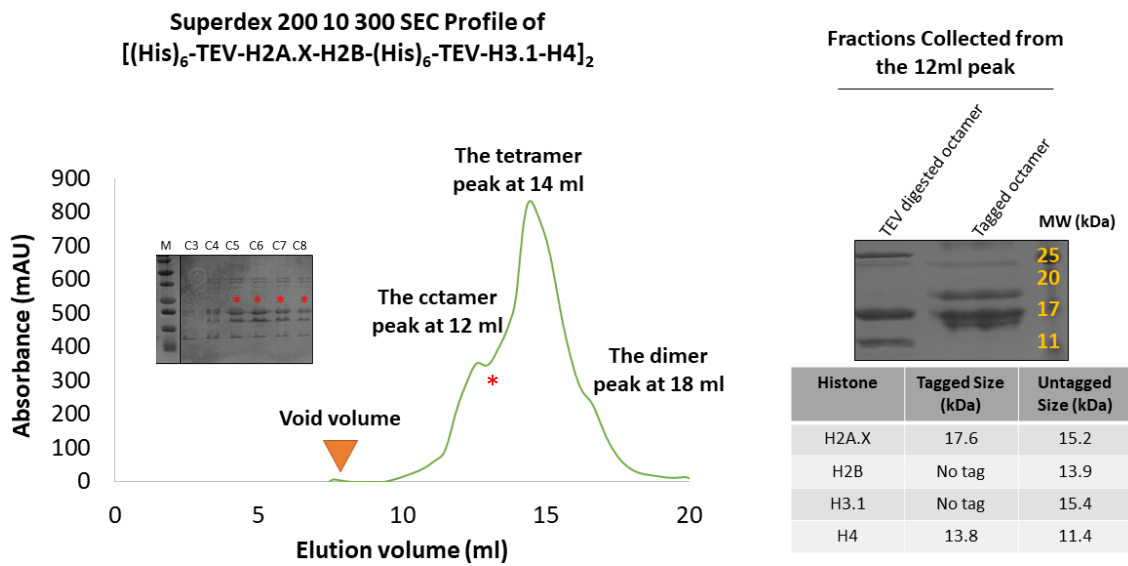


Figure 3.17 Size Exclusion profile of the Co-expressed Histone Oligomers Associated Octamer (2M NaCl) (Image courtesy, Dr. Rashmi Panigrahi).

Concentrated octamer was loaded on a Superdex 200 10 300 size exclusion column. The higher molecular weight contaminant and aggregates eluted out before the void volume (~8 ml). The octamer peak eluted out around 12 ml elution volume. Fractions from the peak region were concentrated and digested with TEV protease. Both digested and undigested octamer were loaded on a 16% SDS PAGE gel to show the presence of the octamer.

3.9.6 Yield of the Histone Oligomers

The yield of the co-expressed histone oligomers was calculated, and table 3.3 listed the approximate amount.

Table 3.3 Yield of the Co-expressed Histone Oligomers. (Yield was calculated by measuring the concentration at A280) (*Data courtesy, Dr. Rashmi Panigrahi)

Histones oligomers	Amount of Protein (mg / 1 liter)
(His) ₆ -TEV-H2A.X-H2B	~20 mg
(His) ₆ -TEV-H2B-H2A.X	~10 mg
[(His) ₆ -TEV-H4-H3.1] ₂	~15 mg*
[(His) ₆ -TEV-H3.1-H4] ₂	~5 mg*

3.10 Discussion: One-step Purification of the Dimer and the Tetramer

In an attempt to purify, the co-expressed dimer, the first construct pETDuet-1-TEV-H2B-H2A.X showed the evidence of H2B being expressed more than H2A; therefore, more H2B were bound on the Ni²⁺ resins than the respective H2A. Upon elution, after some time, there was evidence of precipitation. As a result, this construct was not used further, and we decided to put the hexahistidine tag on H2A.X instead of H2B, and this new recombinant construct had a resolvable size difference as well.

Unlike the first construct, the second construct, pETDuet-1-TEV-H2A.X-H2B showed the presence of both H2A.X and H2B in equal amount, because the excess H2B did not participate in

forming the dimer. Therefore, this excess H2B might have precipitated out in inclusion bodies during the lysis step. The (His)₆-TEV-H2A.X-H2B was eluted out, and the eluent was clear for 12 hours even in higher imidazole concentration. The size exclusion column nicely purified the dimer with high mAU.

The pCDFDuet-1-TEV-H3.1-H4 had the same problems in expression. H3.1 were expressed higher than H4. However, pCDFDuet-1 construct for producing tetramer was still used, and extremely low yield tetramer was obtained from it.

The pACYCDuet-1-TEV-H4-H3.1 had the tag on H4 instead of H3.1. The elution fraction showed the presence of an equal amount of H4 and H3.1. The Ni²⁺ elution for the tetramer was not very good. However, the size exclusion column gave a better purification profile with higher mAU.

Both the (His)₆-TEV-H2A.X-H2B and [(His)₆-TEV-H4-H3.1]₂ were mixed in 2.1:1 ratio to form the octamer. The dimer was mixed in a little bit excess amount so that all the tetramers participate in forming the octamers. The reason behind it is that the octamer peak is not resolvable from the tetramer peak on the Superdex 200 10 300 size exclusion column, but the dimer peak can be easily distinguished. However, the problem here was that the mixture was not incubated for enough time.

In comparison with the refolding method, this co-expressed method significantly reduces steps to form the nucleosome core particle, the octamer.

3.11 Result: One-step Purification of the Octamer

3.11.1 Ni²⁺ Affinity Pull-down Purification of the Octamer

Rosetta 2(DE3) cell line was used to express pETDuet-1-TEV-H2A.X-H2B and pCDFDuet-1-H3.1-H4 constructs together at the same time. pETDuet-1-TEV-H2A.X-H2B and pACYCDuet-1-TEV-H4-H3.1 constructs were expressed together in BL21(DE3). The octamer was purified using Ni²⁺ affinity pull-down purification. The eluents from the Ni²⁺ resins contained mostly the protein of interest, and also some impurities (Figure 3.18). However, pETDuet-1-TEV-H2A.X-H2B and pACYCDuet-1-TEV-H4-H3.1 construct did not work in BL21(DE3) as the size exclusion column showed the presence of only the dimer (data not shown). Each elution volume is 5ml. The purest fraction was loaded on the size exclusion column for further purification.

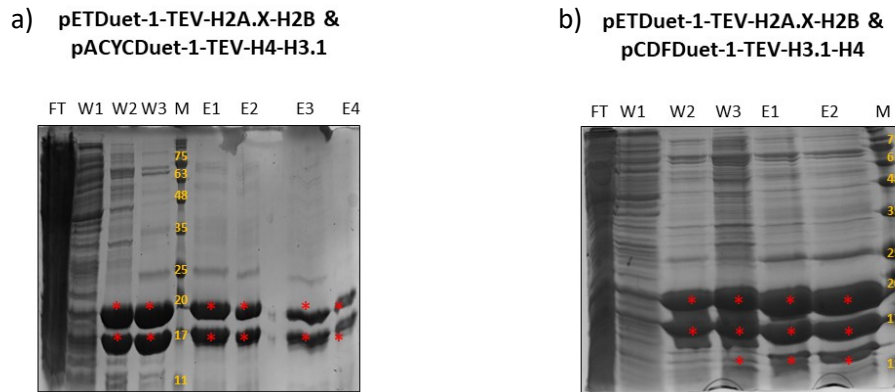


Figure 3.18 Ni²⁺ Affinity Purification of Octamer (Image courtesy, Dr. Rashmi Panigrahi).

On a 16% SDS PAGE gel, FT → Flow through after 2 hours of incubation with the Ni²⁺ resins, W1 → wash of Ni²⁺ resins with 0mM imidazole, W2 → wash of the Ni²⁺ resins with 40mM imidazole, W3 → wash of the Ni²⁺ resins with 80mM imidazole, E1 → 100mM imidazole elution fraction, E2 → 250mM imidazole elution fraction, E3 → 500mM imidazole elution fraction, E4 → 1mM imidazole elution fraction, E5 → 2mM imidazole elution fraction, M → Protein marker (kDa). a) Ni²⁺ affinity purification of [(His)₆-TEV-H2A.X-H2B-(His)₆-TEV-H4-H3.1]₂. However, there was no H3.1 and H4 bands only H2A.X, and H2B bands were present. b) Ni²⁺ affinity purification of [(His)₆-TEV-H2A.X-H2B-(His)₆-TEV-H3.1-H4]. However, only three bands were visible since (His)₆-TEV-H2A.X (17.6 kDa) and (His)₆-TEV-H3.1 (17.83 kDa) were merged together on the gel.

3.11.2 Size Exclusion Chromatography of Octamer

The purest fraction from the Ni^{2+} elution was loaded on Superdex 200 16 60 column, and all three oligomeric peaks were seen on the size exclusion column. In a 120 ml of elution volume column, the octamer (121.2 kDa) peak eluted out around 72 ml, and the dimer (31.5 kDa) came out around 82 ml. Fractions from the peak region were loaded on 16% SDS gel to confirm the presence of the octamer (Figure 3.19).

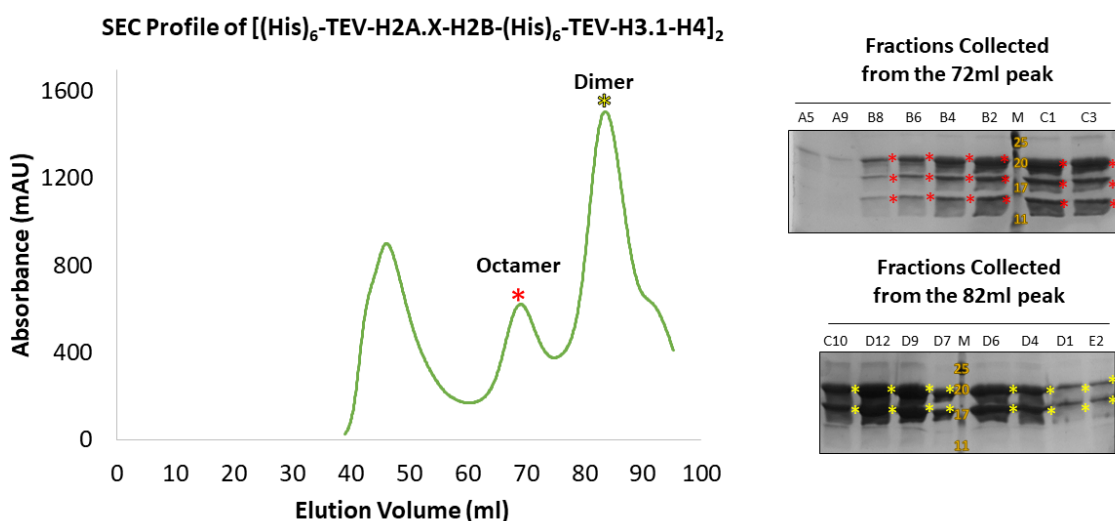


Figure 3.19 Size Exclusion Profile of the Octamer Purified from the One-step Purification System (2M NaCl) (Image courtesy, Dr. Rashmi Panigrahi).

The purest fraction from the Ni^{2+} elution was loaded on Superdex 200 16 60 column. The higher molecular weight contaminant and aggregates eluted out before the void volume (~ 40 ml). The octamer, and the dimer peaks eluted out around 72 ml, and 82 ml elution volumes respectively. Fractions from the peak region were loaded on a 16% SDS PAGE gel to show the presence of the oligomers.

Fractions from the octameric region were assembled and concentrated together to load on the Superdex 200 10 300 column. In a 25 ml of elution volume column, the octamer (121.2 kDa) peak eluted out around 12 ml. Fractions from the peak region were concentrated and digested with TEV protease to remove hexahistidine tag. Both digested and undigested octamer were loaded on a 16% SDS gel to confirm the presence of the octamer (Figure 3.20).

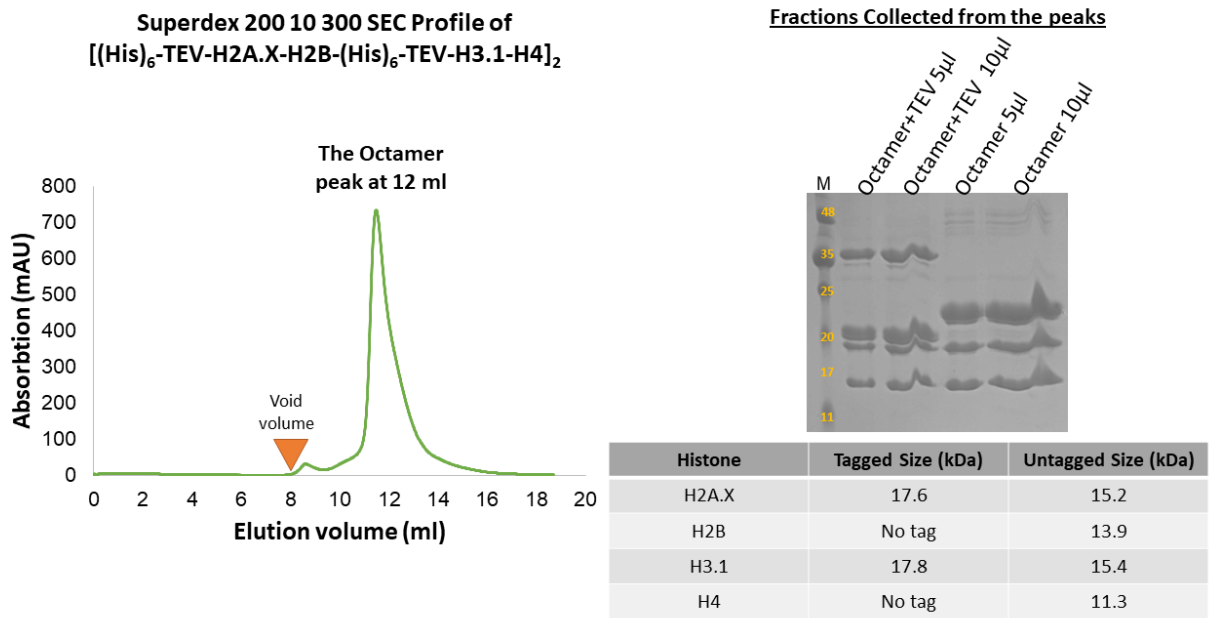


Figure 3.20 Size Exclusion profile of the Octamer in Superdex 200 10 300 after the Superdex 200 16 60 Run (2M NaCl) (Image courtesy, Dr. Rashmi Panigrahi).

The concentrated octamer was loaded on a Superdex 200 10 300 size exclusion column. The higher molecular weight contaminant and aggregates eluted out before the void volume (~8 ml). The octamer peak eluted out around 12 ml elution volume. Fractions from the peak region were concentrated and digested with TEV protease. Both digested and undigested octamer were loaded on a 16% SDS PAGE gel to show the presence of the octamer.

3.11.3 Yield of the Octamer

The yield of the one-step purified octamer was calculated measuring the concentration of the solution. The approximate amount recovered is listed in Table 3.4.

Table 3.4 Yield of the One-step Purified Octamer. (Yield was calculated by measuring the concentration at A280.) (Data courtesy, Dr. Rashmi Panigrahi)

Octamer constructs	Amount of Protein (mg /1 liters)
pETDuet-1-(TEV-H2B-H2A.X) – pCDFDuet-1-(TEV-H3.1-H4) ₂	~ 20

3.12 Discussion: One-step Purification of the Octamer

The pETDuet-1-TEV-H2A.X-H2B and the pACYCDuet-1-TEV-H4-H3.1 construct did not work to form octamer in BL21(DE3). The reason could be the difference between the vector copy numbers, pACYCDuet-1 is a really low copy number (~10) vector, while pETDuet-1 is extremely high (~40). Due to this fact, probably dimer overruled the tetramer expression in these two cell line.

The pETDuet-1-TEV-H2A.X-H2B and the pCDFDuet-TEV-H3.1-H4 construct were expressed together in Rosetta 2(DE3) cell line, and it produced both the oligomers inside the cell to give rise to enough octamer. However, since the tag was associated with both construct, we isolated a non-homologous mixture of the octamer and the other oligomers in the size exclusion column. Since the dimer in the pETDuet-1 construct is more produced, our next aim is to remove the tag from the dimer construct in order to find purely homogenous octamer in the size exclusion column.

3.13 Result: MALDI-IMS confirmation of the H2A.X-H2B Dimer

We performed MALDI-IMS (Matrix-Assisted Laser Desorption Ionization Imaging Mass Spectrometry) analysis in order to figure out the exact size and ratio of each protein present in the histone complexes. Even though 16% SDS gel could not resolve it, but there is an equal amount of both (His)₆-H2A.X and (His)₆-H2B in the dimer formed from the refolding method (Figure 3.21).

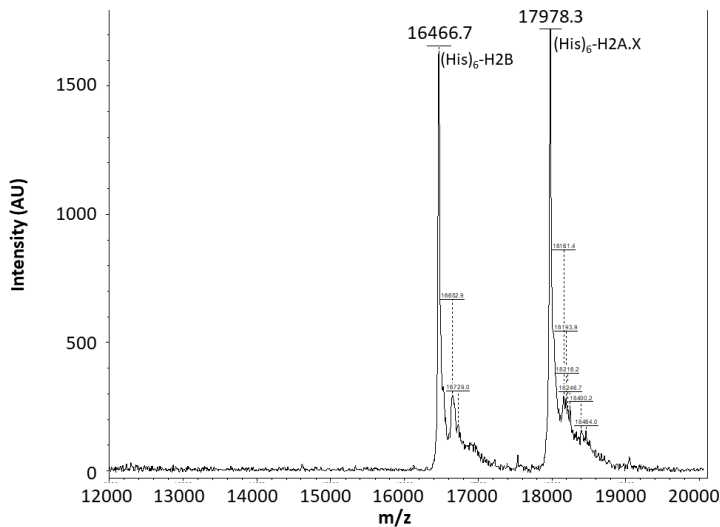


Figure 3.21: MALDI-IMS conformation of the (His)₆-H2A.X-(His)₆-H2B Dimer Prepared from the Modified Refolding System.

MALDI-IMS confirms that (His)₆-H2A.X (17978.3 Da) and (His)₆-H2B (16466.7 Da) are present in the dimer complex reconstituted from the refolding method.

3.15 Discussion: MALDI-IMS Confirmation of the H2A.X-H2B Dimer

MALDI-IMS confirms that all the oligomers have the theoretical amount of respective ratio of histones. No MALDI was performed on the octamer as the octamer is in 2M NaCl, and higher salt concentration solution is not suitable for MALDI-IMS confirmation. MALDI-IMS could not detect the level of γ H2A.X, as phosphate groups are labile to MALDI-IMS environment.

3.15 Result: *In Vitro* Phosphorylation of the H2A.X-H2B Dimer

We predicted that our mutagenized H2A.X is a potential substrate for CK2. In order to test this hypothesis, we performed kinase assay on the dimer prepared from both the refolding and the co-expressed method. 1:20 molar ratio of GST-CK2 to (His)₆-H2A.X-(His)₆-H2B or (His)₆-TEV-H2A.X-H2B dimer was mixed and incubated for 30 minutes at 30°C in presence of 1mM γ ATP. The level of radio-activity increased over time indicating the formation of γ H2A.X over time (Figure 3.22). In the refolded dimer, there was a good amount of non-specific phosphorylation level detected on the H2A.X alanine mutant side, the negative control. It is worth noted again that both the H2A.X and the H2B in the refolded dimer are not separable. Therefore, it is not possible to say from this phosphorscreen image whether H2B also got phosphorylated by CK2.

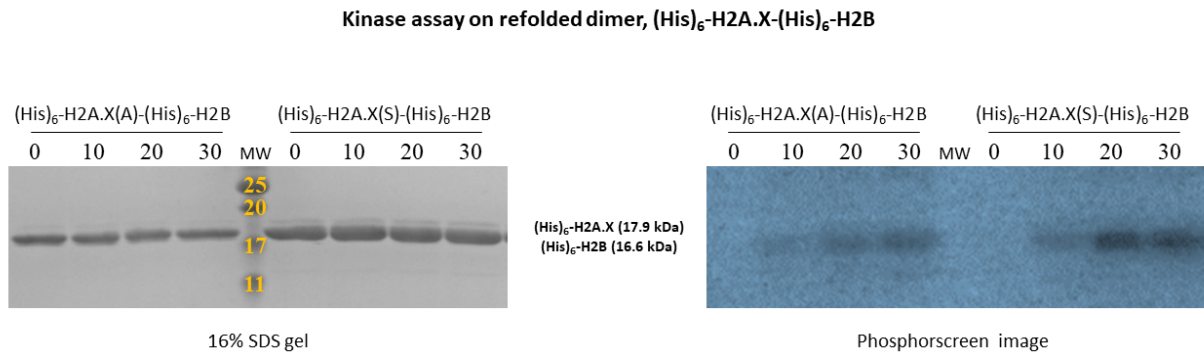


Figure 3.22: Phosphorylation of the Refolded (His)₆-H2A.X-(His)₆-H2B Dimer by the CK2

CK2 mediated phosphorylation of mutagenized H2A.X in order to form γ H2A.X. H2A.X(S139A) was used as a negative control for this assay. Samples were collected every 10 minutes from the reaction mix and were quenched using SDS dye. With time, there was an increase in the level of ³²P incorporation in H2A.X(S). However, a fair level of phosphorylation was detected on the negative H2A.X(A) control.

The dilemma of unresolvable H2A.X and H2B was solved in the co-expressed dimer, where there was a significant size difference between the two histones due to the incorporation of

the tag on only the H2A.X. The kinase assay on the co-expressed dimer confirmed us the source of non-specific phosphorylation. Both the H2A.X(A) and the H2B were phosphorylated by CK2 (Figure 3.23).

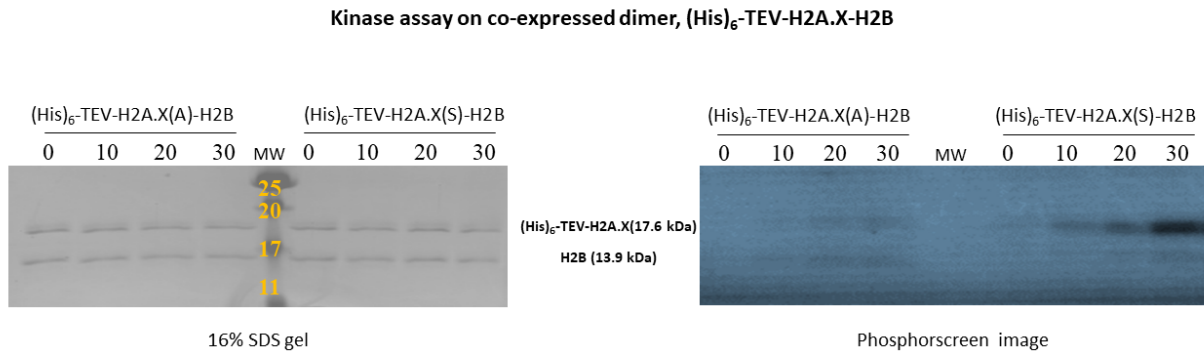


Figure 3.23: Phosphorylation of the Co-expressed (His)₆-H2A.X-H2B Dimer by the CK2

CK2 mediated phosphorylation of mutagenized H2A.X in order to form γ H2A.X. H2A.X(S139A) was used as a negative control for this assay. Samples were collected every 10 minutes from the reaction mix and were quenched using SDS dye. With time, there was an increase in the level of ³²P incorporation in H2A.X(S). However, a low level of non-specific phosphorylation was detected on the negative H2A.X(A) control and also on H2B.

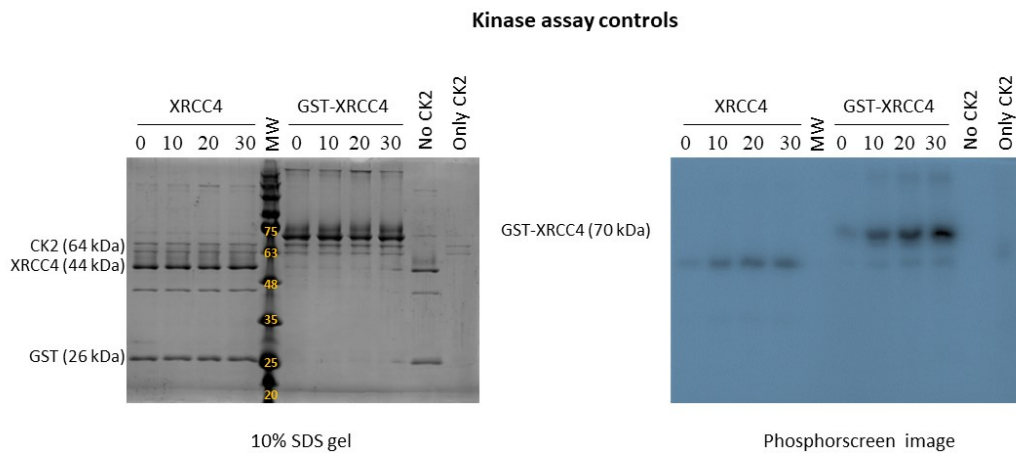


Figure 3.24: Phosphorylation of the XRCC4 by the CK2

CK2 mediated phosphorylation of XRCC4 and GST-XRCC4 were used as a positive control for this kinase assay. The negative controls were CK2 without any substrate (only CK2), and the substrate without any CK2 (No CK2). No signal was detected in the absence of CK2. Minor level of autophosphorylation was detected on CK2 when there was no substrate.

There were some other controls that were tested. Previously, in our lab, we have set up an *in vitro* phosphorylation system for CK2 mediated XRCC4 phosphorylation. Our control showed that CK2 activity was optimal (Figure 3.24).

3.16 Discussion: *In Vitro* Phosphorylation of the H2A.X-H2B Dimer

Kinase assay on the refolded dimer was inconclusive because of the presence of strong non-specific phosphorylation bands on the negative control, H2A.X(A). And, the source of this non-specific phosphorylation was not detectable as H2A.X, and H2B bands were not resolvable on a 16% SDS gel.

However, the source of this non-specific phosphorylation was confirmed from the co-expressed dimer since the co-expressed dimer construct gave resolvable H2A.X and H2B bands. And, it was discovered that both H2A.X(A) and H2B were getting phosphorylated by CK2.

In 2014, Basnet et al. showed that Y57 of H2A is a potential substrate for CK2⁷⁵. Given the fact, H2A.X variant is completely similar in sequence to canonical H2A except that H2A.X has a long C-terminal tail, Y57 is also a potential substrate for CK2 in H2A.X as well. Therefore, this minor level of phosphorylation that was visible on the negative control might rise from pY57.

No evidence of CK2 mediated H2B phosphorylation was reported in the literature. After passing the H2B sequence in the NetPhos 3.1 server, we did not find any potential CK2 phosphorylation site. The highest probability of H2B phosphorylation by CK2 was reported 0.455 on S56 of H2B (--DTG**I**SSKAMG--). Since the dimer used in the kinase assay is not incorporated in the overall nucleosome, the histones in the dimer are more flexible in the solution. Therefore, due to their flexibility, the histones in the dimer are more accessible for the extrinsic proteins.

The CK2 used in this assay was active since it phosphorylated the positive control, XRCC4. There was evidence of the minor level of CK2 autophosphorylation in the assay. The purpose of this CK2 α subunit autophosphorylation is still not understood. According to Donella-Deana et al., Y182 in the CK2 α subunit gets auto-phosphorylated, and this auto-phosphorylation might decrease the catalytic activity of the CK2 enzyme ⁷⁶.

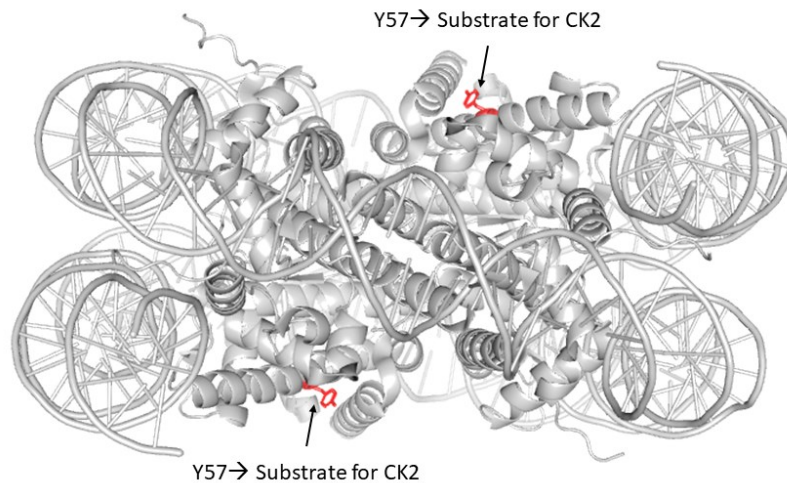


Figure 3.25: Y57 of H2A is a Potential Substrate for the CK2

Y57 of H2A marked in red is a potential CK2 substrate. pY57 regulates transcriptional elongation ⁷⁵.

γ H2A.X was sent for mass spectrometry analysis. However, the mass spectrometry failed to detect the presence of an additional phosphate group on the γ H2A. However, the phosphorylation assay with the radioactive ³²P showed that the mutagenized H2A.X tail could be successfully phosphorylated by the CK2 kinase.

Conclusion & Future Direction

4. Conclusion and Future Direction

In this thesis, we have developed three ways to obtain the histone oligomers. We modified the traditional refolding method for the oligomer reconstitution, where histones were purified under denaturing condition with successive extensive dialysis to reconstitute the histone oligomers. This time and cost ineffective laborious method yielded a lower amount of reconstituted heteromeric histone complexes.

We developed two more purification systems for the histone oligomers based on the duet expression system, where histones pairs were expressed in order to form soluble oligomeric complexes. For the 2nd method, we established a single co-expression purification system where H2A.X, H2B pair, and H3.1, H4 pair are expressed separately in order to form the soluble H2A.X-H2B dimer, and the soluble (H3.1-H4)₂ tetramer respectively. This soluble dimer and the tetramer were mixed together to form the octamer. This process was faster and easier than the traditional refolding method, and the yield for retrieving the histone oligomers was really high as well.

For the 3rd method, we set up a one-step purification of the octamer. For this, we co-co-expressed both H2A.X, H2B and H3.1, H4 pairs at the same time inside the same bacterium in order to extract the (H2A.X-H2B-H3.1-H4)₂ octamer directly without any mixing or dialysis steps. This method was the most cost-effective, and the fastest method that yielded a high amount of the histone octamer. Table 4 shows a comparison between all the different histone oligomer purification process.

The beauty of our purification processes is that if we want to modify (introducing enzymatic PTM markers) the dimer in the overall octamer without modifying the tetramer we might want to use the single co-expression purification system to produce the dimer and the

tetramer separately, and then performing the modification reaction on the oligomer of interest, before reassemble the overall octamer. Our established methods allow us to extract the nucleosomal oligomers in the fastest possible way without repeated hassle (Figure 4.1).

We have also established a quick *in vitro* phosphorylation system to produce the γ H2A.X using the CK2 enzyme. CK2 has a greatly robust activity compared to the uncharacterized ATM kinase that phosphorylates the H2A.X *in vivo* upon DSB. Our radio-labeling kinase assay showed a significant amount of phosphorylation within 30 minutes of the incubation period.

In future, we will produce large quantity of nucleosomal DNA, and will wrap the DNA around the purified octamer to produce the complete nucleosome.

The main purpose of our study is to structurally see how the MDC1-BRCT domain interacts with the γ H2A.X in the context of the overall mono-nucleosome. For that purpose, we have developed purification systems for the nucleosome core particle, and have established an *in vitro* phosphorylation protocol for creating the γ H2A.X. In future, we will perform pull-down assay to see whether our modified γ H2A.X has the capability to interact with MDC1 BRCT domain tightly. We have two constructs of MDC1-BRCT, one with the GST tag and one with the hexahistidine tag. The purpose of having the hexahistidine tagged MDC1-BRCT is to rule out the possibility of seeing an artifact in the MDC1-BRCT-mono-nucleosome interaction due to GST-induced dimerization of MDC1-BRCT.

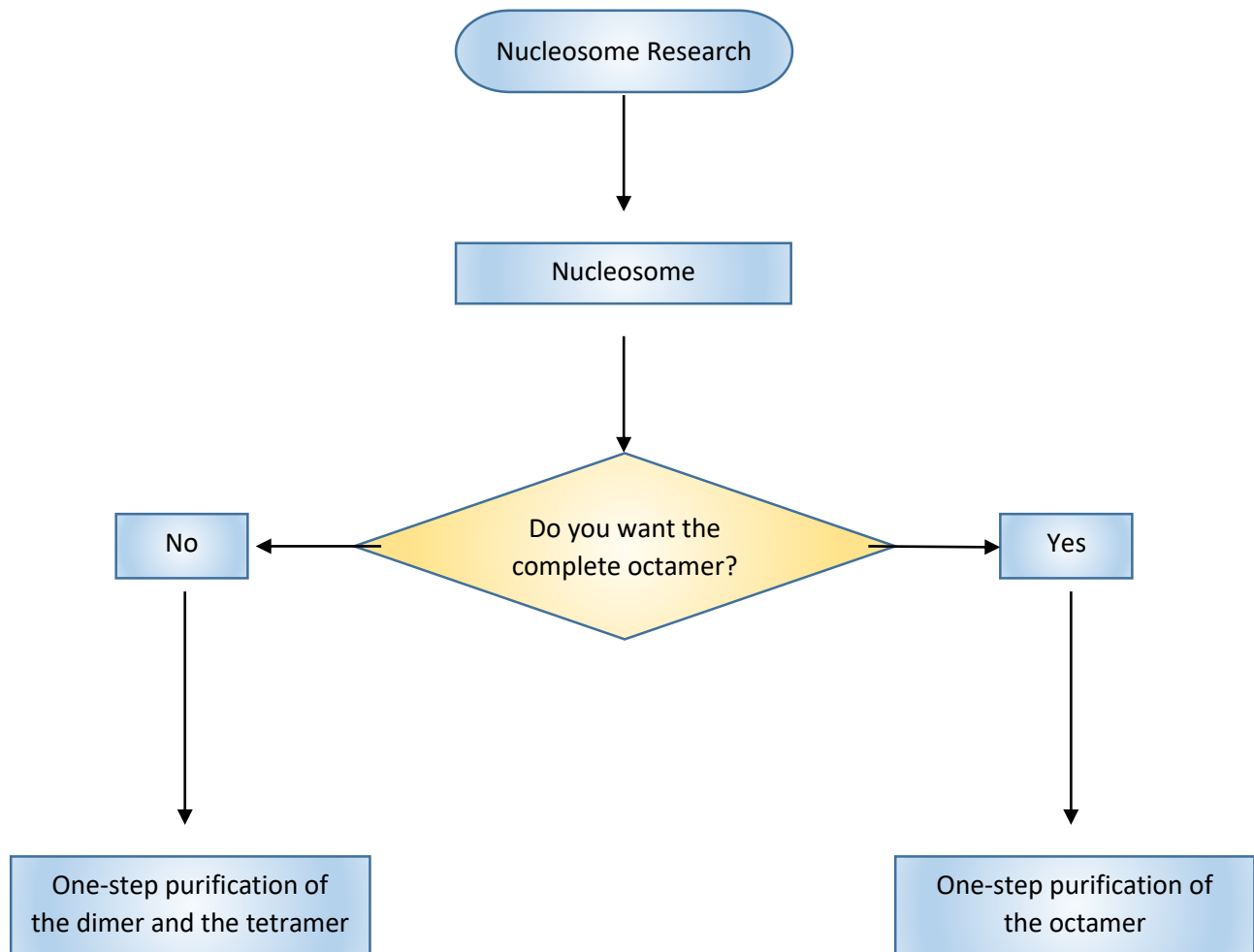


Figure 4.1 Flowchart showing the choice of the histone oligomer purification process.

The two method developed by us will allow the researchers to purify the complete octamer, or to purify the single dimer or the tetramer in order to introduce *in vitro* enzymatic PTMs and hence it would allow them to create modified histone octameric core.

Table 4: A Comparison among all the Purification Processes

Method	Modified refolding of the octamer	One-step purification of the dimer and the tetramer	One-step purification of the octamer
Cell culture	4 liter of each histone = 16 liter	2 liters of TB for the dimer + 4 liters of for the tetramer = 6 liters of TB	4 liters of TB
Urea	3 kg	0 kg	0 kg
NaCl	2 kg	0.5 kg	0.25 kg
Tris-HCl	50 g	20 g	10 g
Glycerol	1.2 liter	0.4 liter	0.2 liter
1M DTT	52 ml	4 ml	2 ml
0.5M EDTA	32 ml	16 ml	8 ml
100mM PMSF	100 ml	50 ml	25 ml
Time	6 days	3 days	2 days
The dimer yield	~30 mg/16 liters	~20 mg/1 liter	0 mg
The tetramer yield	~10 mg/16 liters	~15 mg/1 liter	0 mg
The octamer yield	~5 mg/16 liters	~10 mg/1 liter	~20 mg/1 liter

Following the interaction assay, our aim is to decipher the structural details underlying the interaction between the MDC1-BRCT and the nucleosome. For that purpose, we would like to do a comparative structural analysis using different structure determination techniques. Although high resolution structures of the nucleosome bound different extrinsic protein complexes have been solved using X-ray crystallography, we do not know if the crystallization of MDC1-BRCT bound nucleosome would be feasible. MDC1-BRCT might interact with the nucleosome in a flexible way which might adversely affect its crystallization process. Finding an appropriate crystallization condition might be a lengthy process. On top of that, the protein complex might get orderly arranged in the crystal in a way that might not have any biological significance. Therefore, besides trying to decipher the structure using X-ray crystallography, we would also like to use cryo-electron microscopy (cryo-EM) to decipher the structure. The advantage of cryo-electron microscopy is that it does not require the crystal to be formed and the native state of the sample can be cryo-fixed in the vitreous ice. However, cryo-EM might not provide as high resolution as X-ray crystallography, but it might allow us to decipher different dynamic structures that might be induced by the MDC1-BRCT in the nucleosome remodeling. Lastly, we would also like to perform small angle X-ray scattering (SAXS) to figure out how the complex of MDC1-BRCT-Nucleosome behaves in the solution. SAXS will provide us with spherical averaged low resolution data. SAXS data in combination with cryo-EM data would allow us to create the best 3D-electron density map⁶⁶. Through combining all these different structure determination techniques, we will be able to decipher the most biologically relevant structure of the MDC1-BRCT bound nucleosome.

This MDC1-BRCT bound nucleosome would also allow us to solve the conundrum that involves with the MDC1 independent Ring1A-BMI1 mediated mono-ubiquitination of the nucleosome. It will allow us to see whether the MDC1-BRCT bound γ H2A.X containing

nucleosome can also be mono-ubiquitinated, or whether the mono-ubiquitinated γ H2A.X containing nucleosome can still interact with the MDC1-BRCT domain.

Since the MDC1-nucleosome interaction is one of the early primary events in response to DSB, understanding the structural basis of this interaction will reveal a lot of the elusive DSB repair pathways, and hence, later on, this information might open up a new avenue for battling with the cancers that are associated with the DSB repair defects.

References

1. Alberts, B., Johnson, A., Lewis, J., Raff, M., Roberts, K., & Walter, P. (2002). *The RNA world and the origins of life* (4th ed.). New York: Garland Science.
2. Swenberg, J. A., Lu, K., Moeller, B. C., Gao, L., Upton, P. B., Nakamura, J., & Starr, T. B. (2011). Endogenous versus exogenous DNA adducts: Their role in carcinogenesis, epidemiology, and risk assessment. *Toxicological Sciences*, *120*(suppl_1), S145.
doi:10.1093/toxsci/kfq371
3. Lodish, H., Berk, A., Zipursky, S. L., Matsudaira, P., Baltimore, D., & Darnell, J. (2000). DNA damage and repair and their role in carcinogenesis. *Molecular cell biology* (4th ed.). New York: W. H. Freeman.
4. O'Connor, M. J. (2015). Targeting the DNA damage response in cancer. *Molecular Cell*, *60*(4), 547-560. doi:10.1016/j.molcel.2015.10.040
5. Giglia-Mari, G., Zotter, A., & Vermeulen, W. (2011). DNA damage response. *Cold Spring Harbor Perspectives in Biology*, *3*(1) doi:10.1101/cshperspect.a000745
6. Weinert, T., & Hartwell, L. (1989). Control of G2 delay by the rad9 gene of *Saccharomyces cerevisiae*. *Journal of Cell Science, Supplement 12*, 145–148.
7. Plesca, D., Mazumder, S., & Almasan, A. (2008). Chapter 6 DNA damage response and apoptosis. *Methods in enzymology* (pp. 107-122) Academic Press. Retrieved from <http://www.sciencedirect.com/science/article/pii/S0076687908016066>
8. Zhou, B. S., & Elledge, S. J. (2000). The DNA damage response: Putting checkpoints in perspective. *Nature*, *408*(6811), 433-439. doi:10.1038/35044005
9. Dantuma, N. P., & Attikum, H. (2016). Spatiotemporal regulation of posttranslational modifications in the DNA damage response. *The EMBO Journal*, *35*(1), 6-23.
doi:10.15252/emj.201592595

10. Kolodner, R. (1996). Biochemistry and genetics of eukaryotic mismatch repair. *Genes & Development*, 10(12), 1433-1442. doi:10.1101/gad.10.12.1433
11. Guo-Min Li. (2008). Mechanisms and functions of DNA mismatch repair. *Cell Research*, 18(1), 85-98. doi:10.1038/cr.2007.115
12. Jiricny, J. (2013). Postreplicative mismatch repair. *Cold Spring Harbor Perspectives in Biology*, 5(4), online. doi:doi/10.1101/cshperspect.a012633
13. Caldecott, K. W. (2014). DNA single-strand break repair. *Experimental Cell Research*, 329(1), 2-8. doi:10.1016/j.yexcr.2014.08.027
14. Samuel H Wilson, William A Beard, David D Shock, Vinod K Batra, Nisha A Cavanaugh, Rajendra Prasad, . . . Michelle L Heacock. (2010). Base excision repair and design of small molecule inhibitors of human DNA polymerase β . *Cellular and Molecular Life Sciences : CMLS*, 67(21), 3633-3647. doi:10.1007/s00018-010-0489-1
15. Krokan, H. E., & Bjørås, M. (2013). Base excision repair. *Cold Spring Harbor Perspectives in Biology*, 5(4), a012583. doi:10.1101/cshperspect.a012583
16. Marteijn, J. A., Lans, H., Vermeulen, W., & Hoeijmakers, J. H. J. (2014). Understanding nucleotide excision repair and its roles in cancer and ageing. *Nature Reviews Molecular Cell Biology*, 15(7), 465. 10.1038/nrm3822 Retrieved from <https://www.nature.com/articles/nrm3822>
17. Porro, A. (2016). Editorial: Grappling with the multifaceted world of the DNA damage response. *Frontiers in Genetics*, 7 doi:10.3389/fgene.2016.00091
18. Hoeijmakers, J. H. J. (2001). Genome maintenance mechanisms for preventing cancer. *Nature*, 411(6835), 366. doi:10.1038/35077232

19. Michael R. Lieber. (2008). The mechanism of human nonhomologous DNA end joining. *Journal of Biological Chemistry*, 283(1), 1-5. doi:10.1074/jbc.R700039200
20. San Filippo, J., Sung, P., & Klein, H. (2008). Mechanism of eukaryotic homologous recombination. *Annual Review of Biochemistry*, 77(1), 229-257. doi:10.1146/annurev.biochem.77.061306.125255
21. Blanpain, C., Mohrin, M., Sotiropoulou, P. A., & Passegué, E. (2011). DNA-damage response in tissue-specific and cancer stem cells. *Cell Stem Cell*, 8(1), 16-29. doi:10.1016/j.stem.2010.12.012
22. Annunziato, A. DNA packaging: Nucleosomes and chromatin. *Nature Education*, 1(1), 26. Retrieved from <https://www.nature.com/scitable/topicpage/dna-packaging-nucleosomes-and-chromatin-310>
23. Olins, A. L., & Olins, D. E. (2003). Chromatin history: Our view from the bridge. *Nature Reviews Molecular Cell Biology*, 4(10), 809-814. doi:10.1038/nrm1225
24. Reece, J. B., Urry, L. A., Cain, M. L., Wasserman, S. A., Minorsky, P. V., Jackson, R., & Campbell, N. A. (2010). Chapter 16: The molecular basis of inheritance. *Campbell biology* (9th ed., pp. 305-324). Boston: Pearson.
25. Baxevanis, A. D., & Landsman, D. (1996). Histone sequence database: A compilation of highly-conserved nucleoprotein sequences. *Nucleic Acids Research*, 24(1), 245-247. doi:10.1093/nar/24.1.245
26. Arents, G., Burlingame, R. W., Wang, B. C., Love, W. E., & Moudrianakis, E. N. (1991). The nucleosomal core histone octamer at 3.1 Å resolution: A tripartite protein assembly and a left-handed superhelix. *Proceedings of the National Academy of Sciences*, 88(22), 10148-10152.

27. Dutnall, R. N., & Ramakrishnan, V. (1997). Twists and turns of the nucleosome: Tails without ends. *Structure*, 5(10), 1255-1259. doi:10.1016/S0969-2126(97)00276-1
28. Maze, I., Noh, K., Soshnev, A. A., & Allis, C. D. (2014). Every amino acid matters: Essential contributions of histone variants to mammalian development and disease. *Nature Reviews Genetics*, 15(4), 259. doi:10.1038/nrg3673
29. Strahl, B. D., & Allis, C. D. (2000). The language of covalent histone modifications. *Nature*, 403(6765), 41-45. 10.1038/47412 Retrieved from <http://dx.doi.org/10.1038/47412>
30. Fernandez-Capetillo, O., Lee, A., Nussenzweig, M., & Nussenzweig, A. (2004). H2AX: The histone guardian of the genome. *DNA Repair*, 3(8), 959-967. doi:10.1016/j.dnarep.2004.03.024
31. Robert, X., & Gouet, P. (2014). Deciphering key features in protein structures with the new ENDscript server. *Nucleic Acids Research*, 42(W1), W324. doi:10.1093/nar/gku316
32. Firsanov, D. V., Solovjeva, L. V., & Svetlova, M. P. (2011). H2AX phosphorylation at the sites of DNA double-strand breaks in cultivated mammalian cells and tissues. *Clinical Epigenetics*, 2(2), 283. doi:10.1007/s13148-011-0044-4
33. Kinner, A., Wu, W., Staudt, C., & Iliakis, G. (2008). γ -H2AX in recognition and signaling of DNA double-strand breaks in the context of chromatin. *Nucleic Acids Research*, 36(17), 5678. doi:10.1093/nar/gkn550
34. Kuo, L. J., & Yang, L. (2008). Gamma-H2AX - a novel biomarker for DNA double-strand breaks. *In Vivo (Athens, Greece)*, 22(3), 305-309.

35. Georgoulis, A., Vorgias, C. E., Chrousos, G. P., & Rogakou, E. P. (2017). Genome instability and γ H2AX. *International Journal of Molecular Sciences*, 18(9) doi:10.3390/ijms18091979
36. Celeste, A., Petersen, S., Romanienko, P. J., Fernandez-Capetillo, O., Chen, H. T., Sedelnikova, O. A., . . . Nussenzweig, A. (2002). Genomic instability in mice lacking histone H2AX. *Science (New York, N.Y.)*, 296(5569), 922-927. doi:10.1126/science.1069398
37. McKinnon, P. J. (2004). ATM and ataxia telangiectasia: Second in molecular medicine review series. *EMBO Reports*, 5(8), 772-776. doi:10.1038/sj.embor.7400210
38. Redon, C. E., Nakamura, A. J., Sordet, O., Dickey, J. S., Gouliava, K., Tabb, B., Lawrence, S., Kinders, R. J., Bonner, W. M., Sedelnikova, O. A. (2010). Chapter 14: γ -H2AX Detection in Peripheral Blood Lymphocytes, Splenocytes, Bone Marrow, Xenografts, and Skin. In V. Didenko (Ed.), *DNA Damage Detection In Situ, Ex Vivo, and In Vivo* (pp. 249-270). Totowa, NJ: Humana Press.
39. Daniel, J., Pellegrini, M., Lee, B., Guo, Z., Filsuf, D., Belkina, N., . . . Nussenzweig, A. (2012). Loss of ATM kinase activity leads to embryonic lethality in mice. *The Journal of Cell Biology*, 198(3), 295. Retrieved from https://digitalcommons.wustl.edu/open_access_pubs/1203
40. Cortez, D., & Cimprich, K. A. (2008). ATR: An essential regulator of genome integrity. *Nature Reviews Molecular Cell Biology*, 9(8), 616-627. doi:10.1038/nrm2450
41. Falck, J., Jackson, S. P., & Coates, J. (2005). Conserved modes of recruitment of ATM, ATR and DNA-PKcs to sites of DNA damage. *Nature*, 434(7033), 605-611. doi:10.1038/nature03442

42. Lu, C., Zhu, F., Cho, Y., Tang, F., Zykova, T., Ma, W., . . . Dong, Z. (2006). Cell apoptosis: Requirement of H2AX in DNA ladder formation, but not for the activation of caspase-3. *Molecular Cell*, 23(1), 121-132. doi:10.1016/j.molcel.2006.05.023
43. Rogakou, E. P., Boon, C., Redon, C., & Bonner, W. M. (1999). Megabase chromatin domains involved in DNA double-strand breaks in vivo. *The Journal of Cell Biology*, 146(5), 905-916.
44. Nakamura, A. J., Rao, V. A., Pommier, Y., & Bonner, W. M. (2010). The complexity of phosphorylated H2AX foci formation and DNA repair assembly at DNA double-strand breaks. *Cell Cycle*, 9(2), 389-397. doi:10.4161/cc.9.2.10475
45. Rouse, J., & Jackson, S. P. (2002). Interfaces between the detection, signaling, and repair of DNA damage. *Science (New York, N.Y.)*, 297(5581), 547-551. 10.1126/science.1074740
46. Lamarche, B. J., Orazio, N. I., & Weitzman, M. D. (2010). The MRN complex in double-strand break repair and telomere maintenance. *FEBS Letters*, 584(17), 3682-3695. doi:10.1016/j.febslet.2010.07.029
47. Ying Zhang, Junqing Zhou, & Chang Uk Lim. (2006). The role of NBS1 in DNA double strand break repair, telomere stability, and cell cycle checkpoint control. *Cell Research*, 16(1), 45-54. doi:10.1038/sj.cr.7310007
48. Jager, M. D., Noort, J. V., Gent, D. C. V., Dekker, C., Kanaar, R., & Wyman, C. (2001). Human Rad50/Mre11 is a flexible complex that can tether DNA ends. *Molecular Cell*, 8(5), 1129-1135. doi:10.1016/S1097-2765(01)00381-1
49. Lee, J., & Paull, T. T. (2004). Direct activation of the ATM protein kinase by the Mre11/Rad50/Nbs1 complex. *Science (New York, N.Y.)*, 304(5667), 93-96. doi:10.1126/science.1091496

50. Huen, M. S. Y., Grant, R., Manke, I., Minn, K., Yu, X., Yaffe, M. B., & Chen, J. (2007). RNF8 transduces the DNA-damage signal via histone ubiquitylation and checkpoint protein assembly. *Cell*, *131*(5), 901-914. doi:10.1016/j.cell.2007.09.041
51. Doil, C., Mailand, N., Bekker-Jensen, S., Menard, P., Larsen, D. H., Pepperkok, R., . . . Lukas, C. (2009). RNF168 binds and amplifies ubiquitin conjugates on damaged chromosomes to allow accumulation of repair proteins. *Cell*, *136*(3), 435-446. 10.1016/j.cell.2008.12.041 Retrieved from [http://www.cell.com/cell/abstract/S0092-8674\(09\)00004-X](http://www.cell.com/cell/abstract/S0092-8674(09)00004-X)
52. Horslund, T., Ripplinger, A., Hoffmann, S., Wild, T., Uckelmann, M., Villumsen, B., . . . Mailand, N. (2015). Histone H1 couples initiation and amplification of ubiquitin signalling after DNA damage. *Nature*, *527*(7578), 389. doi:10.1038/nature15401
53. Mattioli, F., Vissers, J. A., van Dijk, W., Ikpa, P., Citterio, E., Vermeulen, W., . . . Sixma, T. (2012). RNF168 Ubiquitinates K13-15 on H2A/H2AX to drive DNA damage signaling. *Cell*, *150*(6), 1182-1195. doi:10.1016/j.cell.2012.08.005
54. Gatti, M., Pinato, S., Maiolica, A., Rocchio, F., Prato, M. G., Aebersold, R., & Penengo, L. (2015). RNF168 promotes noncanonical K27 ubiquitination to signal DNA damage. *Cell Reports*, *10*(2), 226-238. doi:10.1016/j.celrep.2014.12.021
55. Stucki, M., Clapperton, J. A., Mohammad, D., Yaffe, M. B., Smerdon, S. J., & Jackson, S. P. (2005). MDC1 directly binds phosphorylated histone H2AX to regulate cellular responses to DNA double-strand breaks. *Cell*, *123*(7), 1213-1226. doi:10.1016/j.cell.2005.09.038
56. Hofmann, K., Shechter, D., Ishibe-Murakami, S., Patel, D. J., Li, H., Tempst, P., . . . Erdjument-Bromage, H. (2009). WSTF regulates the H2A.X DNA damage response via a novel tyrosine kinase activity. *Nature*, *457*(7225), 57-62. doi:10.1038/nature07668

57. Singh, N., Basnet, H., Wiltshire, T. D., Mohammad, D. H., Thompson, J. R., Héroux, A., . . . Mer, G. (2012). Dual recognition of phosphoserine and phosphotyrosine in histone variant H2A.X by DNA damage response protein MCPH1. *Proceedings of the National Academy of Sciences*, *109*(36), 14381-14386.
58. Rosenfeld, M. G., Cook, P. J., Glass, C. K., Wang, X., Ju, B. G., & Telese, F. (2009). Tyrosine dephosphorylation of H2AX modulates apoptosis and survival decisions. *Nature*, *458*(7238), 591-596. doi:10.1038/nature07849
59. Fyodorov, D. V., Zhou, B., Skoultchi, A. I., & Bai, Y. (2018). Emerging roles of linker histones in regulating chromatin structure and function. *Nature Reviews Molecular Cell Biology*, *19*(3), 192. 10.1038/nrm.2017.94 Retrieved from <https://www.nature.com/articles/nrm.2017.94>
60. Navasona Krishnan, Dae Gwin Jeong, Suk-Kyeong Jung, Seong Eon Ryu, Andrew Xiao, C. David Allis, . . . Nicholas K. Tonks. (2009). Dephosphorylation of the C-terminal tyrosyl residue of the DNA damage-related histone H2A.X is mediated by the protein phosphatase eyes absent. *Journal of Biological Chemistry*, *284*(24), 16066-16070. doi:10.1074/jbc.C900032200
61. Jungmichel, S., Clapperton, J. A., Lloyd, J., Hari, F. J., Spycher, C., Pavic, L., . . . Smerdon, S. J. (2012). The molecular basis of ATM-dependent dimerization of the Mdc1 DNA damage checkpoint mediator. *Nucleic Acids Research*, *40*(9), 3913-3928. doi:10.1093/nar/gkr1300
62. Kolas, N. K., Chapman, J. R., Nakada, S., Ylanko, J., Chahwan, R., Sweeney, F. D., . . . Durocher, D. (2007). Orchestration of the DNA-damage response by the RNF8 ubiquitin ligase. *Science (New York, N.Y.)*, *318*(5856), 1637-1640. doi:10.1126/science.1150034

63. Panier, S., & Durocher, D. (2013). Push back to respond better: Regulatory inhibition of the DNA double-strand break response. *Nature Reviews Molecular Cell Biology*, *14*(10), 661. doi:10.1038/nrm3659
64. Ismail, I. H., Andrin, C., McDonald, D., & Hendzel, M. J. (2010). BMI1-mediated histone ubiquitylation promotes DNA double-strand break repair. *The Journal of Cell Biology*, *191*(1), 45-60. doi:10.1083/jcb.201003034
65. Facchino, S., Abdouh, M., Chatoo, W., & Bernier, G. (2010). BMI1 confers radioresistance to normal and cancerous neural stem cells through recruitment of the DNA damage response machinery. *The Journal of Neuroscience: The Official Journal of the Society for Neuroscience*, *30*(30), 10096-10111. doi:10.1523/JNEUROSCI.1634-10.2010
66. Kim, J. S., Afsari, B., & Chirikjian, G. S. (2017). Cross-validation of data compatibility between small angle X-ray scattering and cryo-electron microscopy. *Journal of Computational Biology*, *24*(1), 13-30. 10.1089/cmb.2016.0139 Retrieved from <http://www.liebertonline.com/doi/abs/10.1089/cmb.2016.0139>
67. Sarno, S., Vaglio, P., Marin, O., Issinger, O., Ruffato, K., & Pinna, L. A. (1997). Mutational analysis of residues implicated in the interaction between protein kinase CK2 and peptide substrates. *Biochemistry*, *36*(39), 11717-11724. 10.1021/bi9705772 Retrieved from <https://doi.org/10.1021/bi9705772>
68. Klug, A., Rhodes, D., Smith, J., Finch, J. T., & Thomas, J. O. (1980). A low resolution structure for the histone core of the nucleosome. *Nature*, *287*(5782), 509. 10.1038/287509a0 Retrieved from <https://www.nature.com/articles/287509a0>
69. Richmond, T. J., Finch, J. T., Rushton, B., Rhodes, D., & Klug, A. (1984). *Structure of the nucleosome core particle at 7 Å resolution* Nature Publishing Group.10.1038/311532a0 Retrieved from <https://www.nature.com/articles/311532a0>

70. Luger, K., Mäder, A. W., Richmond, R. K., Sargent, D. F., & Richmond, T. J. (1997). Crystal structure of the nucleosome core particle at 2.8 Å resolution. *Nature*, 389(6648), 251-260. 10.1038/38444
71. McGinty, R., K., & Tan, S. (2015). Nucleosome structure and function. *Chemical Reviews*, 115(6), 2255-2273. 10.1021/cr500373h Retrieved from <https://www.ncbi.nlm.nih.gov/pmc/articles/PMC4378457/>
72. Lowary, P. T., & Widom, J. (1998). New DNA sequence rules for high affinity binding to histone octamer and sequence-directed nucleosome positioning. Edited by T. richmond. *Journal of Molecular Biology*, 276(1), 19-42. 10.1006/jmbi.1997.1494 Retrieved from <http://www.sciencedirect.com/science/article/pii/S0022283697914947>
73. Zhao, Y., Jordan, I. K., & Lunyak, V. V. (2013). Epigenetics components of aging in the central nervous system. *Neurotherapeutics*, 10(4), 647-663. 10.1007/s13311-013-0229-y Retrieved from <https://link.springer.com/article/10.1007/s13311-013-0229-y>
74. Mermershtain, I., & Glover, J. N. M. (2013). Structural mechanisms underlying signaling in the cellular response to DNA double strand breaks. *Mutation Research*, 750(1-2), 15. 10.1016/j.mrfmmm.2013.07.004 Retrieved from <http://www.ncbi.nlm.nih.gov/pubmed/23896398>
75. Basnet, H., Su, X. B., Tan, Y., Meisenhelder, J., Merkurjev, D., Ohgi, K. A., . . . Rosenfeld, M. G. (2014). Tyrosine phosphorylation of histone H2A by CK2 regulates transcriptional elongation. *Nature*, 516(7530), 267-271. doi:10.1038/nature13736
76. Donella-Deana, A., Cesaro, L., Sarno, S., Brunati, A. M., Ruzzene, M., & Pinna, L. A. (2001). Autocatalytic tyrosine-phosphorylation of protein kinase CK2 α and α' subunits: Implication of Tyr182. *Biochemical Journal*, 357(2), 563. doi:10.1042/0264-6021:3570563

77. Luger, K., Rechsteiner, T. J., & Richmond, T. J. (1999). Expression and purification of recombinant histones and nucleosome reconstitution. *Chromatin protocols* (pp. 1-16) Humana Press. Retrieved from <https://link.springer.com/protocol/10.1385/1-59259-681-9:1>
78. Tanaka, Y., Tawaramoto-Sasanuma, M., Kawaguchi, S., Ohta, T., Yoda, K., Kurumizaka, H., & Yokoyama, S. (2004). Expression and purification of recombinant human histones. *Methods*, 33(1), 3-11. 10.1016/j.ymeth.2003.10.024 Retrieved from <http://www.sciencedirect.com/science/article/pii/S1046202303002883>

Appendices

Appendix i Vectors, Primers, Restriction Enzymes, and Antibiotics

Table i-1 Specifications of the used vectors and the designed primers.

Cloning Vector	Antibiotic Resistance	Pull Down Tag	Cleavage Site	Primer Name [Direction-RE-(Protease)-Histone]	Primer Sequence [green- Restriction site, purple – TEV cleavage site]
pET47b(+) (single expression system)	Kanamycin	Hexa-histidine	HRV-3C Protease	Forward-EcoRI-H2A.X	GGCTCGCGAATTCTATGTCGGGCCGCGGC
				Reverse-HindIII-H2A.X(CK2-S)	GCGGCCGCAAGCTTAGTACTCCTCGGAGTCC
				Reverse-HindIII-H2A.X(CK2-A)	ACCAGAAAGCTTCTATTAGTACTCCTCGCGTCC
				Forward-BamHI-H2B	GGTACCAGGATCCGATGCCAGAGCCAGCG
				Reverse-HindIII-H2B	GCCCCGTAAGCTTGCCTACTTAGCGCTGGT
				Forward-BamHI-H3.1	GGCTCGCGGATCCCATGGCTCGTACTAAC
				Reverse-HindIII-H3.1	CGCCAGGCCAAGCTTCTACGCTCTTTCTCC
				Forward-BamHI-H4	CTTGATGGATCCTATGAGCGGCCGCGGCAAAG
			Reverse-HindIII-H4	CGGGCCAAGCTTCCGTAAACCGCCAAAACC	
			Tev Protease	Forward-BamHI-TEV-MDC1-BRCT	CATATAGGATCCAGAGAACCTCTACTTCCAAGGCACAGCCCCCAAAGTG
Reverse-HindIII-MDC1-BRCT	CGCCCCGCAAGCTTTCAGGTGGATGACATC				
pETDuet-1 (Co-expression system)	Ampicillin	Hexa-histidine (MCS 1)	Tev Protease	Forward-BamHI-TEV-H2B	CAGCCAGGATCCAGAGAACCTCTACTTCCAAGGCATGCCAGAGCCAGCG
				Reverse-HindIII-H2B	GCCCCGTAAGCTTGCCTACTTAGCGCTGGT
		None (MCS 2)	None	Forward-NdeI-H2A.X	GATATACATATGTCGGGCCGCGGCAAGACTG

				Reverse-XhoI-H2A.X(CK2-S)	ACCAGACTCGAGCTATTAGTACTCCTC GGAGTCC
				Reverse-XhoI-H2A.X(CK2-A)	ACCAGACTCGAGCTATTAGTACTCCTC GGCGTCC
		Hexa- histidine (MCS 1)	Tev Protease	Forward-BamHI-TEV-H2A.X	AATTTAGGATCCAGAGAACCTCTACTT CCAAGGCATGTGCGGGCCGCGCAAG
				Reverse-HindIII-H2A.X(CK2-S)	GCGGCCGCAAGCTTAGTACTCCTCGGA GTCC
				Reverse-HindIII-H2A.X(CK2-A)	ACCAGAAAGCTTCTATTAGTACTCCTC GGCGTCC
		None (MCS1)	None	Forward-NcoI-H2A.X	GATATACCATGGGCTCGGGCCGCGGC AAGACTG
		None (MCS 2)	None	Forward-NdeI-H2B	CGCCACATATGCCAGAGCCAGCGAA GTC
				Reverse-XhoI-H2B	CGTGGGCCTCGAGACTACTTAGCGCTG GTG
pACYCDuet-1 (Co-expression system)	Chloramphenicol	Hexa- histidine (MCS 1)	Tev Protease	Forward-BamHI-TEV-H4	CAGCCAGGATCCAGAGAACCTCTACTT CCAAGGCATGAGCGGCCGCGGC
				Reverse-HindIII-H4	CGGGCCAAGCTTCCGTTAACCGCCAAA ACC
		None (MCS 2)	None	Forward-NdeI-H3.1	GATATACATATGGCTCGTACTAAACAG ACAGCTCGG
				Reverse-XhoI-H3.1	ACCAGACTCGAGTTACTACGCTCTTTC TCC
pCDFDuet-1 (Co-expression system)	Streptomycin	Hexa- histidine (MCS 1)	Tev Protease	Forward-BamHI-Tev-H3.1	TAATTAGGATCCAGAGAACCTCTACTT CCAAGGCATGGCTCGTACTAAACAG
				Reverse-HindIII-H3.1	CGCCAGGCCAAGCTTCTACGCTCTTTC TCC
		None (MCS1)	None	Forward-NcoI-H3.1	CGCTCGGCCATGGCTCGTACTAAAC
		None (MCS 2)	None	Forward-NdeI-H4	GATATACATATGAGCGGCCGCGGCAA AGG
				Reverse-XhoI-H4	CGGGGACTCGAGTTATTAACCGCCAAA ACC

Table i-2 List of bacterial expression cell lines with their intrinsic antibiotic resistance.

Cell line	Intrinsic Antibiotic Resistance
BL21(DE3) (Invitrogen Cat. #C600003)	None
BL21(DE3)pLysS (Invitrogen Cat. # C606003)	Chloramphenicol
C41(DE3) (Lucigen Cat. # 60442-1)	None
C43(DE3) (Lucigen Cat. # 60446-1)	None
Rosetta 2 (Novagen Cat. # 71402-3)	Chloramphenicol
Rosetta 2(DE3) (Novagen Cat. # 71400-3)	Chloramphenicol

Appendix ii Protocols

Protocol 1: Polymerase Chain Reaction (PCR): Touch Down

1. Setup the reaction mix in a flat-headed PCR tube (Table ii-p1.1).

Table ii-p1.1: Touch Down PCR Reaction Table.

For Touch Down PCR, each reaction tube will contain the following:

PCR Machine program: Subdirectory 8: Dave, Program #: 7 TCHDWN

Reagents	Volume (µl)
PCR Supermix (Invitrogen, Lot #: 1830570)	45
Forward Primer	1.5
Reverse Primer	1.5
Template DNA	2
	Total = 50

2. Calculate the extension time from the size of the PCR products (Table ii-p1.2).

Table ii-p1.2: PCR product sizes and the calculated PCR extension time:

PCR Product	Size (NTs)	Calculated Extension Time (Seconds) = ((60*Product Size)/1000)	Actual Extension Time (Seconds)
EcoRI-H2A.X(CK2-S)-HindIII	455	27.3	29
EcoRI-H2A.X(CK2-A)-HindIII	455	27.3	29
BamHI-H2B-HindIII	411	24.7	29
BamHI-H3.1-HindIII	440	26.4	29
BamHI-H4-HindIII	340	20.4	29
BamHI-TEV-H2A.X(CK2-S)-HindIII	478	28.7	29
BamHI-TEV-H2A.X(CK2-A)-HindIII	478	28.7	29
NdeI-H2B-XhoI	404	24.2	29

BamHI-TEV-H2B-HindIII	430	25.8	29
NdeI-H2A.X(CK2-S)-XhoI	441	26.5	29
NdeI-H2A.X(CK2-A)-XhoI	441	26.5	29
BamHI-TEV-H3.1-HindIII	459	27.5	29
NdeI-H4-XhoI	336	20.2	29
BamHI-TEV-H4-HindIII	360	21.6	29
NdeI-H3.1-XhoI	420	25.2	29
NcoI-H2A.X(CK2-S)-HindIII	455	27.3	29
NcoI-H2A.X(CK2-A)-HindIII	455	27.3	29
NcoI-H3.1-HindIII	435	26.1	29
BamHI-TEV-MDC1-HindIII	647	38.8	40

3. Run the PCR machine with the following protocol.
 - a. Turn the machine on. It will take some time for the machine to load all the directory.
 - b. Press C “programs”.
 - c. Choose the appropriate subdirectory. For Touch Down PCR, choose “8. Subdirect: Dave !!!”
 - d. Press D “enter”.
 - e. To choose the appropriate program to run, press A “list”.
 - f. Select the program you want to run by pressing the direction arrows. For Touch Down PCR, choose “7. TCHDWN”.
 - g. No alteration to the program is necessary except for the extension time (Table 2.1.1.3). For Touch Down PCR, keep on pressing the downward key until you reach line 21. Press the right direction key, to choose the time, and alter it to the desired value.
 - h. Press C “pgm OK”.
 - i. Press B “start/stop”.

- j. Choose the appropriate subdirectory again. For Touch Down PCR, choose “8. Subdirect: Dave !!!”.
- k. Press D “start”.

Protocol 2: Colony PCR

- 1. Setup the reaction mix in a flat-headed PCR tube (Table ii-p2.1).

Table ii-p2.1: Colony PCR Reaction Table

For Colony PCR, a reaction mix for 10 PCR will contain the following (15µl reaction mix/tubes):

PCR Machine Program: (Subdirectory 1: Mike, Program #: 1 RT-TAQQ)

Reagents	Volume (µl)
ddH ₂ O	61.6
R-Taq 2X Mix (B-Bridge, 1.5mM MgCl ₂ , Lot #: 130320K)	75
Forward Primer	6.7
Reverse Primer	6.7
	Total = 150

- 2. Turn the Bunsen burner on.
- 3. Pick up a single colony with a 10 µl pipette tip, and rub it against the bottom of the PCR reaction tube.
- 4. Store the tip in a 1.5ml Eppendorf tube.
- 5. Add 15µl of reaction mix to each PCR reaction tube (Up to 9 PCR reaction for a 150µl reaction mix)
- 6. Place the PCR reaction tubes in the PCR machine.
- 7. Turn the machine on. It will take some time for the machine to load all the directory.
- 8. Press C “programs”.
- 9. Choose the appropriate subdirectory. For Colony PCR, choose “1. Subdirect.: Mike !!!!”.
- 10. Press D “enter”.

11. To choose the appropriate program to run, press A “list”.
12. Select the program you want to run by pressing the direction arrows. For Colony PCR, choose “1. RT-TAQQ”.
13. No alteration to the program is necessary except for the extension time (Table 2.1.1.3). For Colony PCR, keep on pressing the downward key until you reach line 4. Press the right direction key, to choose the time, and alter it to desired value.
14. Press C “pgm OK”.
15. Press B “start/stop”.
16. Choose the appropriate subdirectory again. For Colony PCR, choose “1. Subdirect.: Mike !!!!”.
17. Press D “start”.
18. After the PCR, confirm the PCR products on a 1.5% agarose gel (Protocol 7).
19. Positive colonies were regrown, and recombinant DNA construct was extracted using Plasmid MiniPrep (Protocol 8).

Protocol 3: PCR Cleanup Protocol

Using TruIn Science PCR Clean-up kit (Cat. # KTS1115), PCR products were cleaned up following the protocol supplied with the kit.

Protocol 4: Double Restriction Digest Reaction

1. Setup a reaction in an Eppendorf tube (Table ii-p4.1).

Table ii-p4.1: Double Digest Reaction Setup

Reagents	Volume (µl)
DNA solution	49
10X FastDigest Buffer (Cat. # B64)	6 (Final Conc. 6X)
1 st Restriction Enzyme	2.5
2 nd Restriction Enzyme	2.5
	Total = 60

2. Use appropriate restriction enzyme pairs (Table ii-p4.2).

Table ii-p4.2: Used Double Digest Pairs:

1st Restriction Enzyme	2nd Restriction Enzyme
FastDigest BamHI (Cat. # FD0054)	FastDigest HindIII (Cat. # FD0504)
FastDigest EcoRI (Cat. # FD0274)	FastDigest HindIII (Cat. # FD0504)
FastDigest NcoI (Cat. # FD0573)	FastDigest HindIII (Cat. #FD0504)
FastDigest NdeI (Cat. # FD0583)	FastDigest XhoI (Cat. # FD 0694)

3. Incubate the reaction tube at 37° C for 3 hours.

Note: For vector digest, add 1µl CIAP (Calf Intestinal Alkaline Phosphatase, Cat. # 18009019) after 2 hours, and incubate with CIAP for one more hour.

4. After digestion, Clean up the digested product using PCR CleanUp Kit from TruIn Science (protocol 3).

Protocol 5: Ligation Reaction

1. Check the concentration of both the vector and the insert using nanodrop.
2. Check the size of the digested vectors (Table ii-p5.1).

Table ii-p5.1 Size of the digested vectors from Serial Cloner 2.6

Digested Product	Restriction Enzyme Pair	Original Size (NTs)	Digested Size (NTs)
pET47b(+)	EcoRI and HindIII	5203	5159
pET47b(+)	BamHI and HindIII	5203	5153
pETDuet-1	NdeI and XhoI	5420	5360
pETDuet-1	BamHI and HindIII	5420	5379
pETDuet-1-TEV-H2B	NdeI and XhoI	5793	5733
pETDuet-1-H2B	BamHI and HindIII	5748	5707
pETDuet-1-H2B	NcoI and HindIII	5748	5670
pACYCDuet-1	BamHI and HindIII	4008	3967
pACYCDuet-1-TEV-H4	NdeI and XhoI	4312	4252
pCDFDuet-1	NdeI and XhoI	3781	3721
pCDFDuet-1-H4	BamHI and HindIII	4042	4001
pCDFDuet-1-H4	NcoI and HindIII	4042	3964

- Calculate the amount of insert required to set up a ligation reaction for 100ng vector using the following formula.

$$\text{Insert mass} = \frac{100 * (\text{Size of the insert in KiloBase})}{\text{Size of the vector in KiloBase}} * (\text{Insert : Vector})$$

[Note: For all my ligation reactions, Insert : Vector = 5 : 1]

- Set up a 20µl reaction (Table p5.2).

Table ii-p5.2 Ligation Reaction Setup

Reagents	Volume (µl)
ddH ₂ O	20 - 5 - X - Y
Vector	X
Insert	Y
5X Ligase Buffer (Cat. # 46300018)	4 (Final Conc. 1X)
T4 DNA Ligase (Cat. # EL0014)	1
	Total = 20

- Incubate the reaction in 16°C for overnight.
- Transform the ligated products into the plasmid amplification cell line, DH5α (Subcloning Efficiency DH5α Competent Cells, Cat. # 18265017) (Protocol 6).

Protocol 6: Recombinant DNA Transformation

- Collect the competent cells from -80°C on ice.
- Collect the appropriate antibiotic-containing plates from 4°C, label it properly, and keep it inverted in the 37°C incubator.
- Turn on the 42°C bath, and fill it with water.
- Add 10µl ligated product, and incubate for 20-30 min.
- Heat shock the cells at 42°C for 45 seconds.

6. Keep the cells on ice for 2 minutes.
7. Add 300-350 μ l Luria Broth (LB) (without antibiotics), and incubate in a 37°C shaker for 45 minutes.
8. After 45 minutes, collect the plate from the 37°C incubator, and turn the Bunsen burner on.
9. Add the complete 350 μ l of culture on the plate, and spread the culture evenly using a sterile plastic yellow loop.
10. Keep the plate on the bench for 5 minutes to have the culture settled on the plate.
11. Put the plate back to 37°C incubate, and incubate inverted for overnight.

Protocol 7: Agarose Gel Casting and Running

1. Set up the agarose gel casting apparatus.
2. In 50ml 1x TAE buffer (40mM Tris pH-8.6, 20mM Acetate, 1mM EDTA), add 7.5g Agarose in a glass Erlenmeyer flask.
3. Heat the flask in the microwave at high for one minute. The agarose should be dissolved completely. If not, keep on heating until all the lenses of agarose completely dissolve.
4. Add 5 μ l Red Safe.
5. Decant the solution in the casting apparatus, and set up the 15 well comb.
6. Let the agarose gel cool down and solidify for 15 minutes.
7. Keep the solidified gel in soaking amount of 1x TAE buffer.
8. Load around 7-15 μ l of PCR product in each well.
9. Run the gel at a constant voltage of 150 V for 20 minutes.
10. Visualize using gel imager.

Protocol 8: Plasmid MiniPrep Protocol

1. Inoculate the colony into a culture tube containing 7ml LB with appropriate antibiotic added.
2. Let the colony grow overnight in a 37°C shaker.
3. Pellet down the cells.
4. Using TruIn Science High Purity Plasmid MiniPrep Kit (Cat. # KTS1015), extract the plasmid from the cells following the supplied protocol with the kit.
5. Measure the concentration using NanoDrop.

Protocol 9: Sequencing the Plasmid to Confirm the Insert

1. In a sequencing tube, add 220ng plasmid to a total volume of 10µl. (22ng/µl plasmid)
2. Add 1µl of 3.2µM either the forward or the reverse primer, but not both the primers.
(0.3µM primer)
3. Submit the total volume of 11µl solution to TAGC for sequencing.

Protocol 10: Overexpression checking

1. Transform the recombinant construct into a bacterial expression cell line (Table i-2).
2. In a culture tube, inoculate single colony in 3ml LB containing appropriate antibiotic.
3. Grow overnight in the 37°C shaker.
4. In a culture tube, take 5ml LB with proper antibiotics, and transfer 250µl of overnight culture (1/20 dilution).
5. Grow the culture in a 37°C shaker. At certain intervals, keep on measuring the optical density (OD) of the culture at an absorbance of 600nm until you reach 0.6-0.9.
6. At OD₆₀₀ = 0.6-0.9,

1. Collect 1ml pre-induction culture
2. Collect 1ml culture and leave it at 37°C shaker to test autoinduction level.
3. Add 1mM IPTG (3µl of 1M IPTG) in the culture tube.
4. Transfer the tube in a shaker with an appropriate temperature of interest (18°C, 30°C, 37°C).
7. Collect 1ml of post-induction samples from the culture tube at 2 hours, 4 hours, and overnight incubation period.
8. Spin down the cells for 1 minute at 13000 RPM.
9. Discard the LB.
10. Resuspend the cells in 200µl ddH₂O.
11. Run the samples on a 16% SDS PAGE gel (Protocol 11).

Protocol 11: SDS PAGE

1. Cast a SDS polyacrylamide gel following the Table p11.

Table ii-p11: SDS Polyacrylamide Gel Casting.

Add the items from left to right order. All Volumes are in ml (10 ml is enough for 2 gels of 1 mm thickness).

Percent Gel	ddH ₂ O	Acrylamide (40%; 29:1)	Tris Buffer*	10% SDS
4%	6.4	1	2.5	0.1
6%	5.9	1.5	2.5	0.1
8%	5.4	2	2.5	0.1
9%	5.15	2.25	2.5	0.1
10%	4.9	2.5	2.5	0.1
11%	4.65	2.75	2.5	0.1
12%	4.4	3	2.5	0.1
14%	3.9	3.5	2.5	0.1
16%	3.4	4	2.5	0.1
18%	2.8	4.5	2.5	0.1
20%	2.3	5	2.5	0.1
22%	1.8	5.5	2.5	0.1
24%	1.3	6	2.5	0.1

*Resolving gel needs 1.5M Tris-HCl, pH 8.8. Stacking gel needs 0.5M Tris-HCl, pH 6.8

10 mL Resolving Gel: polymerize with 100 μ L 10% APS + 15 μ L TEMED

2. 10 mL Stacking Gel: polymerize with 100 μ L 10% APS + 15 μ L TEMED
3. In 30 μ l of the sample, add 10 μ l 4X SDS loading buffer
4. Boil the samples for at least 10 minutes.
5. Spin down the samples for 1 minute at 13000 RPM.
6. Load the samples on an SDS PAGE gel, and run for 1 hour at 200V.
7. When the run is complete, take the gel in a container, and add a soaking amount of Coomassie Blue, and heat in the microwave at high for 1 minute.
8. Incubate the sample on a rotating shaker at room temperature for 10 minutes.
9. Discard the Coomassie solution in a reusing container.
10. Wash out the rest of the Coomassie.
11. Add a soaking amount of destaining buffer in the container, and heat in the microwave at high for 30 seconds.
12. Fold a paper towel, and put it in the container to absorb the stain. Make sure that the towel is not touching the gel.
13. Close the container, and incubate 30 minutes on a rotating shaker. For proper destaining, leave the gel overnight on the shaker adding some water in the destaining solution in order to prevent the gel from drying out.

Protocol 12: Bradford Assay

1. Add 200 μ l Bradford solution in 800 μ l ddH₂O in order to make Bradford mix.
2. In 10 μ l protein solution add 90 μ l of Bradford mix. If protein is present, the solution will turn dark blue.

3. You can use 96 wells plate for it.

Protocol 13: Modified refolding of the Octamer

Overnight pre-inoculum

1. Inoculate transformed BL21(DE3) cells in 500ml LB with Kanamycin (50mg/ml).
2. Let the cells grow for overnight (16 hours) in a 37°C shaker at 200 RPM.

Overexpression of protein

1. Transfer 50ml of the pre-inoculum in 1L LB with Kanamycin (50mg/ml).
2. Let the cells grow in a 37°C shaker at 200 RPM until OD600 = 0.6-0.9.
3. Induce the culture by adding 1mM IPTG.
4. After 5 hours, spin the cells down at 5,000 RPM for 20 minutes at 4°C.
5. Collect 4L pellet in a 50ml conical tube.
6. Store the conical tube at -80°C.

Histone purification

1. Resuspend 4L pellet in 40ml buffer A. In 120ml of Lysis Buffer, add 1ml 100mM PMSF, 300µl Protease Inhibitor, 0.1g Lysozyme.
2. Sonicate at 60% Amplitude, with 10 Seconds pulse on, and 59 Seconds pulse off for 5-7 times.
3. Spin down the lysate at 17,000 RPM for 30 minutes.
4. Collect 20µl of the supernatant for a background check, and discard the rest of the supernatant containing the soluble proteins.
5. Resuspend the pellet in 40ml buffer B. For a better result, take out the pellet nicely in a small beaker and add 40ml Buffer B. Resuspend using magnetic stirrer for 1 hour. The speed of the stirrer should be slow to avoid bubble formation.

6. Spin down the lysate at 17,000 RPM for 45 minutes.
7. Carefully collect the supernatant, and avoid any pellet from coming into the solution.
8. In a 50ml column, collect 5ml Nickel beads (bead volume = 1/20 of the column), and add the supernatant.
9. Incubate for 2 hours on a nutator at 4°C.
10. Collect the Flow Through.
11. Wash the column with 250ml buffer C. Collect a 20µl at the very end for checking on the gel.
12. Add 5ml buffer D, and incubate for 10 minutes.
13. Collect the Elution Fraction in a 15ml conical tube.
14. Add 5ml buffer E, and incubate for 10 minutes.
15. Collect the Elution Fraction in a 15ml conical tube.
16. Repeat step 14 and 15 until Bradford assay provides negative result (Protocol 12).
17. Collect 30µl of each Elution fraction and run it on an SDS PAGE gel (Protocol 11).

Refolding of the histone heteromeric oligomers

1. Measure the concentrations of each fractions using the nanodrop.

Table ii-p13.1 Concentration Calculation for the Histones

Histone Variant	Molecular Weight (Da)	Extinction Coefficient, μ	Concentration Measured at A280 (mg/ml)	Corrected Concentration, [C] = A280 ÷ μ (mg/ml)	Total Volume, V (ml)	Total protein = [C] × V (mg)
(His) ₆ -H2A.X	18117.72	0.411				
(His) ₆ -H2B	16603.13	0.538				
(His) ₆ -H3.1	18103.05	0.329				
(His) ₆ -H4	14066.30	0.530				

2. Molar Ratio of $(\text{His})_6\text{-H2A.X}^* : (\text{His})_6\text{-H2B} = 1.09 : 1$, $(\text{His})_6\text{-H2B} : (\text{His})_6\text{-H2A.X}^* = 0.97 : 1$, $(\text{His})_6\text{-H3.1} : (\text{His})_6\text{-H4} = 1.3 : 1$, and $(\text{His})_6\text{-H4} : (\text{His})_6\text{-H3.1} = 0.77 : 1$
3. Calculate the amount of H2B and H4 required for H2A.X and H3.1 respectively.
4. Cut out the required amount of Dialysis Tube for changing the buffer. (Fisherbrand # 21-152-9, Flat width: 46mm. Vol/cm = 6.74ml. Wall thickness: 28 μm , dry cylinder diameter: 29.3mm. 5015-46. Nominal MWCO 8,000, 15m roll)
5. Wash the tubes with ddH₂O.
6. Soak the tube into buffer E.
7. Clip one end of the tube with a dialysis clip, make sure this end also has an elastic band attached.
8. Pour the Histone mixtures into the tube, and add protease inhibitor in the mixture (100 μl /50ml)
9. Clip the other end of the bag.
10. In a beaker pour 1L of the dialysis buffer E.
11. Put a small magnetic stir bar in the beaker.
12. With a spatula or a stick, hang the Dialysis Tube into the Buffer with the help of the elastic band attached side of the clip.
13. Place the beaker on a stirrer at 4°C for 12 hours.
14. Change into buffer F, and incubate for 6 hours.
15. Change into buffer F, and incubate for 6 more hours. (For both the dimer and the tetramer, you can stop at this step and move on to step 19 unless individual oligomer prep is necessary for other analysis where low salt concentration is needed.)
16. Change into buffer G, and incubate for 2 hours.

17. Change into buffer H, and incubate for 2 hours.
18. Change into buffer I, and incubate for 12 hours.
19. Wash and equilibrate the size exclusion column Superdex 200 16 60 with the last dialysis buffer.

Size exclusion of histone oligomers

1. Concentrate the histone dimer in an Amicon Ultra-15 Centrifugal Filter Unit NMWL 10 kDa (Cat. # UFC901024), the histone tetramer in an Amicon Ultra-15 Centrifugal Filter Unit NMWL 50 kDa (Cat. # UFC905024) at 4000 RPM for 15 minutes.
2. After every 15 minutes, mix the solution so that the protein does not form aggregates.
3. Keep on concentrating until the volume becomes 5ml (3-5mg/ml).
4. Load the concentrated sample on the size exclusion column and collect the fractions.
5. Check the fractions on an SDS-PAGE gel (Protocol 11).
6. Combine the purest fractions and concentrate again for storing at the desired concentration.
7. Flash freeze the histone oligomers and store at -80°C.

Formation of the octamer

1. Calculate the concentration of the dimer and the tetramer.

Table ii-p13.2 Concentration Calculation for the Histone Oligomers

Oligomer Variant	Molecular Weight (Da)	Extinction Coefficient, μ	Concentration Measured at A280 (mg/ml)	Corrected Concentration, $[C] = A280 \div \mu$ (mg/ml)	Total Volume, V (ml)	Total protein = $[C] \times V$ (mg)
(His) ₆ -H2A.X-(His) ₆ -H2B	31568.30	0.472				
[(His) ₆ -H3.1-	58417.97	0.408				

(His) ₆ - H4] ₂						
--	--	--	--	--	--	--

2. Molar ratio calculation, 2.5 (H2A.X-H2B) : [(His)₆-TEV-H4-H3.1]₂ = 78920.75 : 585417.97 = 1.35 : 1, and [(His)₆-TEV-H4-H3.1]₂ : 2.5 (H2A.X-H2B) = 0.74 : 1
3. Mix 2.5 molar of the dimer with 1 molar of tetramer at a concentration of 1mg/ml in a dialysis bag (Fisherbrand # 21-152-9, Flat width: 46mm. Vol/cm = 6.74ml. Wall thickness: 28μm, dry cylinder diameter: 29.3mm. 5015-46. Nominal MWCO 8,000, 15m roll).
4. Dialyze in buffer F for 24 hours. (You can stop at this step and move on to step 32 unless the octamer prep is necessary for other analysis where low salt concentration is needed.)
5. Change into buffer G, and incubate for 2 hours.
6. Change into buffer H, and incubate for 2 hours.
7. Change into buffer I, and incubate for 12 hours.
8. Wash and equilibrate the size exclusion column Superdex 200 10 300 with the last dialysis buffer.

Size exclusion of histone octamer

9. Concentrate the histone octamer in an Amicon Ultra-15 Centrifugal Filter Unit NMWL 100 kDa (Cat. # UFC910024) at 4000 RPM for 10 minutes.
10. After every 10 minutes, mix the solution so that the protein does not form aggregates.
11. Keep on concentrating until the volume becomes 400μl (3-5mg/ml).
12. Load the concentrated sample on the size exclusion column and collect the fractions.
13. Check the fractions on an SDS-PAGE gel (Protocol 11).
14. Combine the purest fractions and concentrate again for storing at the desired concentration.

15. Flash freeze the histone oligomers and store at -80°C .

Protocol 14: One-step Purification of the Dimer and the Tetramer

Overnight pre-inoculum

1. Inoculate pETDuet-1-(His)₆-TEV-H2A.X-H2B transformed Rosetta 2(DE3) cells in 500ml TB with Ampicillin (50mg/ml) and chloramphenicol (34mg/ml). Or, inoculate pACYCDuet-1-(His)₆-TEV-H4-H3.1 transformed BL21(DE3) cells in 500ml TB with chloramphenicol (34mg/ml).
2. Let the cells grow for overnight (16 hours) in a 37°C shaker at 200 RPM.

Overexpression of protein

1. Transfer 50ml of the pre-inoculum in 1L TB with Ampicillin (50mg/ml) and chloramphenicol (34mg/ml), in case of pETDuet-1-(His)₆-TEV-H2A.X-H2B transformed Rosetta 2(DE3), or in 1L TB with only chloramphenicol (34mg/ml) in case of pACYCDuet-1-(His)₆-TEV-H4-H3.1 transformed BL21(DE3).
2. Let the cells grow in a 37°C shaker at 200 RPM until $\text{OD}_{600} = 0.8-1.0$.
3. Induce the culture by adding 1mM IPTG and bring down the temperature to 30°C .
4. After 7 hours, spin the cells down at 5,000 RPM for 20 minutes at 4°C .
5. Collect 4L pellet in a 50ml conical tube.
6. Store the conical tube at -80°C .

Separate purification of the dimer and the tetramer

7. Resuspend 4L pellet in 120ml buffer L. In 120ml of Lysis Buffer, add 1ml 100mM PMSF, 300 μl Protease Inhibitor, 0.1g Lysozyme.
8. Lyse the cells using emulsiflex cell disruptor.
9. Spin down the lysate at 17,000 RPM for 45 minutes at 4°C .

10. Carefully collect the supernatant, and avoid any pellet from coming into the solution.
11. In a 50ml column, collect 10ml Nickel beads (bead volume = 1/10 of the column), and add the supernatant.
12. Incubate for 2 hours on a nutator at 4°C.
13. Collect the Flow Through.
14. Wash the column with 250ml buffer W. Collect a 20µl at the very end for checking on the gel.
15. Add 5ml buffer E1, and incubate for 10 minutes.
16. Collect the Elution Fraction in a 15ml conical tube.
17. Add 5ml buffer E2, and incubate for 10 minutes.
18. Collect the Elution Fraction in a 15ml conical tube.
19. Add 5ml buffer E3, and incubate for 10 minutes.
20. Collect the Elution Fraction in a 15ml conical tube.
21. Add 5ml buffer E4, and incubate for 10 minutes.
22. Collect the Elution Fraction in a 15ml conical tube.
23. Collect 10µl of each Elution fraction and run it on an SDS PAGE gel (Protocol 11).
24. Combine the purest fractions.

Size exclusion of the dimer and the tetramer

25. Pre-equilibrate the Superdex 200 16 60 size exclusion column with buffer S.
26. Concentrate the dimer in an Amicon Ultra-15 Centrifugal Filter Unit NMWL 10 kDa or the tetramer in an Amicon Ultra-15 centrifugal Filter Unit NMWL 50 kDa at 4,000 RPM for 10 minutes.
27. After every 10 minutes, mix the solution so that the protein does not form aggregates.

28. Keep on concentrating until the volume becomes 5ml (3-5mg/ml).
29. Load the concentrated sample on the pre-equilibrated Superdex 200 16 60 size exclusion column and collect the fractions.
30. Check the fractions on an SDS-PAGE gel (Protocol 11).
31. Combine the purest fractions and concentrate again for storing at the desired concentration.
32. Flash freeze the histone oligomers and store at -80°C.

Formation of the octamer

33. Calculate the concentration of the dimer and the tetramer.

Table ii-p14.1 Concentration Calculation for the Histone Oligomers

Oligomer Variant	Molecular Weight (Da)	Extinction Coefficient, μ	Concentration Measured at A280 (mg/ml)	Corrected Concentration, $[C] = A280 \div \mu$ (mg/ml)	Total Volume, V (ml)	Total protein = $[C] \times V$ (mg)
(His) ₆ -TEV-H2A.X-H2B	31568.30	0.472				
[(His) ₆ -TEV-H3.1-H4] ₂	58417.97	0.408				
[H3.1-H4] ₂	53602.92	0.389				

34. Molar ratio calculation, 2.5 (H2A.X-H2B) : [(His)₆-TEV-H3.1-H4]₂ = 78920.75 :

$$585417.97 = 1.35 : 1, \text{ and } [(His)_6\text{-TEV-H3.1-H4}]_2 : 2.5 \text{ (H2A.X-H2B)} = 0.74 : 1$$

35. Mix 2.1 molar of the dimer with 1 molar of tetramer at a concentration of 1mg/ml in a dialysis bag (Fisherbrand # 21-152-9, Flat width: 46mm. Vol/cm = 6.74ml. Wall

thickness: 28 μ m, dry cylinder diameter: 29.3mm. 5015-46. Nominal MWCO 8,000, 15m roll).

36. Dialyze in buffer S for 24 hours. (You can stop at this step and move on to step 38 unless the octamer prep is necessary for other analysis where low salt concentration is needed.)
37. Change into buffer G, and incubate for 2 hours.
38. Change into buffer H, and incubate for 2 hours.
39. Change into buffer I, and incubate for 12 hours.

Size exclusion of histone octamer

40. Wash and equilibrate the size exclusion column Superdex 200 10 300 with the last dialysis buffer.
41. Concentrate the histone octamer in an Amicon Ultra-15 Centrifugal Filter Unit NMWL 100 kDa (Cat. # UFC910024) at 4000 RPM for 10 minutes.
42. After every 10 minutes, mix the solution so that the protein does not form aggregates.
43. Keep on concentrating until the volume becomes 400 μ l (3-5mg/ml).
44. Load the concentrated sample on the size exclusion column and collect the fractions.
45. Check the fractions on an SDS-PAGE gel (Protocol 11).
46. Combine the purest fractions and concentrate again for storing at the desired concentration.
47. Flash freeze the histone octamer and store at -80°C.

Protocol 15: One step purification of the octamer

Overnight pre-inoculum

1. Inoculate [pETDuet-1-(His)₆-TEV-H2A.X-H2B + pCDFDuet-1-(His)₆-TEV-H3.1-H4] transformed Rosetta 2(DE3) cells in 500ml TB with Ampicillin (50mg/ml), streptomycin (50mg/ml), and chloramphenicol (34mg/ml).
2. Let the cells grow for overnight (16 hours) in a 37°C shaker at 200 RPM.

Overexpression of protein

3. Transfer 50ml of the pre-inoculum in 1L TB with Ampicillin (50mg/ml), streptomycin (50mg/ml), and chloramphenicol (34mg/ml).
4. Let the cells grow in a 37°C shaker at 200 RPM until OD₆₀₀ = 0.8-1.0.
5. Induce the culture by adding 1mM IPTG, and bring down the temperature to 30°C.
6. After 7 hours, spin the cells down at 5,000 RPM for 20 minutes at 4°C.
7. Collect 4L pellet in a 50ml conical tube.
8. Store the conical tube at -80°C.

Purification of the octamer

9. Resuspend 4L pellet in 120ml buffer L. In 120ml of Lysis Buffer, add 1ml 100mM PMSF, 300µl Protease Inhibitor, 0.1g Lysozyme.
10. Lyse the cells using emulsiflex cell disruptor.
11. Spin down the lysate at 17,000 RPM for 45 minutes at 4°C.
12. Carefully collect the supernatant, and avoid any pellet from coming into the solution.
13. In a 50ml column, collect 10ml Nickel beads (bead volume = 1/10 of the column), and add the supernatant.
14. Incubate for 2 hours on a nutator at 4°C.

15. Collect the Flow Through.
16. Wash the column with 250ml buffer W. Collect a 20 μ l at the very end for checking on the gel.
17. Add 5ml buffer E1, and incubate for 10 minutes.
18. Collect the Elution Fraction in a 15ml conical tube.
19. Add 5ml buffer E2, and incubate for 10 minutes.
20. Collect the Elution Fraction in a 15ml conical tube.
21. Add 5ml buffer E3, and incubate for 10 minutes.
22. Collect the Elution Fraction in a 15ml conical tube.
23. Add 5ml buffer E4, and incubate for 10 minutes.
24. Collect the Elution Fraction in a 15ml conical tube.
25. Collect 10 μ l of each Elution fraction and run it on an SDS PAGE gel (Protocol 11).
26. Combine the purest fractions.

Size exclusion of the octamer

27. Pre-equilibrate the Superdex 200 16 60 size exclusion column with buffer S.
28. Concentrate the octamer in an Amicon Ultra-15 Centrifugal Filter Unit NMWL 100 kDa.
29. After every 10 minutes, mix the solution so that the protein does not form aggregates.
30. Keep on concentrating until the volume becomes 5ml (3-5mg/ml).
31. Load the concentrated sample on the pre-equilibrated Superdex 200 16 60 size exclusion column and collect the fractions.
32. Check the fractions on an SDS-PAGE gel (Protocol 11).
33. Pre-equilibrate the Superdex 200 10 300 size exclusion column with buffer S.
34. Concentrate the octamer in an Amicon Ultra-15 Centrifugal Filter Unit NMWL 100 kDa.

35. After every 10 minutes, mix the solution so that the protein does not form aggregates.
36. Keep on concentrating until the volume becomes 5ml (3-5mg/ml).
37. Load the concentrated sample on the pre-equilibrated Superdex 200 10 300 size exclusion column and collect the fractions.
38. Check the fractions on an SDS-PAGE gel (Protocol 11).
39. Combine the purest fractions and concentrate again for storing at the desired concentration.
40. Flash freeze the histone oligomers and store at -80°C.

Protocol 16: *In vitro* Phosphorylation of the H2A.X-H2B Dimer

1. Pre-equilibrate the phosphorscreen film by placing it upside down on a turned on SDS gel viewer lamp for at least 15 minutes. It can be longer than 15 minutes, time is not a factor.
2. Prepare 1/15 dilution of the γ ATP stock (in a PCR tube, add 14 μ l ddH₂O and 1 μ l γ ATP from the main stock). Store in the radioactive box.
3. Set up 20 μ l diluted 1mM ATP mix.

Table ii-p16.1 ATP Mix: 1mM ATP

Reagents	Volume (μ l)
ddH ₂ O	15
10X KB (kinase buffer)	2
10mM ATP (pH ~7-8)	2
γ ATP (1/15 dilution)	1
	20

4. Set up 50 μ l reaction mix.

Table ii-p16.2 Kinase Assay Reaction Setup

Reagents	Volume (μl)
ddH ₂ O	10
10X KB	5
H2A.X-H2B (Buffer I)	25 (0.4 $\mu\text{l}/\mu\text{g}$)
CK2	2.5 (1 molar of the 20 molar dimer)
1mM ATP mix	7.5
	50

- For 10 μl SDS sample preparation,

Table ii-p16.3 Quenching of Kinase Reaction

Buffers and samples	Volume (μl)
4X SDS	2.5
1X KB	2.5
Reaction mix	5
	10

- Set the reaction tube on a 30°C heating block.
- Collect 5 μl of the reaction and quench the reaction in the SDS sample prepared.
- Keep on collecting the samples every 10 minutes until 30 minutes.
- Run the samples on a 16% SDS PAGE.

10. Do not let the dye front to run of the gel unless you are fine with contaminating the whole gel apparatus.
11. After the run, cut out the stacking gel, and also cut out portion of gel a little bit above from the dye front. If you do not cut out the dye front it will give you high signal at the bottom.
12. Wrap the gel in a saran wrap. Make sure no bubble got in.
13. Tape the sides of the wrap nicely to prevent air drying of the gel.
14. Place the gel on a phosphorscreen cassette.
15. Quickly place the pre-equilibrated phosphorscreen on the gel as soon as possible without living it outside of the SDS gel view lamp.
16. Close the cassette, and incubate in for 24 hours.
17. Next day, take the cassette to Dr. Fahlman's lab.
18. Use their Typhoon scanner to visualize the phosphorscreen.
19. Turn on the Typhoon scanner, and open the software in the computer.
20. After the machine is ready, lift the scanner lid, and place the phsophorscreen film as soon as possible without exposing it into the light.
21. Close the lid.
22. Mark the region of the gel exposed region on the software, so that the scanner can take the image of only the gel exposed portion. Otherwise, it will take forever to image the full screen.
23. After imagining, save the image.
24. Turn off the Typoon scanner, and take your phosphorscreen film back, and put it in the cassette.

Protocol 17: Size Exclusion Column (SEC)

Size Exclusion Column Manual:

Pump wash:

- Pump → Pump wash purifier → Inlet A1 → ON → Insert

Column wash:

- Pump → Flow → Flow rate = 1.5ml/min → Insert
- Flow path → Column position → position X → Insert
- Alarm → Alarm_Pressure → High Alarm = 0.5 MPa → Insert
- Other → End timer → Acc. Vol → Timeout = 120ml

Loop wash:

- Flow → 2ml/min
- Injection mode → Inject
- Flow path → Column position 1 Bypass
- End timer → 20ml
- Alarm → AirSensor3 → Disable

Table ii-p17.1 Size Exclusion Column Information:

Name	HiLoad 16/60 Superdex 200 prep grade
Height	60.0 cm
Diameter	1.6 cm
Column volume	120.637 ml
Technique	Size Exclusion
Vt	0.0 ml
Vo	39.799999 ml
Max pressure	0.35 MPa
Default flowrate	1.0 ml/min
Typical Peak width at base	10.0 ml
pH High value, longterm	12
pH Low value, longterm	3
pH High value, shortterm	14
pH Low value, shortterm	1
Average particle diameter	34µm
Code no	17-1069-01
Typical loading range	0.6-5ml
Molecular weight range	kDa
Scan rate	Spectra/sec

Table ii-p17.2 SEC Method Information:

Variables	Values
Column	HiLoad 16/60 Superdex 200 prep grade
Wash Inlet A1	OFF
Wash Inlet A2	OFF
Wash Inlet B1	OFF
Wash Inlet B2	OFF
FlowRate Equil	0.500 {ml/min}
Column PressureLimit	0.35 {MPa}
Wavelength 1	280 {nm}
Wavelength 2	254 {nm}
Wavelength 3	OFF {nm}
Averaging Time UV	5.12 {sec}
Pump A Inlet	A1
Pump B Inlet	B1
Start ConcB	0 {%B}
Column Position	Position8
Equilibrate with	0.00 {CV}
System Pump	Normal
System PressLevel	0 {MPa}
System MinFlow	0 {ml/min}
FlowRate WashOut	1.000 {ml/min}
Empty loop with	10.0 {ml}
FlowRate Elution	0.500 {ml/min}
Length Before Frac	0.30 {CV}
TubeType EluateFrac	18mm
Eluate Frac Size	1.000 {ml}
EluateFrac StartAt	FirstTube
TubeType PeakFrac	18mm
Peak Frac Size	0 {ml}
PeakFrac StartAt	FirstTube
Length with Frac	1.00 {CV}

Appendix iii Buffers

Table iii-1 All Buffer Compositions

Buffer Name	Composition	Purpose
Buffer L (Lysis buffer)	<ul style="list-style-type: none"> • 2M NaCl • 50mM Tris pH-7.5 • 5% Glycerol • 1mM TCEP • 1mM PMSF • Protease inhibitor (100µl/50ml) 	<ul style="list-style-type: none"> • One step purification of the dimer and the tetramer • One step purification of the Octamer
Buffer W (Wash buffer)	<ul style="list-style-type: none"> • 2M NaCl • 50mM Tris pH-7.5 • 5% Glycerol • 1mM TCEP • 30mM Imidazole 	
Buffer E (Gradient elution buffer)	<ul style="list-style-type: none"> • 2M NaCl • 50mM Tris pH-7.5 • 5% Glycerol • 1mM TCEP • Imidazole: <ul style="list-style-type: none"> ○ E1: 100mM ○ E2: 250mM ○ E3: 500mM ○ E4: 1M ○ E5: 2M 	
Buffer S (Size exclusion buffer)	<ul style="list-style-type: none"> • 2M NaCl • 25mM HEPES pH-7.5 • 5% Glycerol • 1mM TCEP • 1mM PMSF 	
Buffer A	<ul style="list-style-type: none"> • 2M NaCl • 50mM Tris pH-8.0 • 1mM TCEP • 1mM PMSF • Protease inhibitor (100µl/50ml) 	
Buffer B	<ul style="list-style-type: none"> • 2M NaCl • 50mM Tris pH-8.0 • 6M Urea • 5% Glycerol • 1mM TCEP • 1mM PMSF 	Modified refolding of the Octamer

Buffer C	<ul style="list-style-type: none"> • 2M NaCl • 50mM Tris pH-8.0 • 6M Urea • 5% Glycerol • 1mM TCEP • 10mM Imidazole 	
Buffer D	<ul style="list-style-type: none"> • 2M NaCl • 50mM Tris pH-8.0 • 6M Urea • 5% Glycerol • 1mM TCEP • 300mM Imidazole 	
Buffer E	<ul style="list-style-type: none"> • 2M NaCl • 50mM Tris pH-8.0 • 6M Urea • 5% Glycerol • 1mM TCEP • 2mM EDTA • 1mM PMSF 	
Buffer F	<ul style="list-style-type: none"> • 2M NaCl • 50mM Tris pH-8.0 • 5% Glycerol • 1mM TCEP • 1mM EDTA • 1mM PMSF 	
Buffer G	<ul style="list-style-type: none"> • 1M NaCl • 50mM Tris pH-8.0 • 5% Glycerol • 1mM TCEP • 1mM EDTA • 1mM PMSF 	
Buffer H	<ul style="list-style-type: none"> • 500mM NaCl • 50mM Tris pH-8.0 • 5% Glycerol • 1mM TCEP • 1mM EDTA • 1mM PMSF 	
Buffer I	<ul style="list-style-type: none"> • 250mM NaCl • 50mM Tris pH-8.0 • 5% Glycerol • 1mM TCEP • 1mM EDTA • 1mM PMSF 	

10X KB (Kinase buffer)	<ul style="list-style-type: none"> • 0.5M Tris pH 7.5 • 1.5M NaCl • 0.1 M MgCl₂ • 22M DTT 	In vitro phosphorylation of the H2A.X-H2B dimer
CK2 buffer	<ul style="list-style-type: none"> • 200mM NaCl • 50mM Tris pH-7.5 • 1mM DTT • 1mM EDTA • 50% glycerol 	
CK2 buffer (diluted)	<ul style="list-style-type: none"> • 200mM NaCl • 25mM Tris pH-7 	

Appendix iv Cloning Images

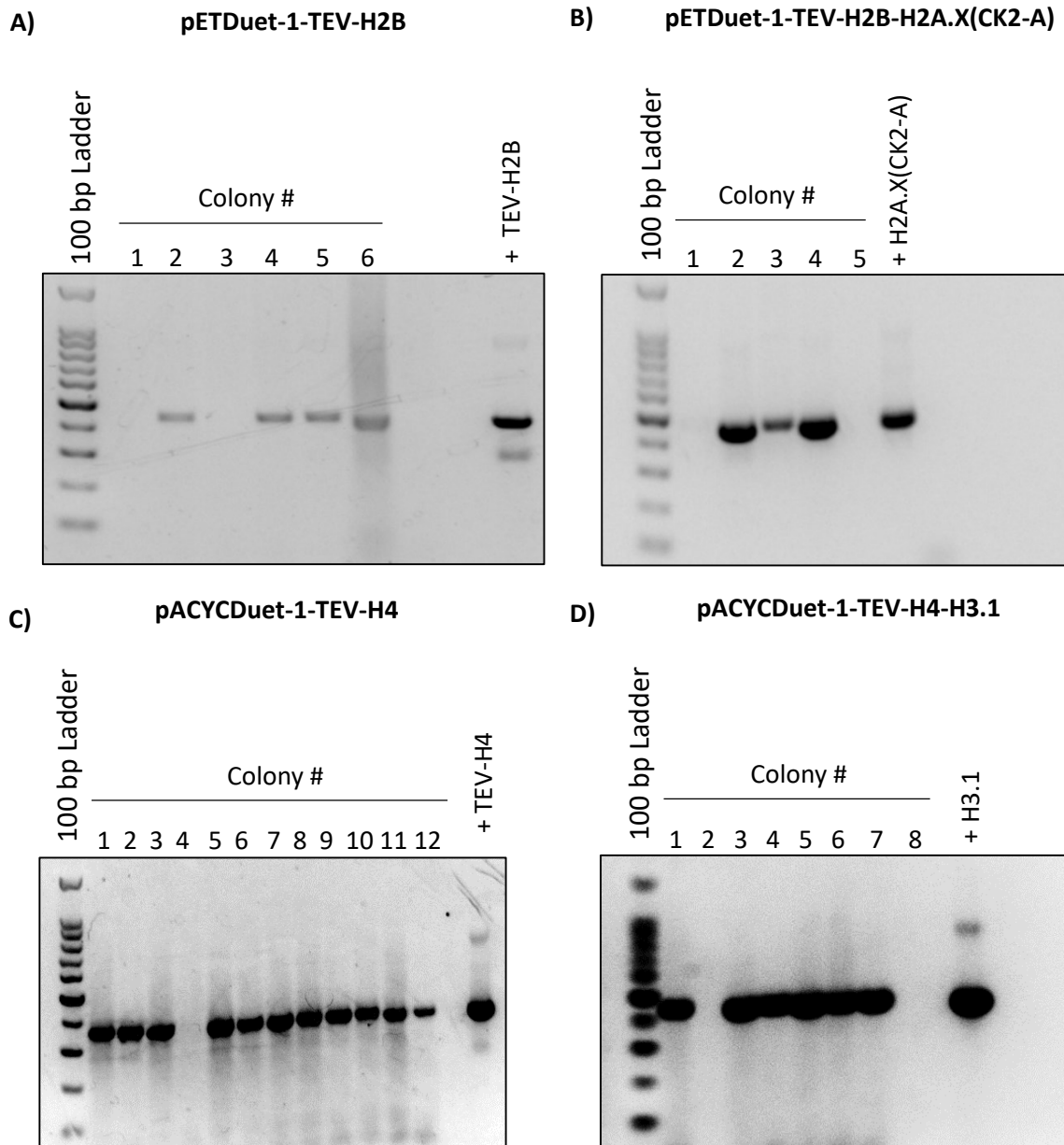


Figure iv-1 Colony PCR Confirmation for Successful Cloning.

The PCR products were run on a 1.5% agarose gel with 150V for 20 minutes. A) TEV-H2B and pETDuet-1 were digested with BamH1 and HindIII. The ligated pETDuet-1-TEV-H2B construct was transformed into DH5 α . The presence of positive colonies was confirmed through colony PCR. B) H2A.X(CK2-A) and pETDuet-1-TEV-H2B were digested with NdeI and XhoI. Ligated pETDuet-1-TEV-H2B-H2A.X(CK2-A) construct was transformed into DH5 α . The presence of positive colonies was confirmed through colony PCR. C) TEV-H4 and pACYCDuet-1 were digested with BamH1 and HindIII. The ligated pACYCDuet-1-TEV-H4 construct was transformed into DH5 α . The presence of positive colonies was confirmed through colony PCR. D) H3.1 and pACYCDuet-1-H4 were digested with NdeI and XhoI. The ligated pACYCDuet-1-TEV-H4-H3.1 construct was transformed into DH5 α . The presence of positive colonies was confirmed through colony PCR.

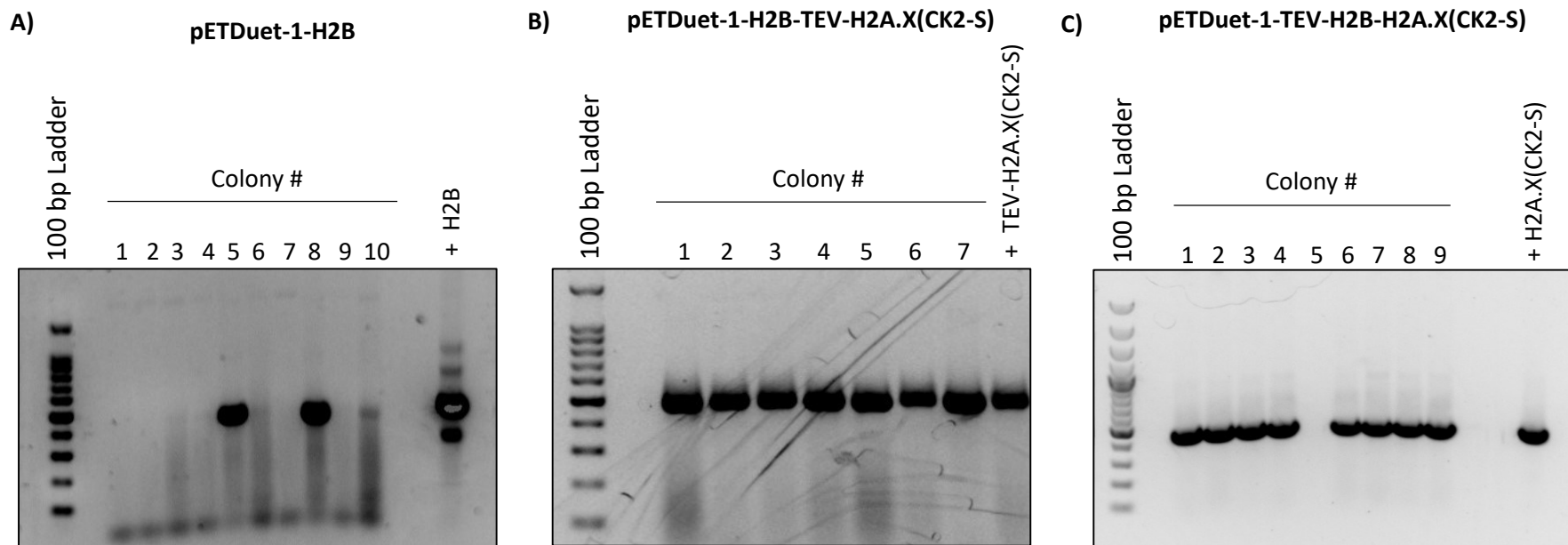


Figure iv-2 Colony PCR confirmation of successful cloning.

The PCR products were run on a 1.5% agarose gel with 150V for 20 minutes. A) H2B and pETDuet-1 were digested with NdeI and XhoI. The ligated pETDuet-1-H2B construct was transformed into DH5 α . The presence of positive colonies was confirmed through colony PCR. B) TEV-H2A.X(CK2-S) and pETDuet-1-H2B were digested with BamHI and HindIII. The ligated pETDuet-1-H2B-TEV-H2A.X(CK2-S) construct was transformed into DH5 α . The presence of positive colonies was confirmed through colony PCR. C) H2A.X(CK2-S) and pETDuet-1-H2B were digested with NcoI and HindIII. The ligated pETDuet-1-H2B-H2A.X(CK2-S) construct was transformed into DH5 α . The presence of positive colonies was confirmed through colony PCR.

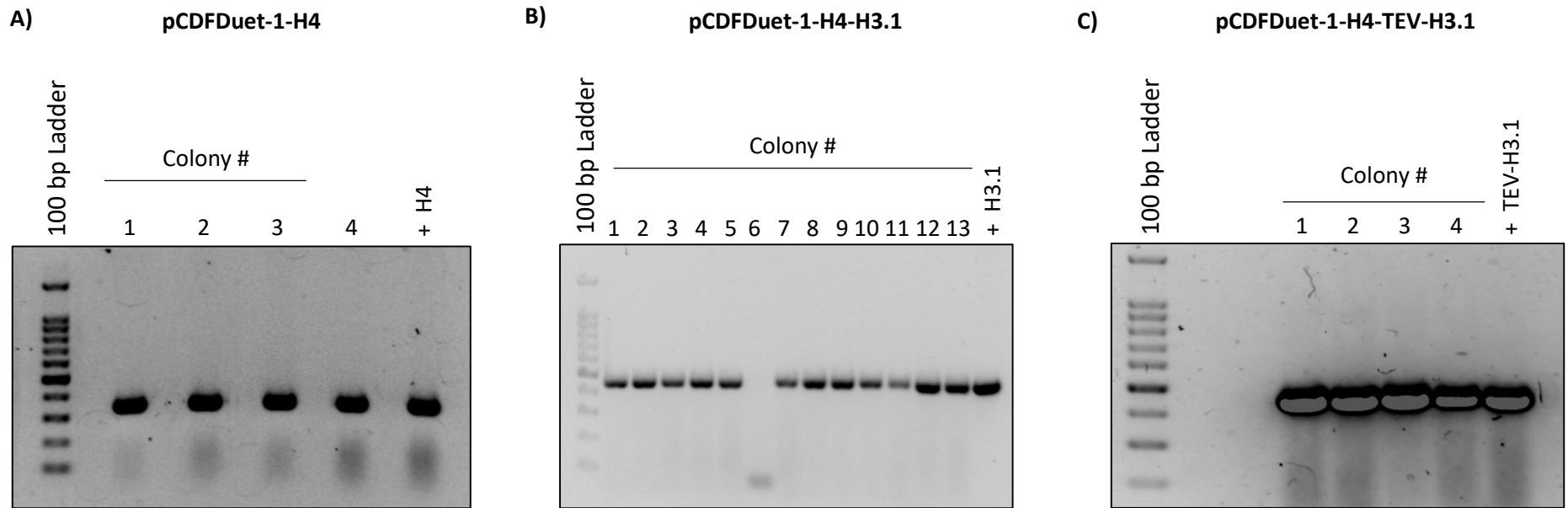


Figure iv-3 Colony PCR confirmation of successful cloning.

The PCR products were run on a 1.5% agarose gel with 150V for 20 minutes. A) H4 and pCDFDuet-1 were digested with NdeI and XhoI. The ligated pCDFDuet-1-H4 construct was transformed into DH5 α . The presence of positive colonies was confirmed through colony PCR. B) H3.1 and pCDFDuet-1-H4 were digested with NcoI and HindIII. The ligated pCDFDuet-1-H4-H3.1 construct was transformed into DH5 α . The presence of positive colonies was confirmed through colony PCR. C) TEV-H3.1 and pCDFDuet-1-H4 were digested with BamHI and HindIII. The ligated pCDFDuet-1-H4-TEV-H3.1 construct was transformed into DH5 α . The presence of positive colonies was confirmed through colony PCR.

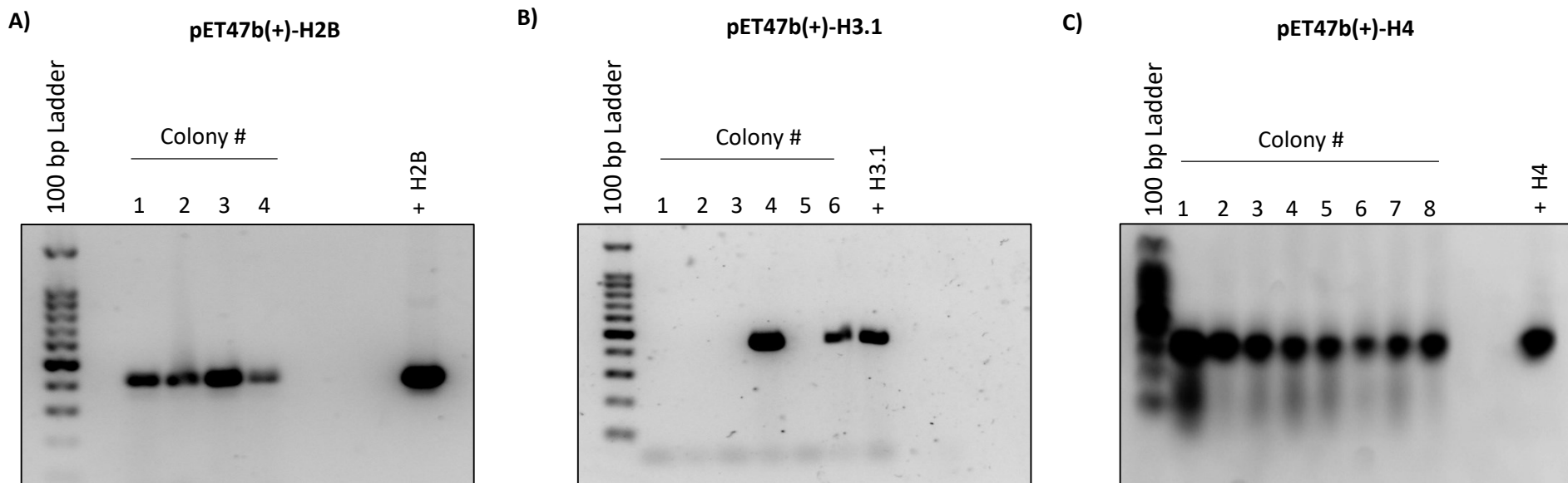


Figure iv-4 Colony PCR confirmation of successful cloning.

The PCR products were run on a 1.5% agarose gel with 150V for 20 minutes. A) H2B and pET47b(+) were digested with BamHI and HindIII. The ligated pET47b(+)-H2B construct was transformed into DH5 α . The presence of positive colonies was confirmed through colony PCR. B) H3.1 and pET47b(+) were digested with BamHI and HindIII. The ligated pET47b(+)-H3.1 construct was transformed into DH5 α . The presence of positive colonies was confirmed through colony PCR. C) H4 and pET47b(+) were digested with BamHI and HindIII. The ligated pET47b(+)-H4 construct was transformed into DH5 α . The presence of positive colonies was confirmed through colony PCR.

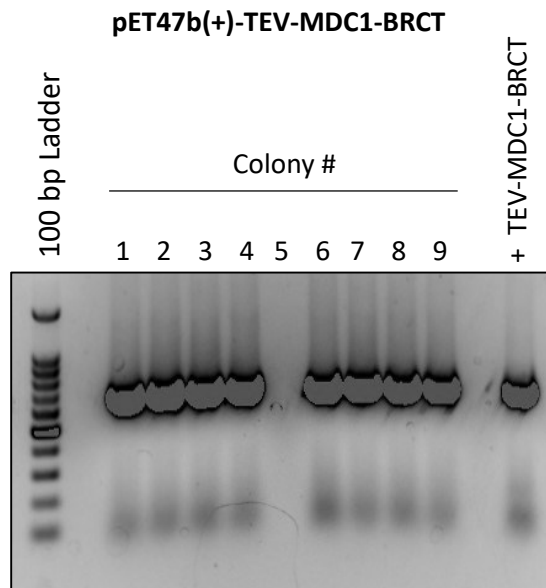


Figure iv-5 Colony PCR confirmation of successful cloning.

The PCR products were run on a 1.5% agarose gel with 150V for 20 minutes. A) TEV-MDC1-BRCT and pET47b(+) were digested with BamHI and HindIII. Ligated pET47b(+)-TEV-MDC1-BRCT construct was transformed into DH5 α . The presence of positive colonies was confirmed through colony PCR.

Appendix v - Cell lines.

Table v-1: Description of the Cell lines Used in this Study.

Cell line	Genotype	Specifications
BL21(DE3) (Novagen, Cat. # 69450)	<i>E. coli str. B</i> <i>F⁻ ompT gal dcm lon hsdS_B(r_B⁻m_B⁻) λ(DE3</i> <i>[lacI lacUV5-T7p07 ind1 sam7 nin5])</i> <i>[malB⁺]_{K-12}(λ^S)</i>	B strain → deficient in lon and OmpT proteases, resistant to phage T1, T7 expression system
BL21(DE3) pLysS (Novagen, Cat. # 69451)	<i>E. coli str. B</i> <i>F⁻ ompT gal dcm lon hsdS_B(r_B⁻m_B⁻) λ(DE3</i> <i>[lacI lacUV5-T7p07 ind1 sam7 nin5])</i> <i>[malB⁺]_{K-12}(λ^S)</i> pLysS[<i>T7p20 ori_{p15A}</i>](Cm ^R)	B strain → deficient in lon and OmpT proteases, resistant to phage T1, stringent T7 inducible expression system
C41(DE3) (Lucigen, Cat. # 60442-1)	<i>E. coli str. B</i> <i>F⁻ ompT gal dcm lon hsdS_B(r_B⁻m_B⁻) λ(DE3</i> <i>[lacI lacUV5-T7p07 ind1 sam7 nin5])</i>	Derived from BL21(DE3) with at least one mutation that prevents recombinant toxic protein associated cell death. This cell line is efficient in expressing toxic and membrane proteins (lucigen).
C43(DE3) (Lucigen, Cat. # 60446-1)	<i>E. coli str. B</i> <i>F⁻ ompT gal dcm lon hsdS_B(r_B⁻m_B⁻) λ(DE3</i> <i>[lacI lacUV5-T7p07 ind1 sam7 nin5])</i>	Derived from C41(DE3) with some more mutations that prevent recombinant toxic protein associated cell death. This cell line is efficient in expressing toxic and membrane proteins (lucigen).
Rosetta 2 (Novagen, Cat. # 71402)	<i>E. coli str. B</i> <i>F⁻ ompT gal dcm lon? hsdS_B(r_B⁻m_B⁻)</i> <i>[malB⁺]_{K-12}(λ^S)</i> pRARE[<i>ileX argU thrU tyrU glyT thrT arg</i> <i>W metT leuW proL</i>](Cm ^R)	Derived from BL21, therefore, all the features of BL21(DE3) are present. However, it helps in producing eukaryotic proteins that contain rare <i>E.coli</i> codons because Rosetta 2 cells are supplied with 7 tRNAs

		<p>that codes for 7 rare codons (AGA, AGG, AUA, CUA, GGA, CCC, and CGG). These tRNA genes are on a chloramphenicol resistant plasmid and are expressed using bacterial native promoters.</p> <p>Since no λDE3 lysogen is present therefore there is no T7 RNA polymerase gene. So expression can only be carried out from the T7 or T7-lac promoter or promoters recognized by E.coli RNA polymerase: e.g. lac, tac, trc, ParaBAD, PrhaBAD and also T5 promoter.</p>
<p>Rosetta 2(DE3) (Novagen, Cat. # 71400)</p>	<p><i>E. coli</i> str. B F^- <i>ompT gal dcm lon?</i> <i>hsdS_B(r_B⁻m_B⁻)</i> λ(DE3 [<i>lacI lacUV5-T7p07 ind1 sam7 nin5</i>]) [<i>malB</i>⁺]_{K-12}(λ^S) pRARE[<i>ileX argU thrU tyrU glyT thrT argW metT leuW proL</i>](Cm^R)</p>	<p>Derived from BL21, therefore, all the features of BL21(DE3) are present. However, it helps in producing eukaryotic proteins that contain rare <i>E.coli</i> codons because Rosetta 2 cells are supplied with 7 tRNAs that codes for 7 rare codons (AGA, AGG, AUA, CUA, GGA, CCC, and CGG). These tRNA genes are on a chloramphenicol resistant plasmid and are expressed using bacterial native promoters.</p> <p>The presence of λDE3 lysogen means there is an IPTG inducible T7 RNA polymerase gene in the bacterial chromosome.</p>

DH5 α (Invitrogen, Cat. # 18265017)	F ⁻ <i>endA1 glnV44 thi-1 recA1 relA1 gyrA96 deoR nupG purB20</i> ϕ 80dlacZ Δ M15 Δ (<i>lacZYA-argF</i>)U169, hsdR17(<i>rK⁻mK⁺</i>), λ^-	Used for large scale plasmid prep because it has endA1, recA1 and relA1 mutation, and it constitutively produces deoxyribose.
---	--	---

Table v-2: Description of the Terminologies Used in the Cell line Specifications.

Terminology	Description
dcm	dcm methyl transferases methylate CCWGG
endA	DNA-specific endonuclease 1. Mutation increase the yield of DNA from minipreps.
F plasmid	Episome (a plasmid that can integrate itself into bacterial genome by homologous recombination) helps in conjugation
fhuA2	Ferric hydroxamate uptake receptor, required by phage T1 to infect bacterial cells
gal	Gal operon of 3 genes: <i>gale</i> , <i>galT</i> , and <i>galK</i>
gyrA	DNA gyrase subunit A. Mutation results in resistance to naladixic acid.
hsdM	<i>E.coli</i> DNA methylase. Mutation blocks sequence-specific adenine methylation
hsdR	<i>E.coli</i> restriction endonuclease. Mutation permits foreign DNA to propagate.
hsdS	<i>E.coli</i> specificity determinant for hsdM and hsdR. Mutation eliminates HsdM and HsdR activity.
lacI	Lac operon repressor protein. LacIq is a mutant of lacI that overproduces the repressor protein.
lacZDM15	A specific N-terminal deletion which permits the α -complementation segment to make a functional LacZ protein
Lon	Cytoplasmic serine protease
malB	Maltose operon protein B
OmpT	Outer membrane aspartyl protease
pLysS	Plasmid carrying chloramphenicol resistance and T7 lysozyme for effective attenuation of T7 RNA polymerase for stringent expression inhibition under non-induced condition
recA	Mutation prevents homologous recombination
relA	Relaxed phenotype. Mutation permits RNA synthesis in the absence of protein synthesis.
thi-1	Mutation requires vitamin B1 (thiamin) for growth in minimal media
λ DE3 lysogen	Carries T7 RNA polymerase under control of the lacUV5 promoter induced by IPTG